Scaling the effects of warming on metabolism from organisms to ecosystems

Submitted by

Daniel Padfield

To the University of Exeter as a thesis for the degree of

Doctor of Philosophy of Biological Sciences

June, 2017

I certify that all material in this thesis which is not my own work has been identified and that no material has previously been submitted and approved for the award of a degree by this or any other University

Signature: ……

Acknowledgements

This thesis is the culmination of three (nearly four) years of hard work and procrastination. Throughout this time, I have received support, guidance and advice from innumerable people that have all contributed, in their own way, to this piece of work. Firstly, I am eternally grateful to my supervisor Gabriel Yvon-Durocher. If/when I succeed in science, the foundations of that success will be traced back to my 3.5 (now close to 4) years with him as my main supervisor. His passion for research and hands-on approach has helped me to think critically and logically about my own work and ideas. On top of that, his excitement for data, graphs and programming was contagious; my love of data, graphs and the R programming language can be traced back to the code snippets and help he provided in the first year of my PhD. The last three years have been the most intellectually challenging and stimulating time of my life and I hope that continues (and that I can grow a beard soon). On top of all that, he is a fantastic person and understood the complexities in my life over the last three years. I have been very lucky to work with him.

Secondly, I owe a huge amount to my co-supervisors Simon Jennings and Angus Buckling who have helped me understand science from perspectives outside of the one I usually occupy, sitting in the lab or on R. Also, a big thanks to Chris Lowe who has provided support even without any direct affiliation to my project, and outside of this has shown me that it is possible to be a success in academia and have something resembling a healthy work-life balance. I would also like to thank the #TeamPhytoplankton lab group including Elisa, Elvire, Sam, Ben, Paqui, Ruth and the undergrads and Masters students who

have come through our lab in that last 4 years. We are an eclectic mix of nationalities and personalities, reflective of how good science should be done.

There are also many people who have helped me collect data along the way. Chris Bryan and Paul Norris for letting me use their CellFacts machine (and helping me fix it when it broke). Genevieve who helped me collect data for *Chapter 2*, even if she faked a burst appendix to get out of lab work! The students of the Iceland field course who grafted with me late into the night collecting metabolism data for Chapter 4. I would like to also thank all the people who have helped me get through the last three years. It has not been anything but easy and special thanks go to Sarah (and Ned) Crowley, Cecily Goodwin, George Swann, James Duffy, Matthew Silk, Peter Stillwell, Lewis Campbell, Guill McIvor, David Fisher, Sean Meaden, Lynda Donaldson, Colin Gardiner, Helen Fielding, Rich Inger, Ed Marffy, and Beth Robinson. Without you all, the last three years would have been nowhere near as enjoyable. Also thanks to my parents and family. It must be hard knowing I am struggling at times and living 8 hours away unable to help in any tangible way. You still give me support and I know you are a safety net when things go awry. This thesis is one way of showing them that I am coping with everything life is throwing at me.

Finally, I would like to thank the most important person in my life. Sophia Galpin has been dealt the toughest of hands in the last 3 years and yet she takes everyday as it comes and continues to make it through. Unbelievably, she has strived and pushed herself to support me when work has been stressful and

she understood when research had me working long hours. She is an inspirational young woman and I am extremely lucky to have her in my life. My main wish is that finishing this thesis and starting a new chapter in my academic journey is accompanied by a similar turning point with respect to her health. To start seeing some improvements so that we are able to explore Cornwall and enjoy our life together more in the next three years.

Publications

The following publications have arisen from this thesis and are presented in Chapters 2 and 4:

- Padfield, D., Yvon-Durocher, G., Buckling, A., Jennings, S., Yvon-Durocher, G (2016) Rapid evolution of metabolic traits explains thermal adaptation in phytoplankton. *Ecology Letters*, **19(2)**, 133-142.

- Padfield, D., Lowe, C., Buckling, A., Ffrench-Constant, R., Schaum, E., Jennings, S., Shelley, F., Ólafsson, J.S., Yvon-Durocher, G. (2017) Metabolic compensation constrains the temperature dependence of gross primary production metabolism. *Ecology Letters (accepted).*

Author Contributions

The work in each chapter represents a collaborative effort, but the majority of work is my own. Primary supervision came from Professor Gabriel Yvon-Durocher, who contributed to the experimental design, analysis, interpretation of results and helped write the published manuscripts. Further supervision

came from Professor Angus Buckling who provided insight into experimental design and provided feedback on published manuscripts and from Professor Simon Jennings who also provided feedback on published manuscripts.

Specifically, in *Chapter 2*, Genevieve Yvon-Durocher helped me collect the metabolism data for the 10 generation lineages. In *Chapter 3*, Chris Lowe gave help and guidance on microbiological techniques that allowed me to quantify community composition and Ruth Warfield and Elisa Schaum helped me collect the metabolic rate data. In *Chapter 4*, I was lucky enough to be part of an Iceland Field Course from which the data was collected by students of BIO 244, alongside Gabriel Yvon-Durocher, Chris Lowe and Elisa Schaum.

Table of Contents

List of figures and tables

Abstract

Understanding the impact of warming on organisms, communities and ecosystems is a central problem in ecology. Although species responses to warming are well documented, our ability to scale up to predict community and ecosystem properties is limited. Improving understanding of the mechanisms that link patterns and processes over multiple levels of organisation and across spatial and temporal scales promises to enhance our ability to predict whether the biosphere will exacerbate, or mitigate, climate warming. In this thesis, I combine ideas from metabolic theory with a variety of experimental approaches to further our understanding of how warming will impact photosynthesis and respiration across scales. Firstly, I show how phytoplankton can rapidly evolve increased thermal tolerance by downregulating rates of respiration more than photosynthesis. This increased carbon-use efficiency meant that evolved populations allocated more fixed carbon to growth. I then explore how constraints on individual physiology and community size structure influence phytoplankton community metabolism. Using metabolic theory, I link community primary production and respiration to the size- and temperature-dependence of individual physiology and the distribution of abundance and body size. Finally, I show that selection on photosynthetic traits within and across taxa dampens the effects of temperature on ecosystem-level gross primary production in a set of geothermal streams. Across the thermal-gradient, autotrophs from cold streams had higher photosynthetic rates than autotrophs from warm streams. At the ecosystem-level, the temperature-dependence of gross primary productivity was similar to that of organism-level photosynthesis. However, this was due to covariance between biomass and stream temperature; after accounting for the effects of biomass, gross primary productivity was independent of temperature. Collectively, this work emphasises the importance of ecological, evolutionary and physiological mechanisms that shape how metabolism responds to warming over multiple levels of organisation. Incorporating both the direct and indirect effects of warming on metabolism into predictions of the biosphere to climate futures should be considered a priority.

Chapter 1: Introduction

"The problem is not to choose the correct scale of description, but rather to recognise that change is taking place on many scales at the same time, and that it is the interaction among phenomena at different scales that must occupy our attention"

Simon Levin, 1992

Few articles have been more influential to ecology in the last 25 years than Simon Levin's Robert MacArthur Award Lecture entitled "The problem with pattern and scale in ecology" (Levin 1992). In it, he emphasises the importance of pattern and scale to our ecological thinking, describing how ecological processes acting at one scale can generate patterns and affect other ecological phenomena at entirely different ones. As ecologists (and PhDs are no exception), we have a tendency to focus on a specific set of research questions and study systems which arbitrarily define the spatial, temporal and organisational scales at which we see the world. For example, macroecologists traditionally ask questions about ecological patterns at very large spatial extents and broad temporal scales, whereas community ecologists are concerned with interactions among species and ecosystem functions at finer resolutions and smaller spatial scales. There is no correct scale at which to describe most ecological processes. Ecosystems and natural communities are complex systems in which organisms are changed by the environment that they themselves modify through evolutionary and ecological processes (Levin 1998). They are complex networks where individuals simultaneously affect and are affected by their biotic and abiotic environments.

Twenty-five years on, the problem of linking patterns and mechanisms across scales remains a central problem in ecology, especially given the rise of climate change as a global issue. From 1880 – 2012, average global temperatures increased by 0.85 ºC and are projected to increase by 3 - 5 ºC over the next century (IPCC 2008). Worryingly, this warming appears to be gathering pace, with nine of the ten warmest years on record being from the turn of the century (NOAA 2017). From September 2015 to August 2016, every month broke all-time temperature records (NOAA 2017). Although the evidence of global warming is overwhelming, regional and local changes in temperature are more complex. The rate of climate warming varies on diurnal and seasonal timescales, with greater warming in summer at mid- to high latitudes and the inverse pattern in some tropical regions (Xia *et al.* 2014). Consequently, global mean changes in temperature only explain around 60% of local temperature change for most of the planet (Sutton *et al.* 2015), but it is at these regional scales that changes in temperature will matter most to individual organisms and populations.

Global responses of species to warming include decreases in body size (Gardner *et al.* 2011), changes in physiology and phenology (Walther *et al.* 2002) and range-shifts (Parmesan 2006). However, at local and regional scales, studies often report more idiosyncratic responses to environmental change (Tylianakis *et al.* 2008). Although the average species response to climate warming is well documented, the response of any given species or community is highly variable and based on many biotic and abiotic factors. For example, decreasing body size has been described as the “third universal

response" to warming, but individual studies regularly find contrasting results (Yvon-Durocher *et al.* 2015) As a consequence, attempts to "scale up" species responses to predict community change has proved difficult due to the alteration and uncoupling of interactions between species that can lead to complex and non-linear community responses and feedbacks (Tylianakis *et al.* 2008; Montoya & Raffaelli 2010; Walther 2010). Consequently, our ability to predict community responses to warming is hindered by our ability to predict aggregate species-level responses. Improving the links between organisational levels and spatiotemporal scales will help build bridges across ecological disciplines and further our ability to predict individual, community and ecosystem responses to climate change.

Carbon cycling, climate warming and phytoplankton

For the last 420,000 years, the climate system has operated within relatively constrained limits of atmospheric carbon dioxide (CO_2) concentrations, cycling between around 180 and 280 ppm (parts per million) in 100,000 year cycles (Petit *et al.* 1999). However, since the Industrial Revolution, the world has left this stable range, and the atmospheric CO_2 concentration now sits consistently above 400 ppm. The biosphere plays an essential role in the carbon cycle (Falkowski *et al.* 2000). Photosynthesis harnesses light energy to convert CO_2 into organic carbon, where it is stored as organic matter and eventually returns to the atmosphere through the process of respiration (Falkowski *et al.* 2000). This release through respiration occurs over vastly different timescales, from near instantaneous return by the plant that photosynthesised that carbon molecule, to being released thousands of years later, after being locked away

in the deep ocean. At the ecosystem level, gross primary production (GPP; the photosynthesis of all the autotrophs within a community) is the largest flux in the global carbon cycle (Beer *et al.* 2010), transferring CO_2 from the atmosphere to the biosphere, fuelling food webs and biological production (Field 1998; Falkowski *et al.* 2008). Understanding how the metabolic response of ecosystems will change with climate warming (i.e. whether they will absorb more or less CO_2) is essential for predicting whether the biosphere will accelerate or mitigate warming.

In terrestrial ecosystems, scientists worry that global warming could be accelerated through a positive feedback between temperature and soil respiration that could lead to widespread loss of soil carbon (Cox *et al.* 2000). Soil respiration increases as a direct result of temperature, as individual metabolic rates are strongly temperature dependent (Davidson & Janssens 2006; Bond-Lamberty & Thomson 2010; Carey *et al.* 2016). Indirect effects of temperature on soil respiration such as thermal adaptation, changes in community composition, or reductions in labile carbon could constrain this increase after long-term warming (Bradford *et al.* 2010; Bradford 2013; Romero-Olivares *et al.* 2017). However, a recent meta-analysis looking at long-term temperature responses of soil respiration across biomes found limited evidence of thermal adaptation (Carey *et al.* 2016). Instead, soil respiration increased exponentially up to 25 ºC but decreased at temperatures above this. There is a need to better understand to what extent thermal adaptation and other indirect effects of temperature may be able to dampen the temperature response of metabolism in the long-term.

Phytoplankton, the mainly microscopic autotrophs of the aquatic world, play a key role in the global carbon cycle. Although phytoplankton comprise only ~0.2% of the global autotrophic biomass, they contribute ~50% of global net primary productivity (Falkowski 1994; Field 1998). Approximately 25% of the carbon fixed in the upper ocean sinks into the interior (Falkowski *et al.* 2000). Most of this is oxidised through heterotrophic respiration in the water column. It is thought that <1% of fixed carbon reaches the open-ocean seafloor, where it is locked away for long periods of time in sediments (Falkowski *et al.* 2000; Lee *et al.* 2004). Through this process, phytoplankton play a key role in the "biological pump" that acts to lock away large amounts of carbon for hundreds of years. Phytoplankton responses to warming are similar to the responses documented for other species. For example, mesocosm experiments (Daufresne *et al.* 2009), macroecological (Moran *et al.* 2010) and palaeoecological studies (Finkel *et al.* 2005) have all found that smaller phytoplankton are likely to be favoured in a warmer world. Smaller phytoplankton have lower sinking rates which could impact the "biological pump" and modify the residence time of carbon in the deep ocean by reducing the carbon export from the upper ocean to the interior (Falkowski 1998; Bopp *et al.* 2005).

Climate warming will also alter phytoplankton communities through changes in species composition (Yvon-Durocher *et al.* 2011) which will be driven by differences in the ability of individual species to adapt (Lohbeck *et al.* 2012; Schaum & Collins 2014; Schlüter *et al.* 2014; Geerts *et al.* 2015) or change their

phenotype (Schaum *et al.* 2013; Magozzi & Calosi 2014). The amount of plasticity and evolutionary potential of key traits (such as growth rate, photosynthesis and respiration) within each species, relative to the variability among species (Thomas *et al.* 2012), will go a long way to determining the extent of species turnover in phytoplankton communities in a warmer world. Phytoplankton metabolic rates will also increase with temperature; phytoplankton photosynthesis is thought to be less sensitive to temperature change than respiration (López-Urrutia *et al.* 2006; Regaudie-de-Gioux & Duarte 2012). Consequently, the ability of ocean ecosystems to sequester carbon is predicted to reduce with climate warming. However, the potential for temperature-driven changes of key traits in phytoplankton communities – due to mechanisms such as thermal adaptation - that could influence ecosystem-level fluxes has not been explored (but see Listmann *et al.* 2016). To date, most studies on adaptation to climate change in phytoplankton have concentrated on the response to elevated CO_2 (Collins & Bell 2004; Lohbeck *et al.* 2012; Schaum & Collins 2014) and generally test the capacity for, rather than the mechanism of, adaptation, and little is known on the impacts on functioning of any adaptive response.

The metabolic theory of ecology

One of the most successful attempts at linking patterns and theory across scales in the last twenty years is undoubtedly the metabolic theory of ecology (MTE) (Brown *et al.* 2004). In the late 1800s, Henrieus van't Hoff and Svante Arrhenius described the temperature-dependence of chemical reactions and by the mid 1900s scientists were regularly demonstrating the temperature-

dependence of biological rates. In seemingly unrelated research, comparative analyses described the allometric scaling of individual metabolic rate with differences in average species body size (Kleiber 1932). Kleiber's law shows that smaller individuals have a higher metabolic rate per-unit-biomass than larger individuals. The seminal paper on MTE (coincidentally another Robert MacArthur Award Lecture) brought together these patterns, and principles from physics, chemistry and ecology, to lay the foundations of a theory that explains ecological processes in terms of energy transfer (Brown *et al.* 2004). Metabolism is the biological processing of energy and sets the pace of life, determining the rates of almost all biological activities. Metabolism controls the uptake of energy, its conversion to other substrates in the body or cell, its transfer to other organisms through consumption, and its eventual excretion back into the environment (Brown *et al.* 2004). MTE was founded on a single equation that links an individual's body size and temperature to its metabolic rate, which is edited slightly here from the original in an attempt to keep notation throughout the thesis consistent.

$$b(T) = b(T_c)m^{\alpha}e^{E(\frac{1}{kT_c}-\frac{1}{kT})} \quad (1.1)$$

$b(T)$ is the rate of metabolism of an individual at temperature, T, in Kelvin (K). Instead of the intercept being at 0 K (-273.15 ºC), $b(T_c)$ is the rate at a common temperature, T_c (K). α is a scaling exponent that describes how metabolic rates change with increases in mass, m. E (eV) is the activation energy that describes the temperature-dependence of metabolism and k is Boltzmann's constant (8.62×10^{-5} eV K^{-1}). Early work on MTE put forward the idea that the values of the size-scaling and temperature-dependence of metabolic rate were constant across species (Gillooly *et al.* 2001; Savage & Allen 2004; Banavar *et al.* 2010),

being $E \approx 0.65$ eV for the relationship of metabolic rates with temperature and $\alpha \approx ¾$ for the size-scaling of metabolism. However, the idea of, and evidence for, such "universal" values received a mixed response, generating considerable scepticism and controversy. Some ecologists argued for alternative universal values ($\alpha \approx \frac{2}{3}$) and others that "universal temperature-dependence" does not allow for taxon-specific deviations or the effects of thermal adaptation or acclimation at longer timescales (Clarke 2004; White *et al.* 2010; Huey & Kingsolver 2011).

More recent work has shown that these values might represent the average, but that there is considerable variation in these parameter values. For example, although an average size scaling exponent of $\approx ¾$ is found across animal species, this is dependent on the taxonomic level at which it is measured, with 50% of taxonomic orders falling outside the range of 0.68 - 0.82 (Isaac & Carbone 2010). In addition, when extended over all the major domains of life, size-scaling has been found to be isometric $(\alpha \sim 1)$ in algae and unicellular protists (DeLong *et al.* 2010; Huete-ortega *et al.* 2017) and super-linear in cyanobacteria and other prokaryotes $(\alpha > 1)$ (DeLong *et al.* 2010; García *et al.* 2015). Along similar lines, the temperature-dependence of metabolism may have an average value of $E \approx 0.65$ eV, but this value has been found to vary across different biological rates (i.e. respiration, velocity, consumption and feeding), between taxa, and between terrestrial and aquatic environments (Dell *et al.* 2011; Pawar *et al.* 2012; Rall *et al.* 2012). Regardless of the constancy of the values of E and α, MTE has provided a theory built up from first principles that gives a set of *a priori,* quantitative, testable predictions (Marquet *et al.*

2015). After all, the role of MTE, and theory generally, is not to capture all the complexity of the natural world, but rather to retain only the essential information. Seen in this light, MTE regularly succeeds in its efforts to capture the key constraints on ecological processes to understand empirical patterns.

With an explicit (some would argue mechanistic) term to explain the effect of temperature on metabolic rate, MTE has proved particularly useful in studying the effects of warming on individuals, populations and ecosystems. At the population-level, the temperature-dependence of growth and reproduction rates can predict potential effects of temperature on population abundance and MTE can predict how warming affects population-level properties (Allen *et al.* 2002; Savage *et al.* 2004). Across-species, mismatches in temperature responses between herbivores and plants, and predator and prey have been used to show how dynamics and species interactions will change with warming (Kordas *et al.* 2011; O'Connor *et al.* 2011; Rall *et al.* 2012; Dell *et al.* 2013). These responses have been scaled up to explain the effect of warming on food-web dynamics (Connor *et al.* 2009; Yvon-Durocher *et al.* 2015; Moorthi *et al.* 2016) and changes in other community properties such as size structure (Yvon-Durocher *et al.* 2011). Individual and community-level responses to warming can be combined to predict ecosystem-level properties. Metabolic scaling theory has been used to combine the effects of temperature on individual physiology and community structure to predict and explain variation in ecosystem functioning (Enquist *et al.* 2003; Yvon-Durocher *et al.* 2011) and global patterns of biodiversity (Allen *et al.* 2002). Throughout this introduction,

and the rest of the thesis, I will expand on some of the applications of metabolic theory summarised here.

Most of the studies using and extending MTE have ignored, or been unable to quantify, indirect effects of temperature on metabolic rates. For example, thermal adaptation (i.e. the change in physiological phenotype due to changes in genotype) and thermal acclimation (i.e. the change in physiological phenotype from a single genotype (West-Eberhard 2003)) could alter the temperature-dependence of metabolism at longer timescales. The ability of Eq. 1.1 to account for the effect of thermal adaptation and acclimation has long been a point of controversy. Previous studies using MTE have measured metabolic rate for many species at each species' average temperature. This shows the relationship between average metabolic rate and average temperature across species (Gillooly *et al.* 2001). These across-species relationships reflect the long-term temperature response of metabolic rate and likely incorporate any effects of thermal adaptation or acclimation. The effects of thermal adaptation and acclimation can be accounted for in MTE through changes in the metabolic normalisation constant, $b(T_c)$. This effect is thought to be small as the temperature-dependence of across-species relationships are similar to the direct effect of temperature on enzyme kinetics (Gillooly *et al.* 2001; Gillooly 2006). This had led many to the conclusion that kinetic constraints on enzymes control metabolic rates from individuals to ecosystems. Despite this line of thinking, multiple studies, from individuals to ecosystems, have documented changing physiological responses after long-term exposure to different temperatures (Bradford *et al.* 2008; Scafaro *et al.* 2016). In the short-

term, metabolism is likely to be determined by biochemical constraints, but in the long-term other indirect effects of temperature on metabolism could become increasingly important. But at present, there is little research using a metabolic theory framework that considers whether the temperature-dependence of metabolism changes through time.

The rest of this introduction describes the impact of some of these indirect effects, with an emphasis on how thermal adaptation or acclimation could affect the temperature-dependence of metabolism across organisational and temporal scales. The within-species response of metabolic rate and temperature describes how the metabolism of a single species responds to short-term temperature change, whereas the across-species temperature response compares metabolic rates among species that differ in average temperature. Thus, within- and across-species responses reflect short- and long-term effects of temperature on species metabolic rate respectively. The ideas presented in the remainder of the introduction can be applied to any level of organisation (e.g. genotypes, populations, communities or ecosystems), where the mechanisms through which temperature influences metabolic rates may differ through time or space.

Thermal adaptation and MTE

The original formulation of MTE includes an exponential temperature response, but rates do not increase forever, and applications of the traditional Boltzmann-Arrhenius function are sensitive to the range of temperatures measured (Pawar *et al.* 2016). Therefore, there is a need to improve the resolution of our data

collection to improve model fitting and further our understanding of the thermal responses of biological traits. Thankfully, physiological ecology has measured the temperature response of organismal rates over a wide range of temperatures for decades. During acute exposure to a range of temperatures, metabolic rates (e.g. respiration and photosynthesis) and other biological rates such as locomotion (Gilchrist 2017) and growth (Eppley 1972) typically increase exponentially up to an optimum before falling off steeply (Figure 1.1). These biological rates are strongly linked to an organism's fitness and generally have a reversible response to acute temperature change (Angilletta 2009). As in MTE, increases in metabolic rates up to the optimum are assumed to be driven by laws of thermodynamics and enzyme kinetics. In contrast, the steep declines after the optimum may be attributable to factors such as protein denaturation and stability (DeLong *et al.* 2017), disruption of cellular membrane structures (Wu 2004) and – in aquatic environments – the nonlinear decrease in the solubility of carbon dioxide, needed for photosynthesis, and oxygen for respiration (Portner & Knust 2007; Schulte *et al.* 2011). These thermal response curves are sensitive to changes in average temperature and thermal variability (Gilchrist 2017), and have been used to show patterns of thermal adaptation within (McLean *et al.* 2005; Knies *et al.* 2009) and across species (Thomas *et al.* 2012). Such response curves have been used to predict competitive interactions between phenotypes (Schaum *et al.* 2017) and to predict the consequences of warming on performance and fitness (Deutsch *et al.* 2008; Vasseur *et al.* 2014), and hence shifts in community composition (Thomas *et al.* 2012).

Many different model formulations have been used to fit thermal response curves (Angilletta 2006; DeLong *et al.* 2017). Throughout this thesis I use a modified version of the Sharpe-Schoolfield curve (Schoolfield *et al.* 1981), which extends the temperature-dependence of the original MTE equation to incorporate a decline in metabolic rates beyond the optimum (Figure 1.1).

$$b(T) = \frac{b(T_c)e^{E(\frac{1}{kT_c}-\frac{1}{kT})}}{1+e^{E_h(\frac{1}{kT_h}-\frac{1}{kT})}} \quad (1.2)$$

This extension of the traditional Boltzmann equation has two extra parameters: E_h (eV) characterises the high temperature-induced inactivation of enzyme kinetics and T_h (K) is the temperature at which half the rate is inactivated due to high temperatures. In this expression, $b(T_c)$ is the rate of metabolism normalised to a reference temperature (e.g. 10 ºC), where no high temperature inactivation occurs. Equation 1.2 yields an optimum temperature, T_{opt}, (K):

$$T_{opt} = \frac{E_h T_h}{E_h + kT_h ln\left(\frac{E_h}{E}-1\right)} \quad (1.3)$$

from which the maximal rate, $b(T_{opt})$, can be calculated. As the Sharpe-Schoolfield model has four parameters, it requires high-resolution data to adequately fit the model, but it is capable of fitting a wide variety of different shaped curves (e.g. it can fit both symmetrical and negatively skewed responses). In addition, other parameters that are known to underlie an organism's susceptibility to climate change (Stillman 2003; Sunday *et al.* 2011, 2012), such as the critical thermal maxima, CT_{max}, and minima, CT_{min}, can be calculated empirically as the temperatures at which rates go below a proportion of the maximal rate (Figure 1.1). These temperatures determine a species' thermal tolerance – the range of temperatures at which an organism can grow – which is expected to be critical for determining species' responses to global

warming (Pörtner; & Farrell 2008; Kearney *et al.* 2009). Approaches using thermal response curves to predict competitive interactions and future distributions typically assume that there is no rapid evolution or local adaptation of the thermal response curves (Sinclair *et al.* 2016), but the importance of evolution in altering responses to climate change is widely acknowledged (Munday *et al.* 2013). Thermal history can influence the shape and position of the thermal response due to local thermal adaptation. For example, optimum temperatures across different phytoplankton and terrestrial autotroph species correlate with their average environmental temperature (Thomas *et al.* 2012). What is not known is the rate at which these evolutionary responses are able to occur with climate change, but rapid evolution has been shown in *Daphnia magna*, that change their thermal limits in response to increased water temperature (Geerts *et al.* 2015). Throughout the thesis, I treat the parameters underlying the shape of the thermal response curve - E, $b(T_c)$, E_h, T_{opt}, $b(T_{opt})$, CT_{max}, CT_{min} (Figure 1.1) - as metabolic traits on which I expect temperature-dependent selection to act on both within and among species.

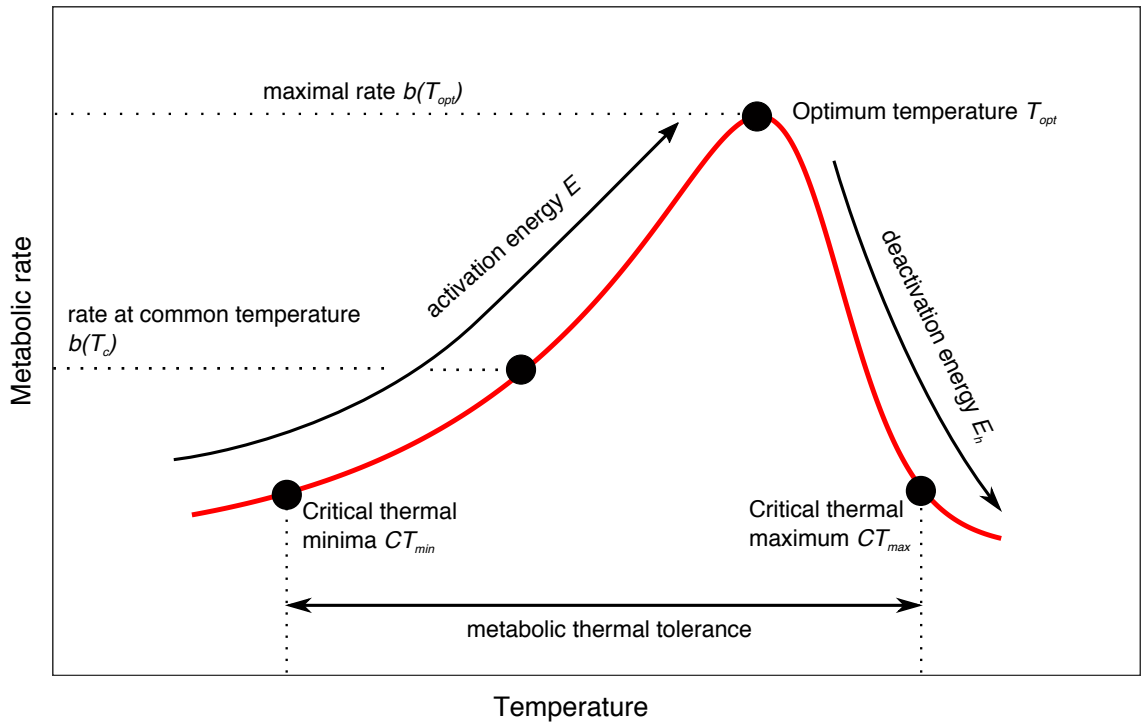

Figure 1.1. A typical thermal response curve.
Rates rise up to an optimum before rapidly declining. The modified Sharpe-Schoolfield model is used to characterise the shape of this curve, from which extra parameters of interest can be empirically estimated. These parameters are treated as "metabolic traits" which are expected to be under temperature-driven selection.

At the intracellular level, enzymes perform better at higher temperatures. Scaling up this logic, the hotter-is-better hypothesis predicts that organisms adapted to lower temperatures (with a lower T_{opt}) have lower maximal rates, $b(T_{opt})$, than organisms at higher temperatures, as adaptation is unable to overcome thermodynamic constraints (Knies *et al.* 2009). This idea has received broad support when looking at estimates of maximal rate across species differing in optimum temperature (Frazier *et al.* 2006; Angilletta 2009; Angilletta *et al.* 2010). Theory suggests that the acute thermal response curve of each species sits on an across-species curve that represents the relationship between maximal rate and optimum temperature (Figure 1.2). Under a special

case of the hotter-is-better hypothesis, the only way to adapt to a new temperature would be for a species to shift its thermal optima, T_{opt}, along this across-species curve. This would result in a corresponding shift in the maximal rate, and a single activation energy governs the short-term temperature response within species and the long-term temperature response across-species (Figure 1.2a). Studies have compared short-term thermal response curves within and across-species of phytoplankton (Eppley 1972) and across-genotypes within a species of bacteria (Knies *et al.* 2009), but more studies are needed to adequately evaluate this hypothesis. These ideas are similar to what MTE has previously found (i.e. the similarity of the across-species temperature-dependence of metabolism to the temperature-dependence at the cellular level), but studies using MTE usually compare rates at average, not maximal, temperatures. As the distance between optimum and environmental temperature narrows as temperatures increase (Thomas *et al.* 2012), these two patterns should not be directly compared. But most species do not operate at their optimum temperature, so it may be more appropriate to analyse the across-species curve at average environmental temperature to understand the impact of metabolic trait differences on performance (Figure 1.2).

Alternatively, long-term warming could result in thermal adaptation and acclimation that may compensate for the effects of low temperature on metabolism (Figure 1.2b). Metabolic-cold adaptation describes the ecological phenomenon where cold-adapted organisms have higher rates of metabolism at a common temperature than warm-adapted organisms (Addo-Bediako *et al.* 2002); $b(T_c)$ decreases with increasing environmental temperature. Previous

work on aquatic and terrestrial autotrophs has shown that they regularly adapt/acclimate to long-term temperature change through alterations in the respiratory and photosynthetic normalisation constants (Atkin *et al.* 2015; Reich *et al.* 2016; Scafaro *et al.* 2016). If complete adaptation occurs, the decrease in the normalisation would be the exact inverse of the activation energy that governs the rise in metabolic rate with acute temperature change. The response of a species to short-term warming is still controlled by biochemical constraints, but decreases in $b(T_c)$ across species completely compensate for the direct effect of temperature on metabolism, such that rates are independent of long-term average temperature (E = 0 eV). However, the metabolic normalisation constant may not be able to completely compensate for the direct effect of temperature on metabolism. In these instances, the across-species temperature-dependence would be greater than zero, but less sensitive to temperature than the average within-species response (Figure 1.2c).

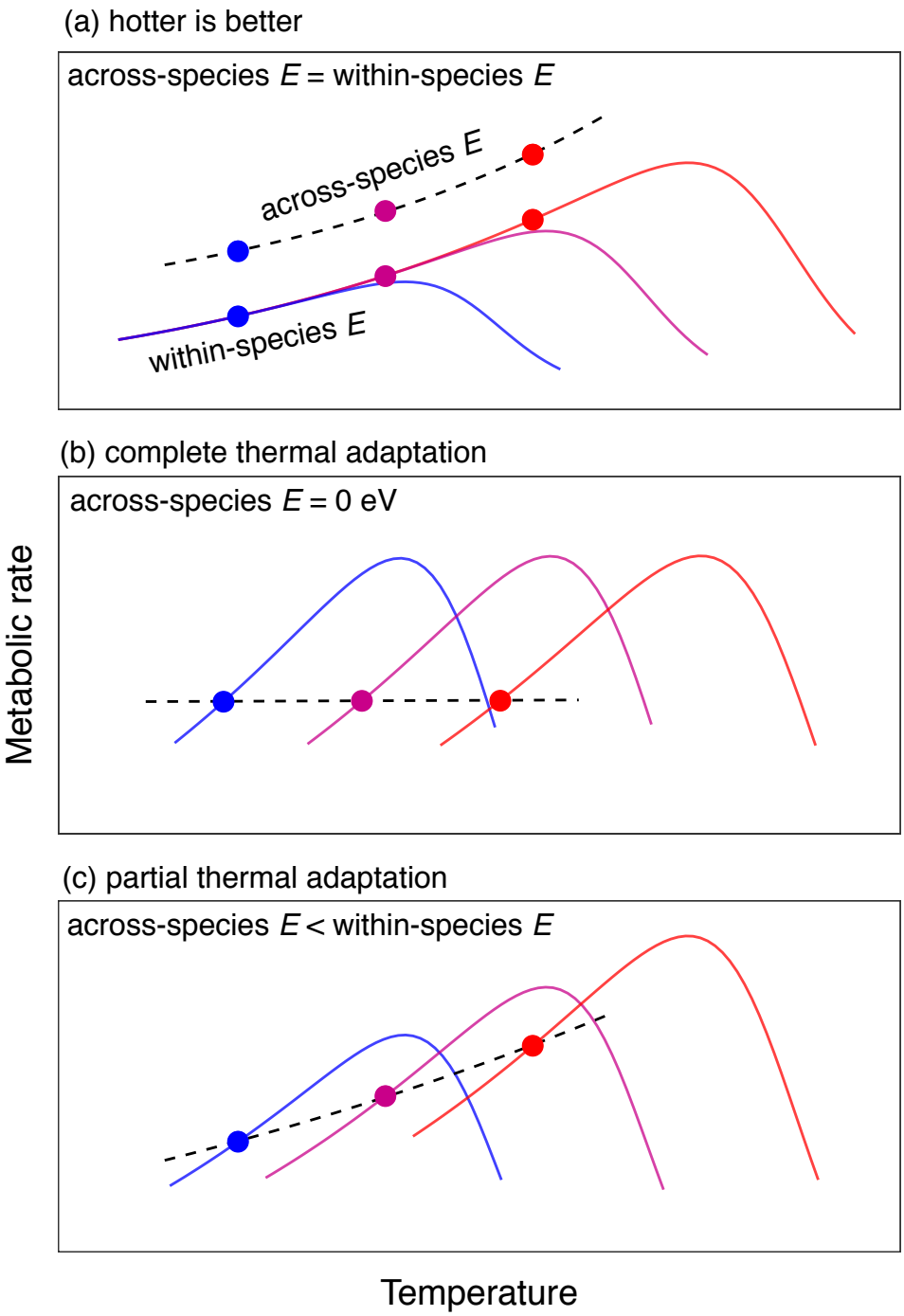

Figure 1.2. Possible models of thermal adaptation.
Under the hotter-is-better hypothesis (a), biochemical constraints alone control metabolic rates. As average and optimum temperatures increase, a corresponding increase in metabolic rate occurs. However complete thermal adaptation (b) may result in long-term effects of temperature on metabolism that override the short-term effect of temperature on metabolism such that rates are invariant with temperature. In (c), partial thermal adaptation results in a partial decrease in the temperature-dependence across species but rates still increase with increases in rates with average temperature.

Plant metabolism: a tale of two fluxes

Traditional MTE assumes that selection acts to maximise metabolic rate within a given individual (Brown *et al.* 2004). This seems relatively straightforward in heterotrophs where there is only a single metabolic process, respiration, that determines rates of energy uptake, transformation to other compounds, and ultimately, allocation to growth. Population and ontogenetic growth rates have been linked to body size and temperature (West *et al.* 2001; Savage *et al.* 2004) and the temperature-dependence of growth in heterotrophs is similar to that of metabolic rate (i.e. respiration) (Savage *et al.* 2004). This suggests that metabolism and growth are closely linked.

In phytoplankton and terrestrial autotrophs, the relationship between fitness and metabolic rate is further complicated by the presence of two metabolic fluxes: photosynthesis and respiration (Raven & Geider 1988). As phytoplankton possess simple lifecycles such that growth (a main component of fitness) is simply proportional to the balance between photosynthesis (the gross fixation of inorganic carbon into organic compounds) and respiration (the total remineralisation of the organic carbon back into the environment). However, previous work has suggested that rates of respiration are often more sensitive to temperature than photosynthesis. This is thought to be due to fundamental differences in their biochemical pathways and rate-limiting enzymes (Allen *et al.* 2005; López-Urrutia *et al.* 2006; Anderson-Teixeira *et al.* 2011; Yvon-Durocher *et al.* 2012). Under light-saturating conditions, the temperature-dependence of photosynthesis is thought to be mainly determined by the net difference between carboxylation (CO_2 fixation) and photorespiration

(O_2 fixation at the site of photosynthesis) at the active site of the Rubisco enzyme (Bernacchi *et al.* 2001). As photorespiration tends to have a stronger response to temperature than carboxylation, light saturated photosynthesis has a shallower activation energy than respiration (Coleman & Colman 1980; Bernacchi *et al.* 2001; Allen *et al.* 2005), whose temperature-dependence is generally thought to be controlled mainly by the response of ATP synthesis.

The model approximating a weaker temperature-dependence of photosynthesis, relative to respiration, was based on the metabolic pathways of C_3 plants, which have no general mechanism to reduce photorespiration (Allen *et al.* 2005). Carbon concentrating mechanisms (CCMs) allow autotrophs to elevate the internal CO_2 concentration relative to O_2. Consequently, the temperature-dependence of photosynthesis might differ across plant types if there are systematic differences in the prevalence of CCMs that transport carbon dioxide into the cell. In terrestrial autotrophs, there are two broad types of CCM: C_4 and CAM (Crassulacean Acid Metabolism). In C_4 plants, the initial fixation of carbon dioxide and subsequent carboxylation by Rubisco are separated in different parts of the cell, whereas in CAM plants these processes occur at different times, with CO_2 fixation occurring in the night and Rubisco carboxylation in the day. A number of CCM variants have been found in different groups of phytoplankton, which are essential to overcome the difficulties of attaining carbon from an aquatic environment (Giordano *et al.* 2005; Raven *et al.* 2011). If these CCMs result in an increase in the concentration of CO_2 then the activation energy of photosynthesis may be higher in phytoplankton compared to the predictions derived based on C_3

photosynthesis (Galmes *et al.* 2015). Further work is needed to quantify the temperature-dependence of photosynthesis and respiration in phytoplankton, and to investigate the extent to which these two fundamental fluxes have different responses to temperature.

If photosynthesis has a lower activation energy than respiration, at temperatures below the optimum, increases in temperature will cause respiration rates to rise relatively more than those of photosynthesis. Consequently, the ratio of respiration to gross photosynthesis (*R/P* ratio) increases as a function of temperature, which means the fraction of carbon available for growth, termed carbon-use efficiency (CUE = 1 – *R/P*) declines as temperatures rise in the short-term. This reduction in energetic efficiency is likely to impose a major selection pressure on phytoplankton physiology when it goes over a certain threshold. However, *R/P* ratios are commonly found to be stable over a range of growth temperatures in terrestrial autotrophs (Gifford 1995; Lewis H. Ziska 1998; Dewar *et al.* 1999; Atkin *et al.* 2007). This suggests that land plants can alter their rates of photosynthesis and/or respiration to offset and counteract the differential temperature sensitivities of respiration and photosynthesis. Downregulation of the respiratory normalisation constant in response to increasing temperature is widespread in plants (Atkin & Tjoelker 2003; Loveys *et al.* 2003; Atkin *et al.* 2015). In plants, these are usually acclimatory adjustments as terrestrial autotrophs are long-living and therefore experience lots of variation in their abiotic environment within a single generation. The same trees can acclimate to seasonal changes in temperature

(Atkin *et al.* 2000) and such responses are likely key for maintaining fitness across a broad range of conditions.

In contrast, phytoplankton have much shorter generation times (hours to days), which limits the exposure of individual phytoplankton to temperature variation. Instead, the opportunity for evolutionary responses to changes in the environment, either through sorting on pre-existing genetic variation within populations, or *de novo* mutation (Lohbeck *et al.* 2012), is much greater in absolute time. Previous work on the temperature response of phytoplankton physiology and metabolism has concentrated mostly on acclimation responses (Vona *et al.* 2004; Staehr & Birkeland 2006). These studies generally measured phytoplankton responses to different temperatures after just 1-10 generations of growth and measure the ability of phytoplankton to rapidly adjust their physiology, metabolism and growth. However, as climate change will occur slowly, over many (hundreds) of generations in phytoplankton, adaptive responses to temperature could be critically important. As of yet, no work has explored the impact of long-term warming (i.e. on evolutionary timescales) on thermal response curves of phytoplankton metabolism and its link to phytoplankton fitness. This is something I will consider in *Chapter 2.*

Using MTE to link individuals to ecosystems

Metabolic theory makes the simple assumption that rates of flux at higher levels of organisation are simply the sum of the metabolic rates of the lower levels of organisation within it. This has allowed body size and temperature constraints on individual physiology to be scaled up to predict community and ecosystem

flux (Enquist *et al.* 2003, 2016; Yvon-Durocher & Allen 2012) and has successfully predicted ecosystem properties (López-Urrutia *et al.* 2006; Enquist *et al.* 2007; Schramski *et al.* 2015). The effects of temperature on rates of ecosystem metabolism are typically assessed in two different types of study. In the first, the temperature-dependence is derived by analysing seasonal variation in metabolism and temperature (Raich & Schlesinger 1992; Lloyd & Taylor 1994; Enquist *et al.* 2003; Yvon-Durocher *et al.* 2010, 2012). Such "within-ecosystem" analyses aim to capture the short-term effects of temperature on ecosystem flux and are somewhat analogous to the acute temperature response measured at the species and population levels. However, even over seasonal temperature variation experienced over several months, phytoplankton will go through many generations and thermal adaptation and changes in metabolic traits due to species turnover may occur in this time.

These within-ecosystem studies may be less informative for understanding how gradual changes in temperature over longer timescales (as to be expected with climate warming) will influence ecosystem properties. To study this, metabolic flux and average temperature are analysed across ecosystems that vary in mean annual temperature along latitudinal or altitudinal gradients (Allen *et al.* 2005; Michaletz *et al.* 2014; Demars *et al.* 2016). Here, 'across-ecosystem' analyses substitute space for time in an attempt to understand how warming will impact ecosystem metabolism. Both within- and across-ecosystem studies have identified temperature sensitivities remarkably similar to those at the species level (Yvon-Durocher *et al.* 2012; Demars *et al.* 2016). Such findings

have inevitably led to the conclusion that biochemical constraints on enzymatic rates control metabolism across different spatial, temporal and organisational scales (Demars *et al.* 2016). Unfortunately, such simplicity is rarely observed in the natural world. This conclusion is likely an example of the many-to-one principle, where the same pattern emerges at different scales from different causal mechanisms.

The direct effect of temperature on enzymes may dictate ecosystem rates in the short term, but even over seasonal temperature changes (even more so over longer timescales) indirect effects of temperature are likely to influence the ecosystem response to warming. For example, if selection acts to decrease the metabolic normalisation constant, thermal adaptation and acclimation within and among species (Enquist *et al.* 2007) that alter species composition (Romero-Olivares *et al.* 2017) and community structure (Yvon-Durocher *et al.* 2011) may dampen the observed temperature response of ecosystem metabolism. In addition, changes in nutrient availability (Behrenfeld *et al.* 2006) that drives variation in standing biomass (Welter *et al.* 2015; Williamson *et al.* 2016) through time (seasonal variation within ecosystems) and space (across ecosystems with different nutrient concentrations) will also alter the observed response of ecosystem-level metabolism to warming. However, whether changes in nutrient availability enhance or constrain the observed ecosystem temperature response will be dependent on whether nutrients positively or negatively covary with warming. Consequently, although the same temperature-dependence may be observed across different timescales and organisational levels, the mechanisms that give rise to the observed

temperature-dependence are likely to be different. I build on these ideas throughout this thesis, and I link organism to ecosystem metabolism in *Chapters 3* and *4*.

Experimental systems

The experimental component of this thesis reflects its scaling theoretical framework in that it spans many temporal, spatial and organisational scales. I use laboratory microcosms to examine how phytoplankton adapt to stressful temperatures. Microcosms are often criticised for the limited applicability to the natural world, but they allow me to implement temperature regimes and measure responses that are yet to occur in nature. Additionally, I can investigate what the temperature-dependence of photosynthesis and respiration is at the organisational level and timescales closest to the proposed mechanisms given by MTE (i.e. the short-term effects of temperature on enzyme kinetics of individuals). Testing the assumptions of MTE at the appropriate scale is essential for improving and developing the theory and its applications (Price *et al.* 2012).

However, I need to scale up my experimental microcosms to understand how the effects of thermal adaptation of individual metabolism might impact ecosystem responses. Thus, I take advantage of a long-term mesocosm experiment where a set of experimental ponds have undergone 4 ºC warming for >10 years. These mesocosms provide an invaluable resource to investigate how community size structure influences community metabolism and test for the relative importance of long-term *vs* short-term warming in determining

community structure and functioning. Mesocosms represent reality much better than experimental microcosms, but both approaches represent only relatively short timescales (relative to the extent of climate warming) and the response of populations and communities to temperature change can vary through time in microcosm (Schlüter *et al.* 2016) and mesocosm experiments (Yvon-Durocher *et al.* 2017).

To combat this, scientists use latitudinal or altitudinal gradients, where a natural thermal cline exists, to study the response of species and ecosystems to long-term temperature differences (Enquist *et al.* 2003; De Frenne *et al.* 2013; Michaletz *et al.* 2014; Zhou *et al.* 2016). These approaches are often confounded by co-variables such as differences in nutrient and light availability (Fukami & Wardle 2005; Bradshaw & Holzapfel 2010) that make it hard to isolate the sole effect of temperature. Natural geothermal stream systems allow me to circumvent this issue as streams and their associated biota have been exposed to differential warming for multiple generations, thereby reflecting long-term evolutionary and ecological responses to warming (O'Gorman *et al.* 2012, 2014). This gives a great opportunity to study both the short- and long-term responses of warming in a completely natural setting, at population and ecosystem scales (O'Gorman *et al.* 2014).

Throughout the rest of this thesis, I develop the ideas and theory outlined here and test quantitative predictions with an appropriate experimental approach to investigate the scaling of metabolism across different spatial, temporal and organisational levels. Specifically, my objectives are to:

Chapter 2: I investigated whether a model phytoplankton species, *Chlorella vulgaris*, can adapt to stressful warming. I expected the metabolic traits underlying the thermal response curves of photosynthesis and respiration to adapt to maximise the carbon-use efficiency at stressful growth temperatures. **After ~ 100 generations *Chlorella vulgaris* adapted to increase their growth rates by decreasing rates of respiration more than photosynthesis and increasing their CUE.** This work highlights the ability of phytoplankton to rapidly adapt to warming and identifies a potential ubiquitous mechanism of metabolic adaptation.

Chapter 3: In this chapter I aimed to understand how community-flux is linked to community structure and individual physiology. I use measurements of phytoplankton community metabolism to test predictions from a metabolic scaling framework. **I find that rates of community-level metabolism are well predicted from individual physiology and community structure and abundance,** suggesting that body size and temperature are the primary drivers of metabolism at multiple levels of organisation.

Chapter 4: Using the theoretical framework outlined in the introduction, I examined how the indirect effects of temperature on ecosystem-level metabolism can dampen the effects of temperature on GPP across catchment of geothermally heated streams. **Rates of population-level photosynthesis decreased at higher stream temperatures such that after accounting for differences in biomass, rates of biomass-specific ecosystem-level GPP were invariant across a 20 ºC gradient in temperature.** The combined

effects of thermal adaptation and temperature-dependent changes in biomass can completely override the direct effects of temperature on metabolic rates.

Chapter 2: Rapid evolution of metabolic traits explains thermal adaptation in phytoplankton.

ABSTRACT

Understanding the mechanisms that determine how phytoplankton adapt to warming will substantially improve the realism of models describing ecological and biogeochemical effects of climate change. Here, I quantify the evolution of elevated thermal tolerance in the phytoplankton, *Chlorella vulgaris*. Initially, population growth was limited at higher temperatures because respiration was more sensitive to temperature than photosynthesis meaning less carbon was available for growth. Tolerance to high temperature evolved after ≈100 generations via greater down-regulation of respiration relative to photosynthesis. By down-regulating respiration, phytoplankton overcame the metabolic constraint imposed by the greater temperature sensitivity of respiration and more efficiently allocated fixed carbon to growth. Rapid evolution of carbon-use efficiency provides a potentially general mechanism for thermal adaptation in phytoplankton and implies that evolutionary responses in phytoplankton will modify biogeochemical cycles and hence food web structure and function under warming. Models of climate futures that ignore adaptation would usefully be revisited.

INTRODUCTION

Phytoplankton play a key role in biogeochemical cycles (Field 1998) and fuel aquatic food webs (Falkowski *et al.* 2008). Novel phytoplankton communities, and the functions they mediate, will emerge as the climate changes through a combination of turnover in species composition (Yvon-Durocher *et al.* 2011), and shifts in the distribution of traits (e.g. body size, metabolic rates, stoichiometry) via phenotypic plasticity (Schaum *et al.* 2013; Magozzi & Calosi 2014) and rapid evolution (Lohbeck *et al.* 2012; Schaum & Collins 2014; Schlüter *et al.* 2014; Geerts *et al.* 2015). The amount of plasticity and evolutionary potential in key traits, relative to their interspecific variability (Thomas *et al.* 2012), will largely determine the extent to which phytoplankton communities are buffered from species turnover in a warmer world (Pörtner & Farrell 2008; Angilletta 2009; Montoya & Raffaelli 2010).

Because of their rapid generation times and high population densities, phytoplankton have substantial capacity for rapid evolutionary responses to climate change (Collins 2011). There is growing evidence for evolutionary responses of phytoplankton *in vitro* to global change drivers, such as elevated CO_2 (Collins & Bell 2004; Lohbeck *et al.* 2012; Schaum & Collins 2014; Schlüter *et al.* 2014), but only a single study has explored responses to warming (Schlüter *et al.* 2014). Studies applying experimental evolution to phytoplankton have focused mainly on identifying the capacity for adaptation and have not investigated the underlying mechanisms that facilitate evolutionary responses. Understanding the capacity for, and mechanisms through which phytoplankton might evolve to cope with novel environments is central to predicting whether

aquatic ecosystems will accelerate or mitigate global warming through changes in their capacity to sequester carbon. Such quantitative and mechanistic understanding will support the development of more realistic models of the ecological and biogeochemical effects of climate futures.

Thermal tolerance – the range of temperatures at which an organism can grow – is expected to be critical for determining species' responses to global warming (Pörtner & Farrell 2008; Kearney *et al.* 2009). Evolution has driven substantial variation in thermal tolerance among species of phytoplankton adapted to different environments (Thomas *et al.* 2012). Experiments on bacteria (Bennett & Lenski 2007), evolving and coevolving viruses (Zhang & Buckling 2011) and zooplankton (Geerts *et al.* 2015) have demonstrated capacity for rapid evolution of elevated thermal tolerance. However, the extent, tempo and mechanisms through which elevated thermal tolerance can evolve in phytoplankton are currently unclear.

Metabolism sets the pace of life (Brown *et al.* 2004) and is a key process that can be used to gain a more mechanistic understanding of evolutionary responses to changes in temperature. Metabolism dictates a host of life-history traits and attributes that determine fitness, including population growth rate (Savage *et al.* 2004), abundance, mortality and interspecific interactions (Dell *et al.* 2011). During acute exposure to a range of temperatures, metabolic rates, $b(T)$, typically increase exponentially up to an optimum, followed by a rapid decline (Figure 2.1a). These unimodal thermal response curves can be

described using a modification of the Sharpe-Schoolfield equation for high temperature inactivation (Schoolfield *et al.* 1981):

$$\ln\big(b(T)\big) = E\left(\frac{1}{kT_c} - \frac{1}{kT}\right) + \ln\big(b(T_c)\big) - \ln\left(1 + e^{E_h\left(\frac{1}{kT_h} - \frac{1}{kT}\right)}\right) \quad (2.1)$$

where $b(T)$, is the metabolic rate per unit biomass (μmol O_2 μg C^{-1} h^{-1}), k is Boltzmann's constant (8.62×10^{-5} eV K^{-1}), E is an activation energy (in eV) for the metabolic process, T is temperature in Kelvin (K), E_h characterises temperature-induced inactivation of enzyme kinetics above T_h and $b(T_c)$ is the rate of metabolism normalised to a reference temperature, T_c = 25 ºC; where no low or high temperature inactivation is experienced (from here on I cal $b(T_c)$I the 'specific rate of metabolism'). Because, $b(T_c)$ is both mass and temperature normalised it enables comparison of metabolic rates across populations which may vary in total biomass and/or ambient temperature. Equation 2.1 yields a maximum metabolic rate at an optimum temperature:

$$T_{opt} = \frac{E_h T_h}{E_h + kT_h \ln\left(\frac{E_h}{E} - 1\right)} \quad (2.2)$$

the parameters $b(T_c)$, E, E_h, and T_{opt}, represent traits that together characterise the metabolic thermal response (see Figure 2.1a).

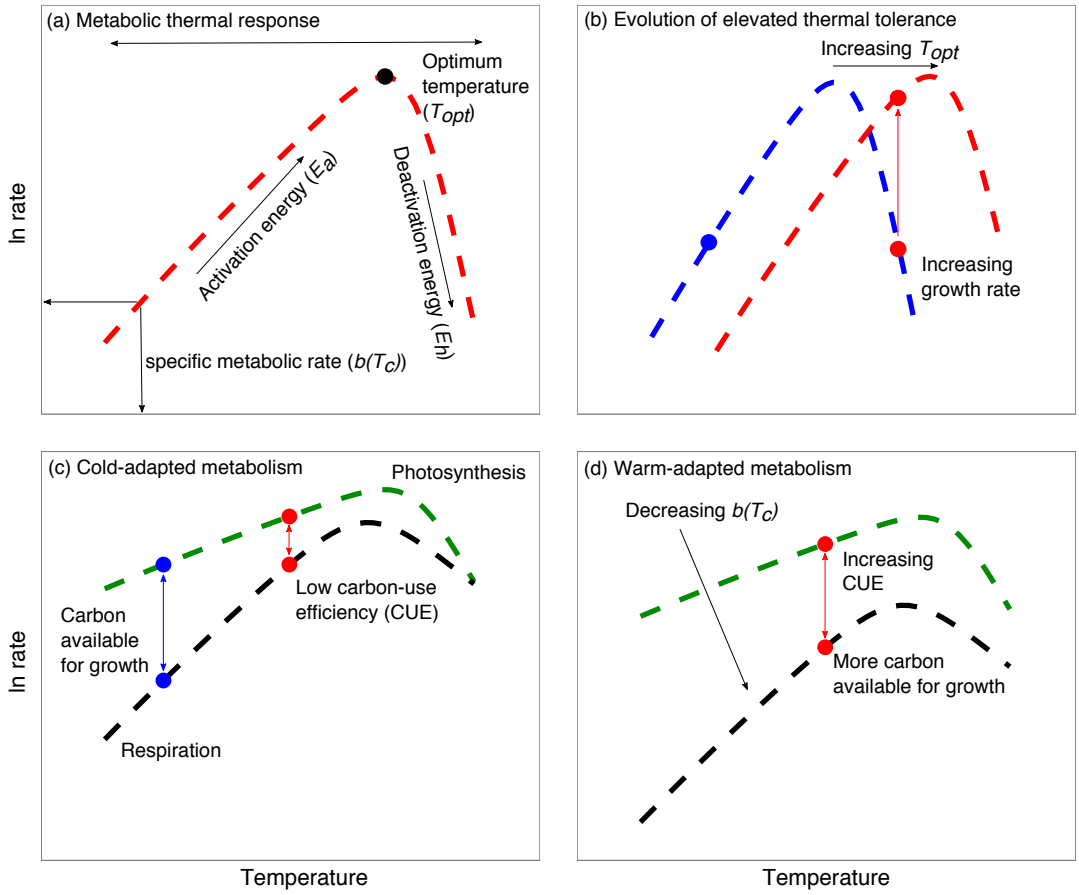

Figure 2.1. Effects of temperature on phytoplankton metabolism.
(a) Metabolic rates, $b(T)$, increase as an exponential function of temperature to an "optimum" temperature (T_{opt}), then decline rapidly. (b) Growth responses for a cold-adapted (blue, point & line) and warm-adapted (red, point & line) phytoplankton. Evolution of elevated thermal tolerance entails increases in T_{opt} and growth rates at elevated temperatures. (c) Thermal responses for photosynthesis (green, P) and respiration (black, R) for a cold-adapted phytoplankton. The relative difference between P and R along the temperature gradient represents the carbon use efficiency (CUE = 1-R/P). Because R is more sensitive to temperature than P, CUE declines (blue to red point) with increasing temperature, limiting growth at high temperatures. As phytoplankton adapt to warmer temperature (d), selection should drive down specific rates of respiration, $R(T_c)$, more than those of photosynthesis, $P(T_c)$, increasing CUE and ensuring they are not limiting for growth.

In phytoplankton, growth rate (a component of fitness) is dependent on two metabolic fluxes: photosynthesis and respiration (Raven & Geider 1988). I hypothesise that selection will operate on the metabolic traits of these two

fluxes as species adapt to new thermal environments. Past work suggests that respiration (activation energy for respiration: E_R ~ 0.65eV) is often more sensitive to temperature than photosynthesis (E_P ~ 0.32eV) (Allen *et al.* 2005; López-Urrutia *et al.* 2006; Anderson-Teixeira *et al.* 2011; Yvon-Durocher *et al.* 2012). As temperatures rise, rates of respiration rise relatively more than those of photosynthesis. Consequently, the ratio of respiration (*R*; i.e., the gross remineralisation of organic carbon (C)) to gross photosynthesis (*P*; i.e., the gross fixation of inorganic C), *R*/*P*, increases as a function of temperature, which means the fraction of C available for growth after satisfying the catabolic demands of the cell, termed carbon-use efficiency (CUE = 1-*R*/*P*), declines as temperatures rise in the short term (Gifford 2003; Allison *et al.* 2010) (Figure 2.1c). This poses a major physiological challenge for photoautotrophic growth at high temperatures (Allison 2014). I hypothesise that adaptation to warmer temperatures (Figure 2.1b) should arise via evolutionary adjustments to metabolic traits that serve to increase CUE (Figure 2.1d) and partially offset intrinsic declines in CUE driven by the differences in the temperature sensitivity of *R* and *P*. When the activation energy for *R* is greater than *P* ($E_R > E_P$), specific rates of respiration, $R(T_c)$, should decline more than those of photosynthesis, $P(T_c)$, resulting in increases in the specific carbon-use efficiency [$CUE(T_c) = 1 - R(T_c)/P(T_c)$] as phytoplankton adapt to higher temperatures (Figure 2.1d). $CUE(T_c)$ reflects the carbon-use efficiency normalised to the reference temperature T_c = 25 ºC and controls for the intrinsic temperature responses of *R* and *P*. Here, I test these hypotheses by combining experimental evolution (Buckling *et al.* 2009; Reusch & Boyd 2013) with

measurements of fundamental physiology to investigate mechanisms of thermal adaptation in the model freshwater alga, *Chlorella vulgaris*.

METHODS

Culture conditions

Chlorella vulgaris is a globally distributed alga and has been found across North & South America, Asia, Europe and Australasia (Algaebase 2015). The particular strain (A60 strain, Sciento) used here was isolated from a pond in northern England 15 years ago and has since been maintained in laboratory culture at 20 ºC. Three replicate populations of the A60 strain of *C. vulgaris* were established at 5 different temperatures and were grown under nutrient and light saturated conditions in Infors-HT shaking incubators (160 r.p.m) on a 12:12 light:dark cycle and with a light intensity of 175 $\mu mol^{-1}\ m^{-2}\ s^{-1}$. Cultures were grown in 200 mL of Bold's Basal Medium, supplemented with $NaHCO_3$ (0.0095 M). These conditions represent typical benign conditions for this strain. Note that I initiated the experimental treatments with populations that presumably contained pre-existing genotypic variation, rather than single clones, to maximise the response to selection and better reflect evolutionary responses expected from natural populations (Reusch & Boyd 2013).

Selection temperatures included the long-term ancestral growth temperature of the strain, 20 ºC, and 4 warming scenarios, 23, 27, 30 and 33 ºC. Initial experiments indicated that 33 ºC was beyond the optimal growth temperature (30 ºC) and was therefore selected as the maximum experimental temperature to investigate the evolution of elevated thermal tolerance (see Figure 2.2a).

Exponential growth was maintained in semi-continuous batch culture; during the mid-log growth phase (identified from pilot growth experiments), 1 x 10^3 cells were transferred into new media to prevent resource limitation. Physiology and growth curve measurements were made twice on each of the three biological replicates at each selection temperature after 10 and 100 generations. The absolute time taken to reach 100 generations varied from 45 to 77 days depending on selection temperature (see Figure 2.2b-f).

Growth rates

Population biomass (µg C mL^{-1}) was measured at each transfer using a particle counter, which uses electrical sensing flow impedance determination to count and size cells (CellFacts™). Measurements of cell volume (μm^3) were transformed into units of carbon (µg C $cell^{-1}$) following Montagnes & Berges (1994). Specific growth rate, µ (d^{-1}), was calculated as:

$$\mu = \frac{\ln(N_1/N_0)}{\Delta T} \quad (2.3)$$

where N_1 is the final biomass (µg C), N_0 represents the initial biomass and ΔT is the time interval (days). The number of generations per transfer (g) is equivalent to the number of doubles and was calculated as follows:

$$g = \frac{\Delta T}{\ln(2)/\mu} \quad (2.4)$$

where ΔT is the time interval of the transfer (days), $\ln(2)/\mu$ is the doubling time (days) and μ is the specific growth rate (d^{-1}). I used linear mixed-effects modelling to quantify trajectories in specific growth rate at the different selection temperatures that allowed me to control for the hierarchical structure of the data (e.g. variance at the replicate level nested within selection temperatures), heteroscedasticity and temporal autocorrelation (Pinheiro & Bates 2006). For

the analysis, μ was the dependent variable, time (days) and selection temperature were fixed effects, while slopes and intercepts were treated as random effects at the level of replicates nested within selection temperature (Table 2.1). I controlled for heteroscedasticity by modelling changes in variance with selection temperature, and temporal autocorrelation using an autoregressive moving average function at the level of the random effect. Significance of the parameters was assessed using likelihood ratio tests, comparing models with common slopes and intercepts to models with different slopes and intercepts for each selection temperature (Table 2.1). Multiple comparison tests using Tukey's least significant difference were used to determine pairwise parameter differences between selection temperatures and significant differences from 0 (Appendix Table 1). Model selection was carried out on models fitted using maximum likelihood, while multiple comparison tests were carried out on the most parsimonious model fitted using restricted maximum likelihood.

Exponential population growth rates (r (d^{-1})) were calculated from logistic growth curves, measured after 10 and 100 generations at each selection temperature (Figure 2.2a & Appendix Figure 2). Samples were taken twice daily to estimate biomass, and once the stationary phase had been reached, I fitted the logistic growth equation to the biomass data using non-linear least squares regression:

$$N(t) = \frac{K}{1+Ae^{-rt}}\ ;\ A = \frac{K-N_0}{N_0} \qquad (2.5)$$

where $N(t)$ is the number of individuals at time, t, K is the carrying capacity, N_0 is the number of individuals at the start of the sampling period and r is the rate of exponential growth.

Characterising the metabolic thermal response

Responses of photosynthesis and respiration to acute temperature variation were determined across a broad range of temperatures (10 ºC – 49 ºC) to characterise the metabolic thermal response of *Chlorella vulgaris* (Figure 2.1). 10 mL aliquots of the populations were concentrated through centrifugation and acclimatised to the assay temperature for 15 minutes in the dark before measuring metabolic rates. Photosynthesis and respiration were measured through oxygen evolution in the light, and oxygen consumption in the dark, on a Clark-type oxygen electrode (Hansatech Chlorolab2). Photosynthesis was measured at increasing light intensities in intervals of 30 $\mu mol^{-1}\ m^{-2}\ s^{-1}$ up to 300 $\mu mol^{-1}\ m^{-2}\ s^{-1}$, and then in intervals of 100 $\mu mol^{-1}\ m^{-2}\ s^{-1}$ up to 1000 $\mu mol^{-1}\ m^{-2}\ s^{-1}$. This yielded a photosynthesis irradiance curve (PI) at each assay temperature. PI curves were fitted to the photoinhibition model (Platt *et al.* 1990) using non-linear least squares regression (Appendix Figure 3):

$$P(I) = P_s(1 - e^{\frac{-\alpha I}{P_s}} . e^{\frac{-\beta I}{P_s}}) \quad (2.6)$$

where $P(I)$ is the rate of photosynthesis at light intensity, I, P_s is a scaling coefficient that sets the relative rate of *P*, α controls the rate at which *P* increases up to a maximal rate, and β determines the extent to which *P* declines after the optimal light intensity due to photoinhibition. The photosynthetic maximum, P_{max}, was then calculated from Eq. 2.6.

$$P_{max} = \frac{P_s}{(\frac{\alpha+\beta}{\alpha})(\frac{\beta}{\alpha+\beta})^{\frac{-\beta}{\alpha}}} \quad (2.7)$$

Rates of respiration were measured in the dark. Gross photosynthesis (*P*) was then estimated as $P = P_{max} + R$. By using P_{max}, I controlled for any potential light-temperature interactions in the characterisation of the thermal response for *P*. Rates of *P* and *R* at each acute temperature were normalised by dividing by the biomass measured in each aliquot.

Acute responses of biomass normalised *P* and *R* to temperature were fitted to a modified Sharpe-Schoolfield equation for high temperature inactivation (see Eq. 2.1) using non-linear least squares regression. Fits were determined using the 'nlsLM' function in the 'minpack.lm' (Elzhov *et al.* 2009) package in R statistical software (v3.2.0) (R Core Team 2014), which uses the Levenberg-Marquardt optimisation algorithm. Model selection using the Akaike Information Criterion (AIC) was carried out to identify the parameter set which best characterised the data. This entailed running 1000 different random combinations of starting parameters drawn from a uniform distribution and retaining the parameter set that returned the lowest AIC score. The goodness of fit of the selected models were examined both graphically and through computation of a pseudo-R^2 value, recognising the caveats associated with calculating R^2 for non-linear models (Spiess & Neumeyer 2010). I tested for the effects of 'selection temperature' on the metabolic traits (parameters of Eq. 2.1 for *P* and *R*) using the Boltzmann-Arrhenius function:

$$\ln\big(b(T)\big) = E\left(\frac{1}{kT_c} - \frac{1}{kT}\right) + \ln(b(T_c)) \quad (2.8)$$

where $b(T)$ is the metabolic trait at the selection temperature, T, $b(T_c)$ is the

rate at temperature T_c, where T_c = 25 ºC, and E is the activation energy that determines how quickly the trait varies as a function of T. I used Eq. 2.8 in an Analysis of Covariance to test for the effects of 'selection temperature', 'exposure' (e.g. long-term vs. short-term warming), and 'metabolic flux' (either *P* or *R*) on the parameter estimates (Table 2.2).

In plant physiology, the carbon-use efficiency (CUE) represents the fraction of fixed carbon that is available for allocation to growth (Gifford 2003), and can be estimated from rates of gross photosynthesis (*P*) and respiration (*R*) as: CUE = 1-*R*/*P*. CUE and specific carbon-use efficiency [$CUE(T_c)$] were estimated for each replicate after 10 and 100 generations from rates of *R* and *P* measured at their selection temperature and from the specific rates of *R*, $R(T_c)$, and *P*, $P(T_c)$, respectively. Because the cultures experienced a 12:12 hour light-dark cycle, integrated over 24 hours, populations will be photosynthesising for 12h but respiring for 24h. In estimating CUE, rates of *R* and *P* were integrated over 24 and 12 hours respectively, to account for the diel population-level carbon budget. I then analysed the estimates of CUE and $CUE(T_c)$ using linear regression centred to a normalised temperature (T - T_c) in an Analysis of Variance so that the intercept of the linear model represented the CUE at T_c, where T_c = 25 ºC. 'Selection temperature' and 'exposure' (e.g. long-term vs. short-term warming) were included as potentially interacting factors.

RESULTS

The rate of exponential population growth (r) increased with selection temperature and after 10 generations, peaked at 30 ºC. Growth at 33 ºC was

lower than predicted from the exponential relationship between temperature and population growth (Figure 2.2a). However, following 100 generations of selection at 33 ºC, growth increased 1.4 fold (Tukey post-hoc test comparing long- and short-term growth rates at 33 ºC, t = -6.9, d.f. = 18, $P < 0.001$) to the level predicted from the initial (10 generation data) relationship between temperature and growth rate (Figure 2.2a). Trajectories of specific growth rate (μ) suggest that fitness did not change over the course of the selection experiment in the ancestral lineages (20 ºC) and those at 23 ºC. However, between 27 and 33 ºC, fitness increased over the course of 100 generations (Figure 2.2b-f). The most marked response to selection (e.g. the steepest fitness trajectory) was at 33 ºC (Figure 2.2f; Table 2.1 & Appendix Table 1).

Consistent with previous work (López-Urrutia *et al.* 2006; Yvon-Durocher *et al.* 2012), R was more sensitive to temperature than P in all lineages (Figure 2.3a-b; Appendix Figure 1 & Table 2.2) and consequently, CUE decreased with increasing selection temperature in the lineages that had experienced 10 and 100 generations at each selection temperature (ANCOVA $F_{1,26}$ = 70.27; $P < 0.001$; Figure 2.4a). Indeed, the low CUE at 33 ºC was initially (after 10 generations) limiting for growth (Figure 2.2a), explaining why lineages at 33 ºC showed the strongest response to selection (Figure 2.2f).

I hypothesised that evolution of elevated thermal tolerance should arise via increases in CUE, particularly at the temperature that was initially the most stressful (33 ºC), by selection driving down $R(T_c)$ more than $P(T_c)$ with increasing temperature (Figure 2.1d). In line with my hypothesis, CUE

increased significantly between lineages exposed to 10 and 100 generations at each temperature regime (ANCOVA comparing intercepts between levels of 'exposure'; $F_{1,26}$ = 9.73; P = 0.004; Figure 2.4a). Furthermore, in the 100 generation lineages $R(T_c)$ and $P(T_c)$ declined exponentially with increasing selection temperature (Figure 2.4b-c), with the activation energy for $R(T_c)$ = -0.88 eV (95% CI: -1.48 to -0.46 eV), double that of $P(T_c)$ = -0.47 eV (95% CI: -0.82 to -0.17 eV). Consequently, the specific carbon-use efficiency [$CUE(T_c)$ = 1- $R(T_c)$ / $P(T_c)$] increased linearly with increasing selection temperature (ANCOVA $F_{1,13}$ = 12.87; P = 0.003; Figure 2.4d).

I found no evidence for shifts in most of the other metabolic traits – e.g. E, T_{opt}, T_h – in response to temperature, after 10 or 100 generations (Table 2.2; Appendix Figure 1). Beside the documented declines in $R(T_c)$ and $P(T_c)$, the deactivation energy, E_h, which dictates the rate at which metabolism declines past the optimum, increased with selection temperature for both *P* and *R* (Table 2.2; Appendix Figure 1). Thermal optima for *P* and *R* were always higher than the selection temperatures for all lineages (Appendix Table 2). Thus, increases in E_h, resulting in more rapid declines in metabolic rates after the optimum, would not impact growth or fitness. Decreases in specific rates of metabolism, $R(T_c)$ and $P(T_c)$, and increases in the deactivation energy, E_h, do however suggest that metabolic thermal responses became more specialised in the lineages evolved to higher temperatures, where the strength of selection was greatest.

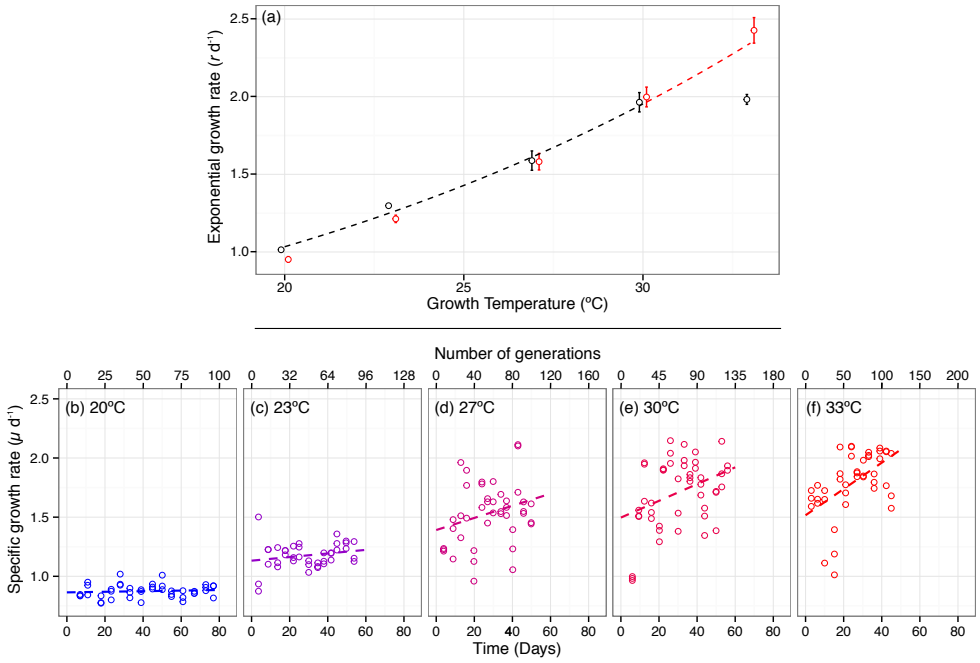

Figure 2.2. Growth rate trajectories for Chlorella vulgaris at different selection temperatures.

(a) Exponential rates of population growth (r) at the five different selection temperatures after 10 generations (black circles) and 100 generations (red circles). The broken black line shows the temperature dependence of growth rate for the all lineages up to 30 ºC after 10 generations and the broken red line predicts the expected growth rate at 33ºC from these data fitted to the Boltzmann-Arrhenius model (see Methods). (b – f) Trajectories of specific growth rate (μ) for populations at 20 ºC (the ancestral temperature), 23 ºC, 27 ºC, 30 ºC and 33 ºC respectively. Broken lines in (b-f) show growth trends based on the fixed effects of a linear mixed effect model (see Methods).

Table 2.1. Results of the linear mixed effects model analysis for trajectories of specific growth rate.
Random effects on the slope and intercept were determined at the level of replicates nested within selection temperatures. The results of the model selection procedure on the fixed effect terms are given and the most parsimonious model is highlighted in bold. Analyses reveal that growth rates changed significantly through time and that growth trajectories were significantly different between selection temperatures.

Model	**d.f.**	**AIC**	**Log Lik**	***L*-ratio**	***p***
random effects structure					
random = ~1 | id					
corr. structure = varPower() & corARMA(q = 1)					
fixed effects structure					
1. **growth rate ~ 1 + time * selection temp**	14	-140	84		
2. growth rate ~ 1 + time + selection temp	10	-123	71.3	25.4	< 0.001
3. growth rate ~ 1 + time	6	-53	32.9	77.0	< 0.001

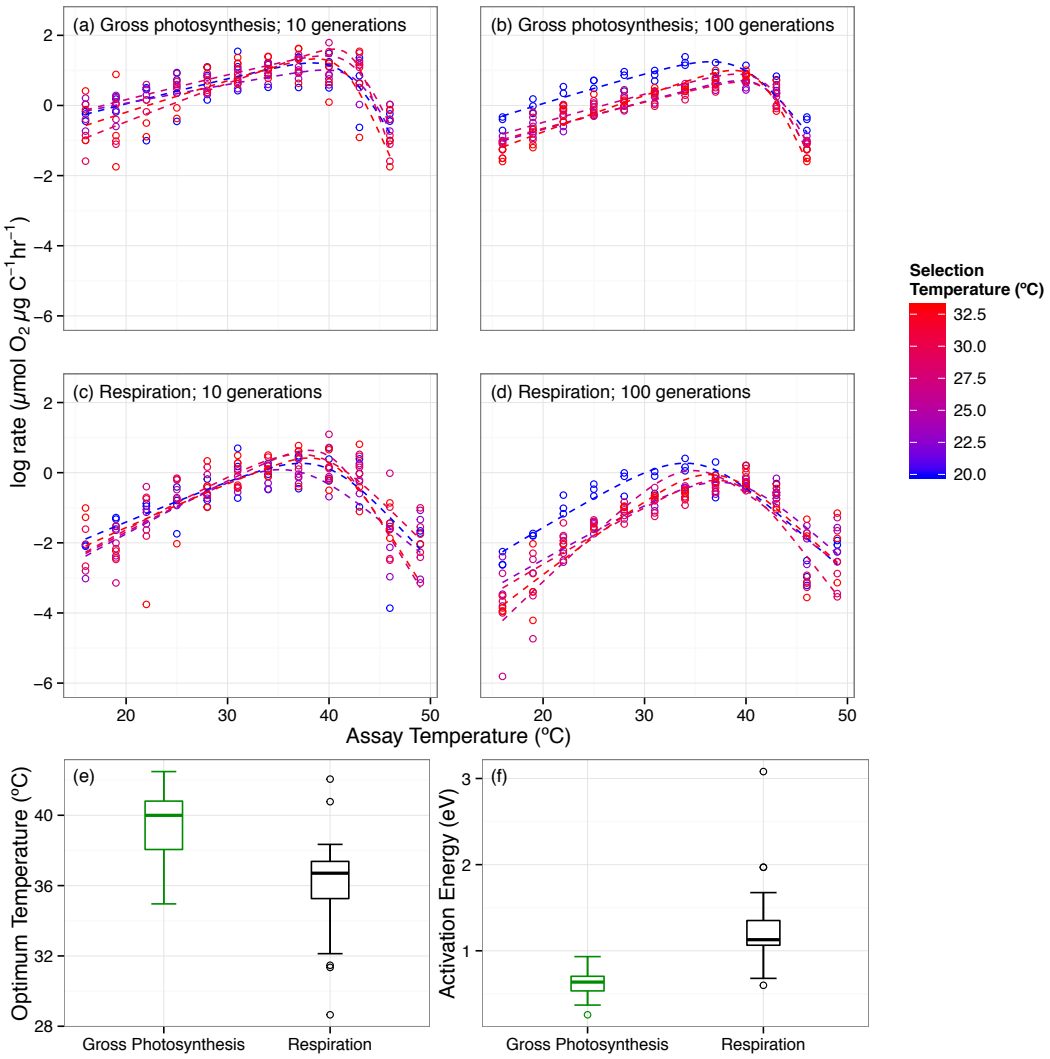

Figure 2.3. Acute effects of temperature on gross photosynthesis and respiration.

Acute thermal response curves for gross photosynthesis (P; a, b) and respiration (R; c, d) were measured for populations following short-term (10 generations, a, c) and long-term warming (100 generations; b, d) at 20 ºC (blue), through to 33 ºC (red). In (a – d), fitted lines are based on mean parameters at each growth temperature across replicates (n = 3) derived from non-linear least squares regression using the modified Sharpe-Schoolfield model (see Eq. 2.1). (e & f) Activation energies and thermal optima are pooled across all replicates and selection temperatures from both short- and long-term responses; tops and bottoms of box-whisker plots represent the 75th and 25th percentiles and black horizontal lines the medians.

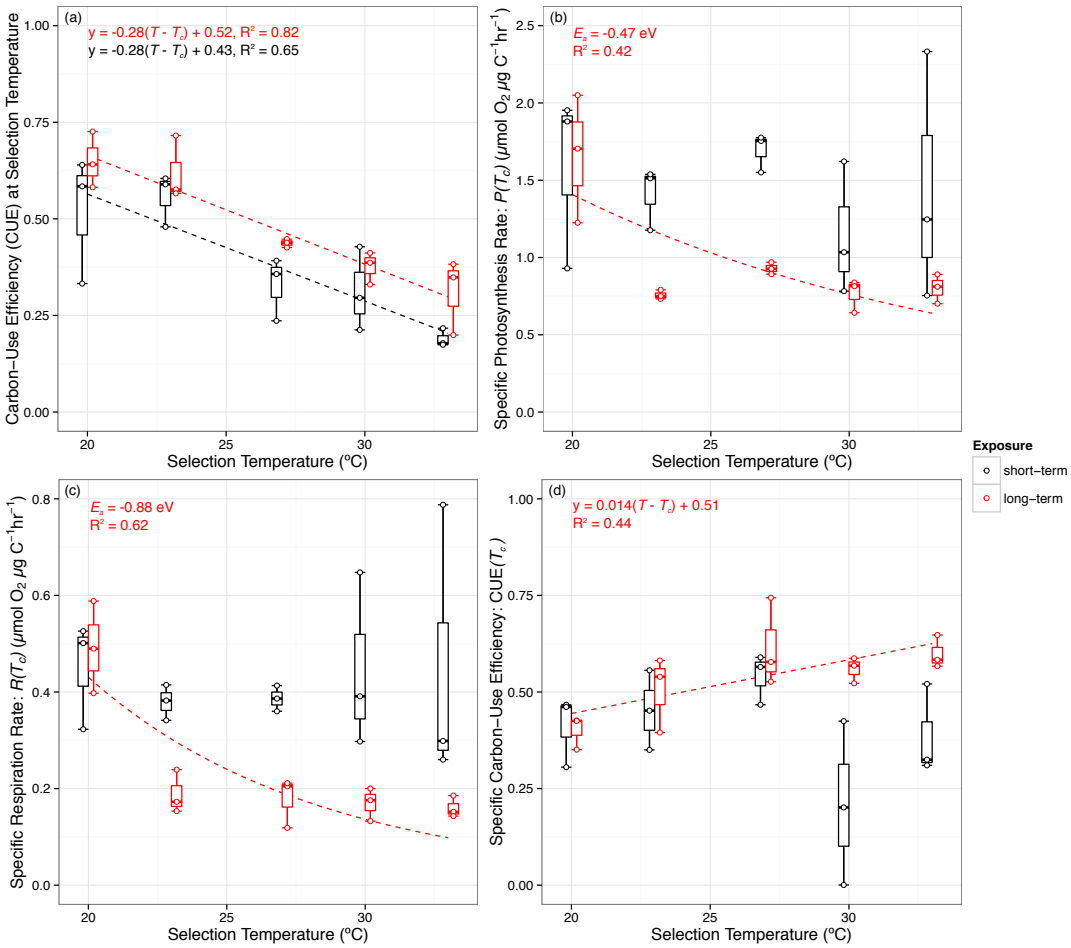

Figure 2.4. Effects of selection temperature on carbon-use efficiency and specific rates of metabolism.
(a) Carbon use efficiency (CUE) declined with increasing selection temperature after 10 (black bars) and 100 generations (red bars). However, CUE increased over the course of 100 generations (relative to the values after 10 generations), with the most marked increase at the temperature that was initially stressful (33 ºC). (b-c) Specific rates of gross photosynthesis, $P(T_c)$ and respiration, $R(T_c)$ for cultures after 10 (black) and 100 (red) generations. Neither of these metabolic traits varied with selection temperature after 10 generations, but both declined exponentially following 100 generations. (d) Specific carbon-use efficiency, $CUE(T_c)$, increased with increasing selection temperature over the course of 100 (red bars) but not after 10 generations (black bars). Fitted lines in (a, d) represent fits to a temperature-centred linear regression and in (b, c) represent fits to the Boltzmann-Arrhenius equation (Eq. 2.8; see Methods).

Table 2.2. Results of an Analysis of Covariance for each metabolic trait. Parameters included in the most parsimonious model are highlighted in bold.

Parameter	Effect	d.f.	F value	P value
$b(T_c)$	**selection temperature**	1,52	13.7	**< 0.001**
	metabolic flux	1,52	274.58	**< 0.001**
	exposure	1,52	40.9	**< 0.001**
	selection temperature*metabolic flux	1,52	0.198	0.65
	selection temperature*exposure	1,52	6.93	**< 0.05**
	metabolic flux*exposure	1,52	2.38	0.13
	selection temperature*metabolic flux*exposure	1,52	1.36	0.25
E_a	selection temperature	1,52	2.44	0.11
	metabolic flux	1,52	56.8	**< 0.001**
	exposure	1,52	7.29	**< 0.01**
	selection temperature*metabolic flux	1,52	0.0004	0.98
	selection temperature*exposure	1,52	0.024	0.88
	metabolic flux*exposure	1,52	4.8	**< 0.05**
	selection temperature*metabolic flux*exposure	1,52	0.91	0.34
E_h	**selection temperature**	1,52	4.71	**< 0.05**
	metabolic flux	1,52	17.5	**< 0.001**
	exposure	1,52	1.78	0.19
	selection temperature*metabolic flux	1,52	0.42	0.52
	selection temperature*exposure	1,52	0.09	0.76
	metabolic flux*exposure	1,52	0.39	0.53
	selection temperature*metabolic flux*exposure	1,52	0.002	0.96
T_h	selection temperature	1,52	0.15	0.34
	metabolic flux	1,52	36.4	**< 0.001**
	exposure	1,52	4.73	**< 0.05**
	selection temperature*metabolic flux	1,52	0.335	0.57
	selection temperature*exposure	1,52	0.211	0.65
	metabolic flux*exposure	1,52	1.38	0.25
	selection temperature*metabolic flux*exposure	1,52	0.23	0.64
T_{opt}	selection temperature	1,52	2.23	0.133
	metabolic flux	1,52	28.8	**< 0.001**
	exposure	1,52	2.75	0.10
	selection temperature*metabolic flux	1,52	0.04	0.85
	selection temperature*exposure	1,52	0.02	0.88
	metabolic flux*exposure	1,52	5.81	**< 0.05**
	selection temperature*metabolic flux*exposure	1,52	0.0001	0.99

DISCUSSION

I hypothesised that the higher temperature dependence of respiration (*R*) relative to photosynthesis (*P*) would constrain growth at elevated temperatures in the model phytoplankton, *C. vulgaris*, because of reductions in carbon-use efficiency (CUE). I therefore expected elevated thermal tolerance to evolve through down-regulation of *R* relative to *P*, enabling more efficient allocation of fixed carbon to growth. Results from the evolution experiment were consistent with these hypotheses.

Acclimation - i.e. the change in physiological phenotype from a single genotype (West-Eberhard 2003) - typically occurs over 1 to 10 generations in phytoplankton (Staehr & Birkeland 2006). In my experiment, growth rates increased exponentially between 20 and 30 ºC after 10 generations, though at 33 ºC, the capacity for physiological acclimation to facilitate further increases in growth was insufficient. In line with my expectations, CUE declined with increasing selection temperature, and at 33 ºC growth was presumably limited by low CUE.

Evolutionary responses in phytoplankton, either via selection on pre-existing genotype variation (Lohbeck *et al.* 2012) or *de novo* mutations, are frequently observed within 100 generations (Schaum & Collins 2014; Schlüter *et al.* 2014), and in this experiment, after 100 generations, growth at 33 ºC had increased to levels predicted from the exponential relationship between temperature and growth. Consistent with my hypothesis, elevated thermal tolerance evolved via increases in CUE mediated by greater down-regulation of specific rates of

respiration, $R(T_c)$ relative to those of photosynthesis, $P(T_c)$. These findings provide direct evidence that selection on metabolic traits provides a mechanistic explanation for the evolution of elevated thermal tolerance in a model phytoplankton.

Down-regulation of $R(T_c)$ under warming is well documented in vascular plants (Loveys *et al.* 2003; Atkin *et al.* 2015), and adjustments to $R(T_c)$, $P(T_c)$ and CUE occur within a single generation through acclimation. For plants that experience substantial variation in the environment over the course of a single generation, the capacity for physiological acclimation is likely to be key for maintaining fitness across a broad range of conditions. Phytoplankton have much shorter generation times (hours to days) and therefore the opportunity for evolutionary responses to changes in the environment, either through sorting on pre-existing genotype variation, or *de novo* mutation and selection (Lohbeck *et al.* 2012), is much greater in absolute time. Whether mediated by acclimation or evolutionary change, the net effect of down-regulating specific rates of respiration to facilitate growth at elevated temperatures, appears to be conserved across both vascular plants (Loveys *et al.* 2003; Atkin *et al.* 2015) and the green alga studied here. Developing a detailed understanding of the molecular and biochemical mechanisms that underpin the responses of metabolic traits to temperature should be a priority for further research.

A recent comparative analysis coupled to an eco-evolutionary species distribution model, demonstrated that geographic variation in thermal niches of phytoplankton closely matched the temperature regime of their natal

environment and suggests that thermal tolerance is a key trait shaping the response of phytoplankton communities to warming (Thomas *et al.* 2012). The rate at which thermal tolerance evolves to track changes in temperature in the Thomas *et al*. (2012) model is a key parameter for determining whether a species can persist in a given location under warming. However, due to the lack of data on rates of thermal adaptation for phytoplankton, this parameter could not be empirically constrained in the investigation by Thomas *et al*. (2012). My experiment demonstrates that for a model species of green algae, 100 generations (45 days) was sufficient to evolve elevated rates of population growth (1.4 fold increase) at a temperature that initially constrained growth and therefore provides an empirical basis for parameterising thermal trait evolution in eco-evolutionary models of phytoplankton dynamics. This work also reveals the metabolic mechanisms that underpin the evolution of elevated thermal tolerance and provides a basis for refining models by linking evolution and physiology to better predict the responses of phytoplankton communities to climate change.

While these experiments focused on a single species and strain, I consider that the rapid evolution of carbon-use efficiency will provide a mechanistic explanation for thermal adaptation in other phytoplankton. This is because the greater sensitivity of respiration to temperature, relative to photosynthesis is well established in a wide range of autotrophs (Allen *et al.* 2005; López-Urrutia *et al.* 2006; Staehr & Birkeland 2006; Anderson-Teixeira *et al.* 2011; Yvon-Durocher *et al.* 2012) and because phytoplankton have been shown to evolve rapidly in response to changes in their environment (Collins & Bell 2004;

Lohbeck *et al.* 2012; Schaum & Collins 2014; Schlüter *et al.* 2014). Absolute rates of evolution will depend on generation times and genotypic variation within populations, and will intrinsically vary among species as well as being dependent on past interactions with the environment. The rates of adaptation found here may not be consistent with those in the natural environment because experimental conditions in the laboratory are vastly simplified relative to the complex selection environment faced in nature. My results might, for example, overestimate rates of evolution because cultures were maintained in exponential growth. Phytoplankton in the natural environment likely spend a proportion of their life cycle at carrying capacity and/or under nutrient limitation, and thus have longer generation times than those achieved under laboratory conditions. On the other hand, my results could be conservative if the more heterogeneous environments experienced by natural populations result in high standing genetic variation. Indeed, a recent review of studies of genetic variation in natural populations using genetic markers demonstrated high standing gene and clonal diversity in diatoms, coccolithophores, dinoflagellates and a raphidopyte (Collins *et al.* 2013). Finally, rates of thermal adaptation in nature might be amplified or retarded relative to those observed in the laboratory, depending on how co-evolutionary interactions with other species affect evolutionary responses to changes in the abiotic environment (Lawrence *et al.* 2012).

Models used to assess biogeochemical and ecological futures under climate change tend to resolve phytoplankton into either taxonomic, functional or trait-based groups (Anderson 2005; Schneider *et al.* 2008; Vancoppenolle *et al.*

2013). More experiments are clearly needed to define the range of adaptive responses to warming among different groups of phytoplankton. Notwithstanding, these findings suggest that warm adapted phytoplankton could evolve elevated carbon fixation, which might offset some of the predicted declines in carbon sequestration under warming in aquatic ecosystems (Allen *et al.* 2005; López-Urrutia *et al.* 2006; Yvon-Durocher *et al.* 2010, 2012). I propose that the effects of thermal adaptation could be generalised within models based on these results, at least to test the sensitivity of model predictions to the rates of adaptation I have quantified and to challenge alternate model outputs (e.g. based on no adaptation vs. adaptation or to different rates of adaptation) with data (Stow *et al.* 2009). This will provide important insights into how the effects of thermal adaptation are expected to modify biogeochemical cycles, and hence predictions of elemental fluxes and the structure and functioning food webs, under warming.

CONCLUSION

I demonstrate the ability of an aquatic alga, *Chlorella vulgaris*, to adapt to novel thermal environments. After 10 generations at higher temperatures, growth was limited as respiration is more sensitive to temperature than photosynthesis. However, rapid evolution (increased thermal tolerance occurred after just ~45 days growth) is driven by a down-regulation of respiration rates relative to photosynthesis that results in an increase in the carbon-use efficiency that allowed a higher proportion of fixed carbon to be allocated to growth. Rapid-evolution of carbon-use efficiency could be a general mechanism of thermal

adaptation in phytoplankton and suggests that evolutionary responses could modify long-term temperature response of metabolism.

Chapter 3: Abundance, temperature and body-size predict community-level metabolic rates in phytoplankton communities.

ABSTRACT

Quantifying variation in primary production is critical to predicting the impacts of environmental change on the aquatic carbon cycle. Here, I used a metabolic scaling framework to investigate how body size and temperature influence phytoplankton community metabolism. I used phytoplankton sampled from an outdoor mescosom experiment in which communities had been either experimentally warmed (+ 4 ºC) for a decade or left at ambient temperature. Warmed and ambient phytoplankton communities differed substantially in their taxonomic composition and size structure, where communities from the warmed mescosms were dominated by larger phytoplankton. Community metabolism (photosynthesis and respiration) across all treatments could be robustly predicted using a model that accounted for the size- and temperature-dependence of individual metabolism, and the distribution of abundance, body size and biomass. These findings demonstrate that the key metabolic fluxes that determine the carbon balance of planktonic ecosystems can be predicted using metabolic scaling theory, with only knowledge of the individual size distribution and the ambient temperature.

INTRODUCTION

At the global scale, phytoplankton are responsible for around half of the carbon fixed by the biosphere, despite accounting for <1% of global autotrophic biomass (Falkowski 1994; Field 1998). Most of this carbon, fixed through photosynthesis, is quickly remineralised by respiration (Falkowski *et al.* 2000) and the difference between community respiration and gross primary production represents the amount of carbon available for sequestration to the deep ocean and to fuel aquatic food webs (Falkowski *et al.* 2008). Despite its importance to the global carbon cycle and ocean ecosystems, there is disagreement as to whether community respiration generally exceeds gross primary production in large areas of the ocean (del Giorgio *et al.* 1997; Duarte *et al.* 2013; Williams *et al.* 2013). If true, this would mean that large areas of the oligotrophic ocean are heterotrophic and release more CO_2 to the atmosphere through respiration than they fix via photosynthesis (Duarte *et al.* 2013).

The disagreement and uncertainty in the spatiotemporal coverage of heterotrophy in the ocean is partly caused by the different approaches for estimating planktonic metabolism and their associated limitations and uncertainties (del Giorgio & Duarte 2002; Robinson & Williams 2005; Serret *et al.* 2015). Traditional bottle-incubation measurements, where the metabolism of small samples of sea water (~125 mL) are measured *in vitro* for short periods of time (hours to days) (Robinson & Williams 2005; Serret *et al.* 2015), represent the metabolism of a single community at a specific time and place. In contrast, *in situ* methods measure ocean metabolism at much broader and coarser scales, by monitoring concentrations of gases that control or indicate

phytoplankton metabolism (such as O_2 and N_2) in large bodies of water (many km^2) over long periods of time (weeks to months) (Hansell *et al.* 2004; Williams *et al.* 2013). These methods necessarily incorporate the effect of multiple abiotic drivers (e.g. temperature, light) and integrate the metabolism of multiple communities that occur and change through time and space in the water mass (Serret *et al.* 2015). New approaches to estimate phytoplankton metabolism that can link across the spatial and temporal scales at which the current methods measure metabolism are needed to improve our understanding of the carbon cycle in aquatic ecosystems.

Here I approach this problem by linking aspects of community structure (e.g. size distribution and abundance) and individual physiology (i.e. gross photosynthesis and respiration) to the community metabolic flux. Previous work has shown that scaling up individual metabolism to the community-level can successfully predict ecosystem-level properties (López-Urrutia *et al.* 2006; Mcgill *et al.* 2006; Edwards *et al.* 2013a; Schramski *et al.* 2015). Metabolic scaling theory links organism to ecosystem metabolism using the fundamental relationships between temperature, body size and metabolic rate (Enquist *et al.* 2003; Brown *et al.* 2004). Metabolic theory has proven especially useful in helping to explain and predict the impact of warming on population, community and ecosystem-level phenomena (Enquist *et al.* 2003; Savage *et al.* 2004; Connor *et al.* 2009; Pawar *et al.* 2012). In phytoplankton, warming will alter the carbon cycling of communities directly through increases in metabolic rates (López-Urrutia *et al.* 2006; Padfield *et al.* 2016; Schaum *et al.* 2017). At the community-level, gross primary production (GPP) tends to be less sensitive to

changes in temperature than community respiration (CR). Consequently, it is expected that climate warming will shift the metabolic balance of phytoplankton communities towards heterotrophy (López-Urrutia *et al.* 2006; Regaudie-de-Gioux & Duarte 2012).

However, temperature also influences many aspects of community structure that in turn can influence phytoplankton community metabolism such as standing biomass (Chust *et al.* 2014; Yvon-Durocher *et al.* 2015), community composition (Markensten *et al.* 2010; Thomas *et al.* 2012), local adaptation (Berry & Bjorkman 1980), community size structure (Daufresne *et al.* 2009; Moran *et al.* 2010; Yvon-Durocher *et al.* 2011) and biodiversity (Hillebrand *et al.* 2011; Lewandowska *et al.* 2011, 2014; Yvon-Durocher *et al.* 2015). To successfully predict the impact of warming on phytoplankton metabolism, these indirect effects of warming need to be considered alongside the direct effect of temperature on metabolic rates.

Previous studies linking aspects of community structure to functioning in phytoplankton have generally focused on a subset of these direct and indirect relationships in isolation. For example, the relationship between body size, metabolic rate and abundance (Huete-Ortega *et al.* 2014; García *et al.* 2015; Huete-ortega *et al.* 2017), body size and temperature (Moran *et al.* 2010; López-Urrutia & Morán 2015), and metabolic rate, temperature and biodiversity (Lewandowska *et al.* 2011; Yvon-Durocher *et al.* 2015). How community-level metabolism emerges from the combined effects of temperature and body size on individual physiology and community structure remains largely unexplored

(but see López-Urrutia *et al.*, 2006). Here, I investigate how GPP and CR in phytoplankton communities are influenced by the effect of temperature and body size on individual metabolic rate and community structure. I do this by testing the predictions of a model derived from metabolic scaling theory against empirical data from a warming experiment with phytoplankton communities.

THEORY

Metabolism sets the pace of the life (Brown *et al.* 2004) and is a key process that can link patterns and mechanisms across levels of organisation by quantifying the relationships between metabolic rate, body size and temperature (Enquist *et al.* 2003; Brown *et al.* 2004). The central equation from metabolic scaling theory (MST) predicts individual metabolic rate (i.e. photosynthesis or respiration), b_i, at temperature, T (in Kelvin):

$$b_i(T) = b_i(T_c) m_i^a e^{E(\frac{1}{kT_c} - \frac{1}{kT})} \quad (3.1)$$

where $b_i(T_c)$ is an individual-level normalisation constant, at T_c (in K), and k is Boltzmann's constant (8.62 x 10^{-5} eV K^{-1}). m_i^a is the mass-dependence of metabolic rate characterised by an exponent, α, which is thought to reflect mass-dependent changes in the density of metabolic organelles (Allen *et al.* 2005). The exponent, α, was originally thought to be ¾ across all organisms (West *et al.* 2002), but recent empirical studies have found the size-scaling exponent to be steeper and close to isometric (α = 1) in phytoplankton (Marañón 2008; Huete-ortega *et al.* 2017) and super-linear in bacteria (α > 1) (DeLong *et al.* 2010; García *et al.* 2015). E (eV) is the activation energy that describes the temperature-dependence of the metabolic process. Previous work indicates that the activation energy of gross photosynthesis is weaker than

that of respiration across both terrestrial and aquatic autotrophs (Allen *et al.* 2005; Anderson-Teixeira *et al.* 2011; Padfield *et al.* 2016; Schaum *et al.* 2017).

The effect of body size and temperature on individual metabolic rate in Eq. 3.1 can be combined and summed across all individuals within a given community, j, to give an estimate of community metabolic rate B_j at temperature T (Enquist *et al.* 2003; Yvon-Durocher & Allen 2012):

$$B_j(T) = B_j(T_c)e^{E(\frac{1}{kT_c}-\frac{1}{kT})} \quad (3.2)$$

where $B_j(T)$ is the rate of metabolism of community j, at temperature T, in Kelvin (K), n_{tot} is the total number of individual organisms, i, that comprise all the organisms in j. $B_j(T_c)$ is the community-level normalisation ($= \sum_{i=1}^{n_{tot}} b_i(T_c)\, m_i^a$) at T_c (= 18 ºC [291.15 K]), and accounts for changes in abundance, size structure and individual metabolic normalisation constant between communities. In Eq. 3.2, E represents the temperature-dependence of community metabolism which is assumed to be similar to the average temperature-dependence of individual metabolism (Allen *et al.* 2005; Demars *et al.* 2016).

Total biomass, $M_{tot} = \sum_{i=1}^{n_{tot}} m_i$, is commonly used to normalise metabolic rates between communities. However, if the size-scaling of metabolism is not isometric ($\alpha \neq 1$) then biomass and metabolism will not be directly proportional (Allen & Gillooly 2009). By multiplying total biomass by a biomass-weighted average of the relationship between body size and metabolic rate m_i^{a-1} ($= \left(\sum_{i=1}^{n_{tot}} b_i(T_c)\, m_i^{\alpha}\right) / \left(\sum_{i=1}^{n_{tot}} m_i\right)$), mass-corrected biomass, $M_{tot}(m_i^{a-1})$, can

account for the size-scaling of metabolic rate with changes in body size. Mass-corrected biomass is predicted to be proportional to the total metabolic capacity (i.e. gross primary production or community respiration) of the biomass pool of a community. Thus, by rearranging Eq. 3.2 to control for the direct effect of temperature, T, on metabolism, mass-corrected biomass can be used to compare metabolism estimates among communities that differ in size structure, standing biomass and temperature (Barneche *et al.* 2014).

$$B_j(T)e^{E(\frac{1}{kT_c}-\frac{1}{kT})} = M_{tot}(m_i^{a-1}) \quad (3.3)$$

Here, $M_{tot}(m_i^{a-1})$ is an estimate of the metabolic flux of the community. This incorporates any effect of temperature on the metabolic normalisation constant, which is necessary as terrestrial and aquatic autotrophs are able to upregulate their metabolic normalisation constants $b(T_c)$ at low temperature and down-regulate them at high temperature to compensate for the constraints of thermodynamics on enzyme kinetics (Atkin *et al.* 2015; Padfield *et al.* 2016; Reich *et al.* 2016; Scafaro *et al.* 2016). After controlling for the direct effect of temperature, T, Eq. 3.3 predicts that gross primary production and community respiration should be directly proportional (the slope of the log-log relationship should be 1) to the mass-corrected biomass of the community. However, this key prediction of metabolic scaling theory has never been adequately tested due to the challenge of simultaneously measuring community metabolism and the complete size distribution (but see Yvon-Durocher and Allen, 2012).

The framework described in Eq 3.2 predicts community flux from the effect of temperature and body size on individual metabolic rates. However, it also emphasises that variation in total abundance, n_{tot}, between communities could

significantly alter community flux. Changes in total community abundance are expected to be intrinsically linked to the influence of body size and temperature on metabolic rate (White *et al.* 2007). The relationship between body size and abundance is often modelled by a power-law. Damuth's rule describes the phenomenon where the relationship between average body size of a species and abundance is the inverse of the relationship between body size and metabolic rate (Damuth 1987). These ideas of energetic equivalence can be applied to whole communities; the cross-community scaling relationship describes how variation in size-structure between communities results in simultaneous inverse changes in total community abundance. Under constant resource conditions, Eq. 3.2 predicts a trade-off between shifts in community size structure, temperature and total community abundance (Enquist *et al.* 2003). Under zero-sum dynamics, metabolic theory predicts that any change in the average rate of gross photosynthesis of a community, driven by changes in size structure or temperature, will result in a proportional decrease in the total number of individuals within that community, (Enquist *et al.* 1998; White *et al.* 2004; Ernest *et al.* 2009). The trade-off between the number of individuals and the total metabolic rate of those individuals predicts that when there is no change in the resource supply between communities, community rates should remain similar regardless of changes in the size structure.

METHODS

Overview of long-term mesocosm experiments

Twenty freshwater mesocosms, each holding 1 m^3, were set up in 2005 to mimic shallow lake ecosystems. They are situated at the Freshwater Biological

Association's river laboratory (2º 10' W, 50º 13' N) in East Stoke, Dorset, UK. Of the twenty, ten mesocosms have been warmed by 4 ºC above ambient temperature for more than 10 years. The mesocosms were seeded in December 2005 with organic substrates and a suite of organisms from surrounding natural freshwater habitats and subsequently left open to natural colonisation. These mesocosms have previously shown that warming can alter community structure and the metabolic balance of ecosystems (Dossena *et al.* 2012; Yvon-Durocher *et al.* 2015). As this system retains some of the aspects of natural ecosystems while maintaining the control of an experiment, it provides a powerful tool to investigate how individual- and community-level properties influence ecosystem functioning and the impact of warming on these links.

Experimental setup and maintenance

I sampled all twenty mesocosms (~200 mL) and set them up in a reciprocal transplant experiment in April 2016. I inoculated microcosms with a starting density of 200 cells mL^{-1} in water collected from the mesocosms supplemented with Bold's Basal Medium (BBM) and placed the microcosms in incubators (Infors-HT) at 16 ºC and 20 ºC (the temperatures of the mesocosms on the day of sample collection). Each mesocosm was passed through a 40 µm filter prior to inoculation to remove zooplankton from the microcosms. Phytoplankton communities were maintained on a 12:12 light:dark cycle with a daily light intensity of 175 μmol^{-1} m^{-2} s^{-1}. This resulted in 40 communities with 10 replicates of each combination of short- and long-term warming (i.e. warmed mesocosm in warm incubator, ambient mesocosm in ambient incubator,

warmed mesocosm in ambient incubator and ambient mesocosm in warm incubator). Autotroph counts were tracked daily using flow cytometry (BD Accuri C6). After ~17 days of culture, most communities showed a slowing of biomass accrual due to density dependence and resource limitation. The communities were then maintained in resource replete conditions by replacement of 50% of the culture with new medium (mesocosm water supplemented with BBM).

Measuring community flux

After ~30 days of culture (enough time for acclimation responses to short-term warming to occur [1-10 generations in phytoplankton] (Staehr & Birkeland 2006)) I measured metabolism at incubator temperature (16 ºC or 20 ºC) on communities below carrying capacity. Aliquots (30 mL) of each community were concentrated through centrifugation (~1500 rpm for 30 minutes at 4 ºC) and resuspended in 5 mL and acclimatised to the measurement temperature for 15 minutes in the dark prior to measuring metabolic flux. Primary production and community respiration were measured through oxygen evolution in the light and oxygen consumption in the dark respectively on a Clark-type electrode (Hansatech Ltd, King's Lynn UK Chlorolab2). Primary production was measured at increasing light intensities in minutely intervals of 50 $\mu mol^{-1}\ m^{-2}\ s^{-1}$ to 200 $\mu mol^{-1}\ m^{-2}\ s^{-1}$ and then in intervals of 100 $\mu mol^{-1}\ m^{-2}\ s^{-1}$ up to 1800 $\mu mol^{-1}\ m^{-2}\ s^{-1}$ that yielded a photosynthesis irradiance (PI) curve (Appendix Figure 5). Rates of respiration were measured for two minutes in the dark at the end of each PI curve to ensure respiration was not limited by available photosynthate during the measurement period.

Each individual PI curve was fit to a modification of the Eiler's curve for photoinhibition that incorporates community respiration. This model allows allow for negative rates of net primary production at low light levels where community respiration is greater than gross primary production (Eilers & Peeters 1988):

$$NPP(I) = \frac{NPP_{max} I}{(NPP_{max}/\alpha {I_{opt}}^2)\, I^2 + \left(1 - \left(\frac{2NPP_{max}}{\alpha I_{opt}}\right)\right) I + \frac{NPP_{max}}{\alpha}} - CR \quad (3.4)$$

where $NPP(I)$, is the rate of net primary production at irradiance, I, NPP_{max} is the maximal rate of net primary production at optimal light, I_{opt}, α controls the gradient of the initial slope and CR is community respiration, the rate of oxygen consumption in the dark. Gross primary production (GPP) at light saturation was then found by adding community respiration onto maximal net primary production ($GPP = NPP_{max} + CR$).

The community size distribution was measured by flow cytometry on the sample from the respirometer immediately after metabolic rate measurements. Cell size was calculated by converting values of forward scatter from the flow cytometer into values of diameter (d; µm) (Schaum *et al.* 2017). The biovolume of each cell was then calculated by assuming each particle was spherical (biovolume $= \frac{4}{3}\,\pi\,(\frac{d}{2})^3$) and converted into units carbon (µg cell^{-1}) using a conversion factor of 0.109 x 10^{-6} (Montagnes & Berges 1994). I also measured the community size distribution prior to centrifugation using similar methods. Here, I also quantified heterotrophic bacterial abundance using a SYBR gold stain (1:10000 dilution of initial stock). Bacteria represented <5% of total carbon

biomass in all but one of the microcosms (Appendix Figure 6) and are therefore unlikely to have a significant impact on measurements of community metabolism. Thus, all analyses use only the size distribution of the autotrophic communities.

Quantifying community diversity

Alongside measurements of community flux, I took samples to quantify microbial community composition and diversity by sequencing the V4 hyper-variable region of the 16S rDNA gene. On the sampling day, 50 mL of each microcosm was centrifuged in falcon tubes at 3000 rpm for 45 minutes at 4 ºC. The supernatant was then removed and the pellet transferred to 1.5 mL Ependorf tubes and centrifuged again for 30 minutes at 10000 rpm. The supernatant was then removed and the samples were frozen at -80 ºC prior to DNA extraction. DNA was extracted from samples using a Qiagen DNeasy Plant Mini Kit (Qiagen, Düsseldorf, Germany) following the manufacturer's instructions. Genomic DNA was purified and concentrated using Agencourt AMPure XP beads (Beckman Coulter, California, USA) at a ratio of 1:1.4. The products of this clean up were eluted into ~25 µL 10mM TRIS. Subsequent PCR amplification and sequencing of the 16S V4 region was undertaken by the Centre for Genomic Research (Liverpool, UK) following the Illumina MiSeq 16S Ribosomal RNA Gene Amplicons workflow.

Sequence data was analysed in R (v 3.3.2) (Team 2014) using the packages *'dada2'* and '*phyloseq'* (Callahan *et al.* 2015, 2016). Reads were truncated at 250 bp. I then followed the full stack workflow to estimate error rates, infer and

the merge sequences, construct a sequence table, remove chimeric sequences and assign taxonomy (Callahan *et al.* 2016). Sequence inference was done by pooling all the samples to improve the detection of rare variants that are seen just once or twice in an individual sample, but many times across all samples. I combined multiple rRNA databases to create my own database from which I assigned taxonomy. PhytoREF (Decelle *et al.* 2015), provides a reference database for the plastidial 16S rRNA gene for photosynthetic eukaryotes. Consequently, in a single amplicon sequencing run of the 16S v4 region I quantified both bacterial and eukaryotic autotroph diversity. I combined the PhytoREF database with the Ribosomal Database Project (Cole *et al.* 2014) that contains ribosomal RNA sequences of prokaryotes and 2700 16S rDNA cyanobacterial references (Decelle *et al.* 2015). Using CD-HIT (Li & Godzik 2006) I created a clustered database that aligned sequences with >97% similarity. I then preferentially assigned clustered sequences as originating from 1) PhytoREF, 2) cyanobacteria or 3) the Ribosomal Database Project as previous work has shown erroneous assignments of chloroplast plastidial sequences as being of bacterial origin (Decelle *et al.* 2015). I used the R package '*taxise'* (Chamberlain & Szöcs 2013) to reconcile each species in the reference database with its higher taxonomy. Samples were filtered if under 1000 total reads and standardised to the total number of operational taxonomic units (OTUs) through rarefaction to account for biases between coverage depth and number of OTUs present. I then filtered for autotrophic OTUs which resulted in samples from 36 of the 40 communities that could be used for downstream analysis.

Statistical analyses

To compare the composition between phytoplankton communities, I examined the impact of short- and long-term warming on Unifrac distance. Differences in community composition between communities were explored using the rarefied samples of each community and unweighted Unifrac distances using the R packages '*phyloseq'* (Callahan *et al.* 2016) and '*vegan'* (Oksanen *et al.* 2007). Unifrac distances compare the phylogenetic distance between sets of taxa based on shared branch length. Permutational ANOVA tests were run using the "adonis" function from the '*vegan'* package in R using short- and long-term warming as main effects and Unifrac distances as a response term with 999 permutations. The distance metric used (i.e. weighted Unifrac or Bray-Curtis dissimilarity) did not alter the results so only the results of the Unifrac distance are presented. After visualising rarefaction curves for all samples, the sequencing depth was found to be insufficient to analyse differences in alpha diversity, but the sequencing is still adequate to test for differences in the dominant species between communities.

I fit Eq. 3.4 to the measurements of oxygen flux using non-linear least squares regression using the R package '*minpack.lm*' (Elzhov *et al.* 2009). Model selection was done on each individual fit using Akaike Information Criterion (AIC) which entailed running up to 1000 iterations of the fitting process with start parameters drawn from a uniform distribution and retaining the fit with the lowest AIC score. I then calculated GPP as described earlier that was used alongside measured CR as the fluxes in the metabolic scaling framework (Eq. 3.2). I analysed the effect of short- (ambient or warm incubator) and long-term

warming (ambient or warm mesocosm) on raw community flux using an Analysis of Covariance in a mixed effects model framework. A random effect was included to account for the hierarchical structure of the data (community microcosms nested within mesocosms). A separate model was ran for each flux and model selection was carried out by comparing nested models using likelihood ratio tests.

The combined effects of community size structure and short-term warming on community metabolism were assessed using maximum likelihood. To do this, I fit the complete size distribution of each community to flux measurements. When the size distribution of a community is known, the approach taken here allows an estimation of the individual size-scaling exponent, m_i^a, instead of the size-scaling exponent of the average sized individual of the community or size class, $\overline{m_i^a}$. This approximation is prone to error unless all individuals are the same mass (Savage 2004; White *et al.* 2004, 2007) and becomes less accurate as the variation around average size, $\overline{M_i}$, increases. I fit Equation 3.2 to the rate of GPP and CR and the size distribution of each community to simultaneously estimate a value for the activation energy and size-scaling exponent. Analyses were done in R using the package '*bbmle'* (Bolker & Team 2010), with separate models for each flux (GPP and CR). The effect of long-term warming (ambient or warm mesocosm) was added as a potentially interacting factor on the metabolic normalisation constant, $b(T_c)$, activation energy, E, and individual size-scaling exponent, α. Model selection was carried out by comparing nested models using likelihood ratio tests.

I then investigated how well the scaling framework predicts community flux. To do this, I used Eq. 3.3 and the parameter estimates ($b(T_c)$, E and α) from the maximum likelihood approach to calculate temperature-corrected flux and mass-corrected biomass for both GPP and CR. I used standardised major axis (SMA) regression to investigate the slope of the relationship between temperature-corrected flux and mass-corrected biomass (Warton *et al.* 2006). SMA is useful here as I am testing for an expected slope (e.g. slope = 1) where it does not matter which variable is the response and which is the predictor. I then tested this relationship against the expected slope of 1 derived from the scaling framework.

I used the pre-centrifuged size distribution of each community to investigate whether zero-sum dynamics resulted in a trade-off between total community abundance and average individual metabolic rate. Pre-centrifuged communities were used to account for potential differences in sinking rates within and across communities that may distort the total community abundance after centrifugation. I calculated total community abundance, $\ln n_{tot}$, and estimated the average individual metabolic rate, $\overline{m_i^a}$, from the values of the maximum likelihood approach for GPP by abundance correcting Eq. 3.1 ($\overline{m_i^a} = \frac{M_{tot}(m_i^{a-1})e^{E(\frac{1}{kT_c}-\frac{1}{kT})}}{n_{tot}}$). Thus, $\overline{m_i^a}$ controls for the effect of temperature, changes in the metabolic normalisation constant and size structure on average metabolic rate. I then tested the slope of the relationship between average individual metabolic rate and abundance using SMA regression against an expected slope of -1.

RESULTS

Effect of warming on community composition and size structure

For the communities from which I had samples (n = 36), I found that long-term warming significantly altered the autotrophic community composition of the phytoplankton communities (Figure 3.1a). Long-term warming was a significant predictor of community composition (i.e. the phylogenetic dissimilarity among communities, unweighted Unifrac, Figure 3.1a, PERMANOVA, $F_{1,35}$ = 6.79, partial R^2 = 0.16, P = 0.001), whereas short-term warming had no effect on community composition (PERMANOVA, $F_{1,35}$ = 1.67, partial R^2 = 0.04, P = 0.078). The difference in community composition had a significant impact on size structure (Figure 3.1b). Communities from the ambient mesocosms had fewer large phytoplankton (average size = 3.6×10^{-5} µg C) compared to those from the warm mesocosms (average size = 1.06×10^{-4} µg C) with the average individual size being a magnitude bigger due to long-term warming.

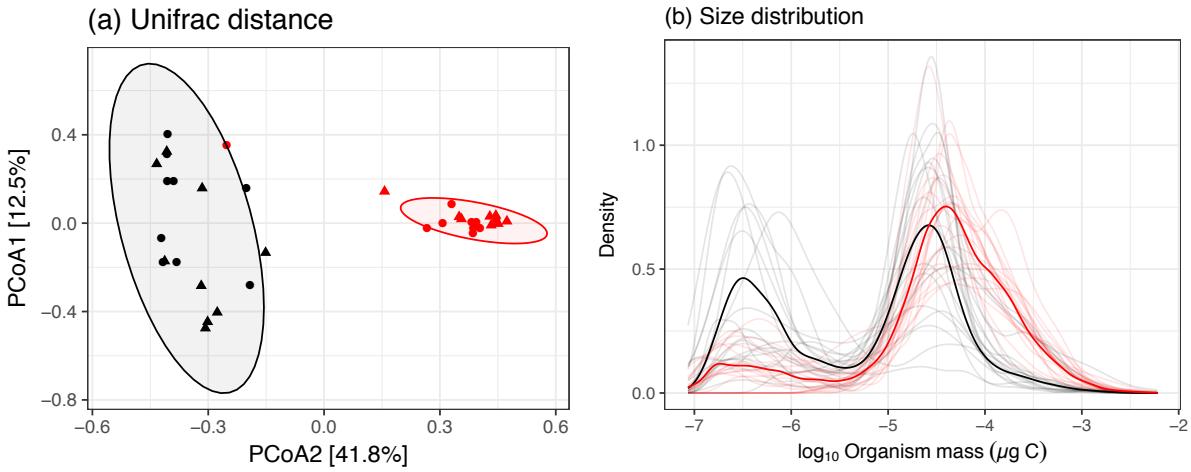

Figure 3.1. Effects of long-term warming on community structure. (a) Principal Coordinate (PCoA) plot of communities based on Unifrac distances. The percentage of variation explained is shown on each axis (calculated from the relevant eigenvalues). Long-term warming alters community composition while short-term warming (triangles) had no impact. (b) Probability density function for the size distribution of ambient and warm mesocosms. Warm mesocosms are dominated by larger phytoplankton. In both panels, different colours are used to represent ambient (black) and warm (red) mesocosms. In (a) triangles represent the warm incubator and circles the ambient incubator, shaded areas over communities represent the t-distribution based on the differences in community composition calculated from a PERMANOVA (see Methods). In (b) the pronounced line represents the size distribution of the pooled communities while the faded lines show the size distribution of each individual community.

Effect of short- and long-term warming on community metabolism

There was no significant effect of short- or long-term warming on rates of gross primary production or community respiration (Figure 3.2, Appendix Table 3). This is surprising given the large differences in the size structure and community composition due to long-term warming and the well documented effects of short-term warming on community metabolic rates.

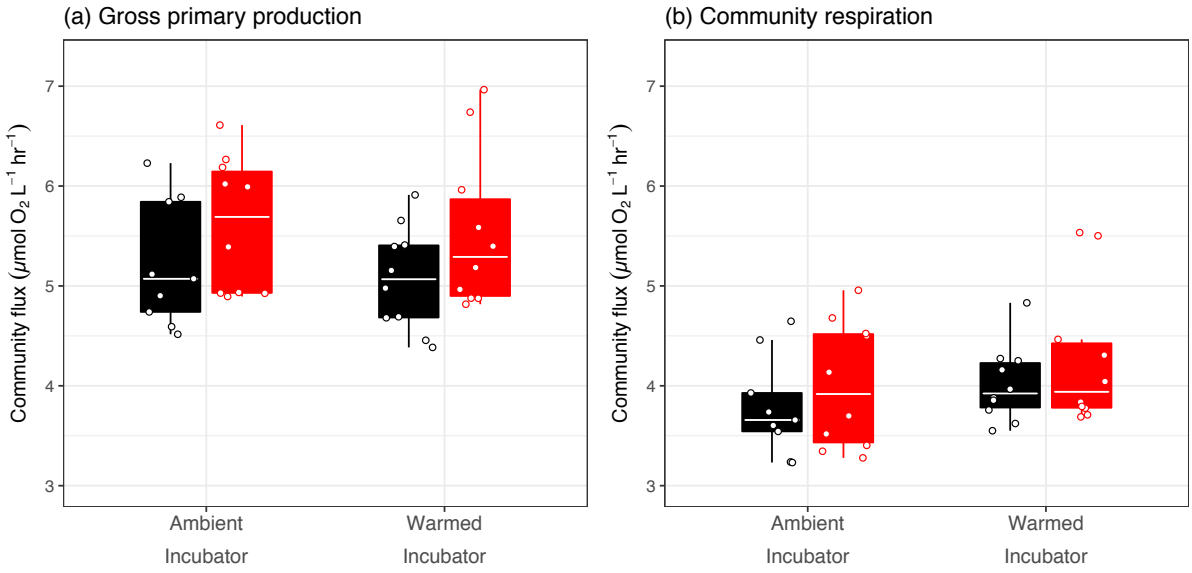

Figure 3.2. The effect of short- and long-term warming on (a) gross primary production and (b) community respiration.
The maximum likelihood framework found that short-term warming increases GPP and CR in both ambient (black) and warm (red) mesocosms. Long-term warming resulted in large shifts in community composition, size structure and a decrease in the community normalisation of CR. However, there was no significant effect of either short- or long-term warming on either GPP or CR. Each point represents the flux of one community; tops and bottoms of box-whisker plots represent the 75th and 25th percentiles and the white horizontal line represents the median.

Temperature-dependence and size-scaling of community metabolism

I fitted Eq 3.2 to the measurements of community metabolic rate (Figure 3.2). In line with our predictions, short-term warming had a direct effect on community metabolic rates, with the temperature-dependence of gross primary production (E_{GPP} = 0.74 eV; 95% CI = 0.20 – 1.29 eV) weaker than that of community respiration (E_{CR}= 1.42 eV; 95% CI = 0.85 – 1.98 eV). The maximum likelihood approach also estimated the size-scaling exponent of gross primary production (α_{GPP}= 0.87; 95% CI = 0.58 – 1.17) and community respiration (α_{CR}= 1.14; 95% CI = 0.74 – 1.41) which are not significantly different (they have overlapping 95% confidence intervals) from previously found ¾, or isometric

scaling (α = 1) that has been found in phytoplankton. As in previous studies, long-term warming significantly decreased the normalisation constant of community respiration, $\ln CR(T_c)$, in warm mesocosms (likelihood ratio test on nested models χ_1^2= 4.66, p = 0.03). Long-term warming had no impact on the temperature-dependence and size-scaling of GPP or CR or the metabolic normalisation constant of GPP (Table 3.1 & Appendix Table 4).

Table 3.1. Results of the maximum likelihood model fitting.
This entailed estimating the parameters below simultaneously by fitting Eq. 3.2 to gross primary production, community respiration and the community size distribution.

parameter	units	estimate	95% confidence interval
E_{GPP}	eV	0.741	0.196 - 1.286
E_{CR}	eV	1.417	0.853 - 1.982
α_{GPP}	-	0.887	0.567 - 1.174
α_{CR}	-	1.101	0.743 - 1.412
$\ln GPP(T_c)$	μmol O_2 L^{-1} hr^{-1}	-3.426	-6.335 - -0.989
$\ln CR(T_c)$ (ambient mesocosm)	μmol O_2 L^{-1} hr^{-1}	-2.717	-5.943 - -0.150
$\ln CR(T_c)$ (warm mesocosm)	μmol O_2 L^{-1} hr^{-1}	-3.110	-6.126 - -0.650

Mass-corrected biomass predicts GPP and CR

After estimating the temperature-dependence and size-scaling of metabolic rate for GPP and CR, there is a need to determine how well the scaling framework actually predicts community-level flux. To this end, I used Eq. 3.3 and calculated the mass-corrected community biomass, $M_{tot}(\overline{m_i}^{a-1})$, and the temperature-corrected community rate, $B_j(T)e^{E(\frac{1}{kT_c}-\frac{1}{kT})}$, of GPP and CR for each community using the parameter estimates from the best fit maximum likelihood model (Table 3.1). I then fitted the data to an SMA to test how well my metabolic scaling approach predicts observed community flux. After accounting for the effect of short-term warming and mass on metabolic rate,

temperature-corrected flux should increase proportionally (1:1) with mass-corrected biomass on a log-log scale (Figure 3.3; dashed lines). For GPP, the SMA regression had an intercept of 0.12 (95% CI = -0.88 – 1.12), a slope of 0.95 (95% CI = 0.79 – 1.15) and an R^2 of 0.68 (Figure 3.3a). For CR, the SMA regression had an intercept of 0.50 (95% CI = -0.27 – 1.26), a slope of 0.87 (95% CI = 0.70 – 1.07) and an R^2 of 0.59 (Figure 3.3b). The relationships between predicted and observed flux for both GPP and CR had values of the slopes and intercepts that were not significantly different from the expected values (slope = 1; intercept = 0). This indicates that our modelling framework can predict community flux purely from data on the size distribution and temperature (Figure 3.3). Fitting the same model to all the data using OLS regression returned similar results.

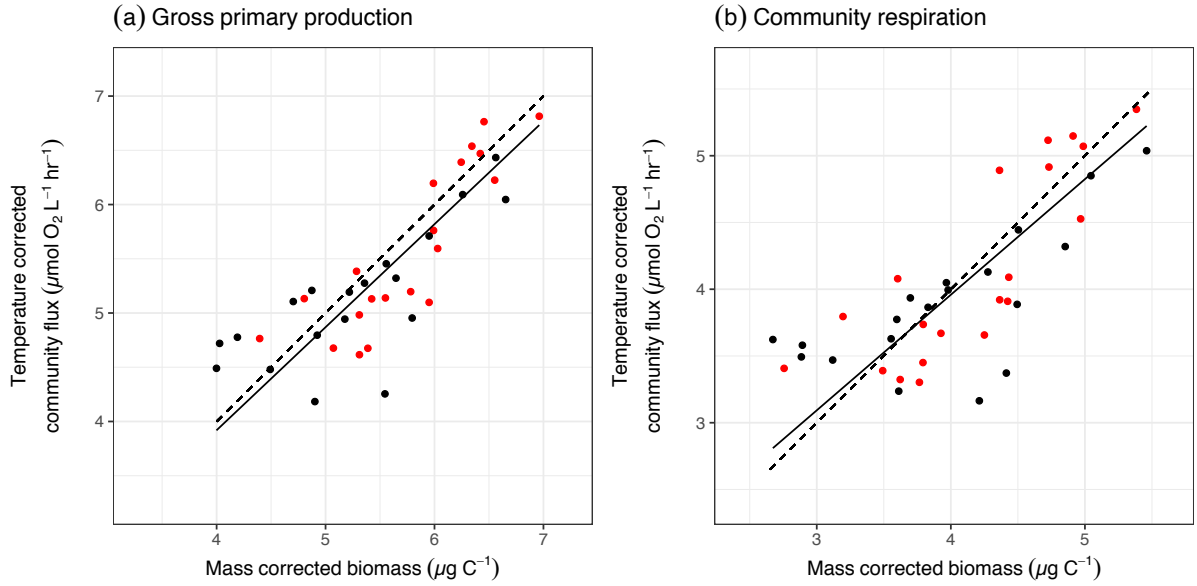

Figure 3.3. Relationship between (a) temperature-corrected community gross primary production and mass-corrected community biomass, and (b) temperature-corrected community respiration and mass-corrected community biomass.

Community flux can be predicted from changes in community abundance, body size and short-term temperature. Fluxes were temperature normalised using the empirically derived values of E_{GPP} = 0.74 eV in (a) and E_{CR} = 1.42 eV in (b). Mass-corrected biomass was calculated using the values of α and $b(T_c)$ from

the maximum likelihood approach (Table 1). The warm mesocosm communities are denoted by red points and the ambient mesocosms by black points. The fitted lines represent the predictions of standardised major axis regression investigating whether the slope between observed and expected metabolism is significantly different from the predicted slope of 1. The dashed line represents a 1:1 line as predicted from metabolic scaling theory.

Energetic equivalence across communities

Across communities, under zero-sum dynamics, metabolic scaling theory predicts that any increase in average individual metabolic rate should trade-off with a decrease in total abundance. I calculated average individual metabolic rate of each community using the parameter values for GPP from the maximum likelihood approach (Table 3.1) and looked at the relationship between total community abundance and average individual metabolic rate using SMA regression. Total community abundance decreased with increases in average individual metabolic rate (slope = -0.95, 95%CI = -1.17 - -0.76; intercept = 16.6, 95% CI = 16.46 – 16.80; R^2 = 0.46; Figure 3.4). This slope is not significantly different from the predicted value -1 (test comparing slope to -1, r = -0.08, d.f. = 38, P = 0.61) and indicates that these communities adhere to zero-sum dynamics.

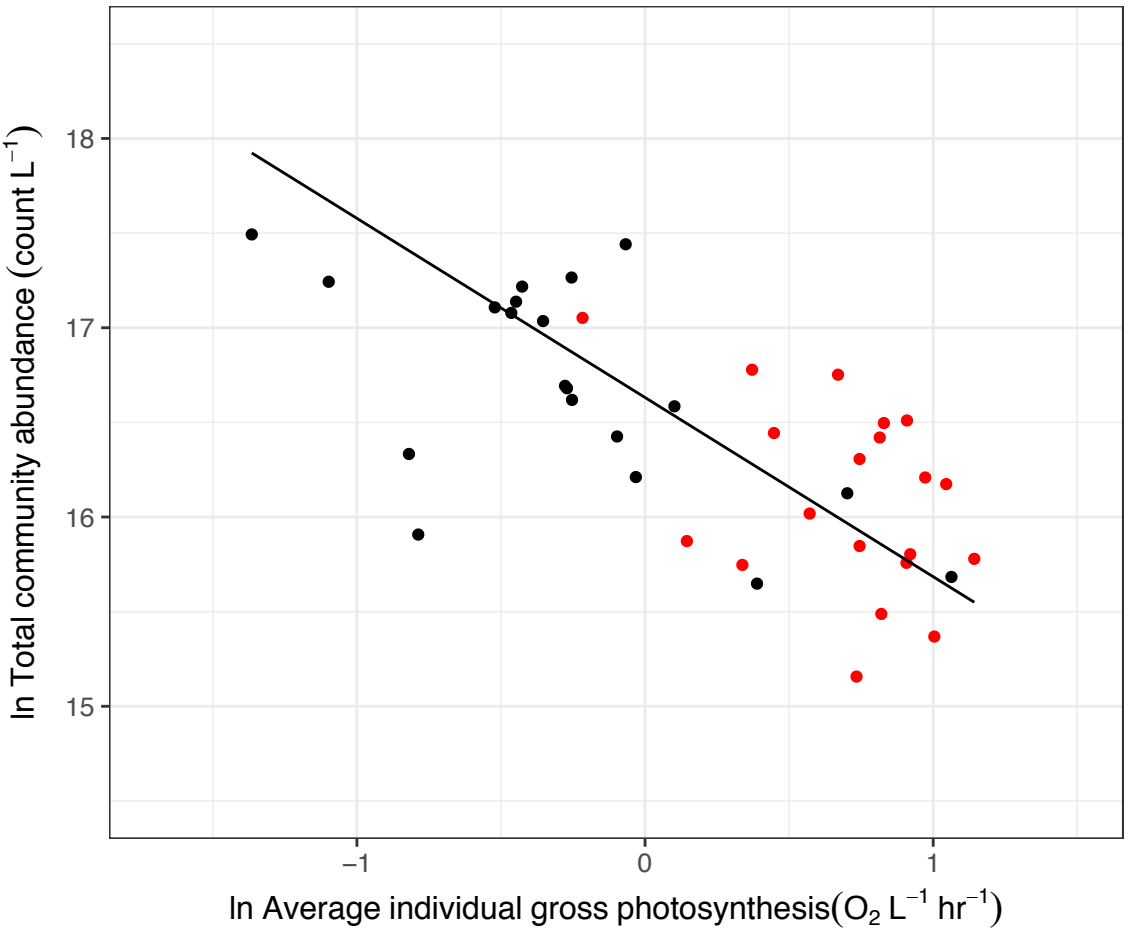

Figure 3.4. Relationship between average individual gross photosynthesis and total community abundance.
Average individual gross photosynthesis was calculated from the values of the maximum likelihood approach for gross primary productivity (see methods). Consistent with zero sum dynamics, increases in average individual gross photosynthesis resulted in a compensatory decrease in total community abundance. The exponent, fitted using standardised major axis regression on log-transformed data, is -0.92, which is not significantly different from the predicted value of -1. Warm mesocosms (red) have higher average individual metabolic rates than ambient mesocosm communities (black) due to being dominated by larger individuals. Each point represents a community and the fitted line is the predicted fit of the SMA regression.

DISCUSSION

Measurements of ocean metabolism *in situ* and *in vitro* have led to contrasting conclusions as to whether the oligotrophic ocean is net autotrophic or heterotrophic (Duarte *et al.* 2013; Williams *et al.* 2013). These differences are

partly driven by the different mechanisms that influence metabolism at the vastly different scales at which the measurements are taken. In the hope of better understanding the carbon cycling of ocean communities, previous work has linked individual physiology and community size structure to predict phytoplankton community metabolism in the ocean (López-Urrutia *et al.* 2006). Here, I extend this work by coupling measurements of phytoplankton community metabolism with a model that links phytoplankton community rates of GPP and CR with the effects of body size and temperature on individual physiology and the community size distribution. In contrast to previous work, I examine the effect of both short- and long-term warming on community metabolism. Long-term warming resulted in marked shifts in community composition which shifted communities towards larger phytoplankton species and resulted in a downregulation in the rates of community respiration. Despite this, rates of both GPP and CR were well predicted from the size-distribution of communities and the effects of body size and temperature on individual metabolic rate. However, our results show that warming may influence the metabolic rates of phytoplankton communities in ways that are more complex than the short-term response to warming alone.

As well as predicting community flux purely from the size-structure of phytoplankton communities, the metabolic scaling framework presented here allows me to evaluate how fundamental constraints on individual metabolism influence community-level properties. For example, temperature increased rates of metabolism per-unit-biomass and I found that short-term warming strongly influenced community flux (Table 3.1). As in a previous study that

measured GPP and CR *in situ* in these mesocosms, I found no effect of long-term warming on the temperature-dependence of metabolism (Yvon-Durocher & Allen 2012). In addition, similar to predictions from metabolic theory, gross primary production was less sensitive to temperature change than community respiration (Table 3.1), with values of the activation energy of GPP and CR at the community-level similar to those recently found at the population-level (i.e. gross photosynthesis and respiration) for single species of phytoplankton (Padfield *et al.* 2016; Schaum *et al.* 2017). These findings are consistent with ideas from metabolic theory that the effect of temperature on metabolism is controlled by fundamental constraints on enzyme activity and is a key driver of community-level flux.

Previous studies have used the short-term temperature sensitivities of GPP and CR to predict the impact of long-term warming on phytoplankton communities. Specifically, as respiration will increase more than photosynthesis in the short-term, the metabolic balance of phytoplankton communities may shift towards heterotrophy (López-Urrutia *et al.* 2006). This would significantly alter the amount of carbon dioxide that would be captured by the ocean and would potentially exacerbate climate warming. However, using short-term responses to temperature to predict the impacts of long-term warming (as is expected of climate warming) on community metabolism is not straightforward. In the long-term, warming is known to affect phytoplankton composition, size structure (Yvon-Durocher *et al.* 2011; Dossena *et al.* 2012) and standing biomass (Yvon-Durocher *et al.* 2015) which can all influence metabolic rates.

In this study, long-term warming had profound effects on some of these community-level properties, significantly altering community composition and shifting the size distribution towards larger phytoplankton (Figure 3.1). This shift in size structure is thought to be a result of enhanced top-down regulation of adjacent trophic levels by increasing temperature-dependent consumption rates (Connor *et al.* 2009; O'Connor *et al.* 2011; Yvon-Durocher *et al.* 2015) and is in contrast to previous studies that find that phytoplankton generally get smaller due to warming (Daufresne *et al.* 2009; Moran *et al.* 2010). Somewhat surprisingly, differences in the size structure were maintained throughout the ~30 days of culture in the laboratory, even though the zooplankton were absent for the entire growth period. The absence of an effect of short-term warming on community composition or size structure is likely due to the absence of key community processes in the microcosms. These processes, such as dispersal and immigration, ultimately control species turnover and local diversity in natural environments (Leibold *et al.* 2004). Changes in the size structure are therefore likely to be primarily driven by size differences between the dominant species in each community, in contrast to body size plasticity within species. This is at odds with the temperature-size rule (Atkinson 1994) and previous studies on phytoplankton that have shown that species reduce their body size in response to warming (Peter & Sommer 2012; Schaum *et al.* 2017).

The effect of long-term warming on the size structure and community composition can alter community metabolism. Recent work has shown that rapid evolution to warming can shift the metabolic normalisation constant of gross photosynthesis and respiration to maximise the energetic efficiency of

individuals at increasing temperatures (Padfield *et al.* 2016). This allows a larger proportion of gross photosynthesis to be allocated to growth and biomass production (Padfield *et al.* 2016). In line with this hypothesis, long-term warming had no effect on the metabolic normalisation constant of GPP, $GPP(T_c)$ (Figure 3.2a), but the metabolic normalisation constant of community respiration was lower in the warm mesocosms (Figure 3.2b). Instead of rapid evolution within species, this decrease was driven by shifts in the community composition after long-term warming. In these semi-natural communities, wider regional-species pools and immigration and extinction processes control local biodiversity. Thus, the downregulation of $CR(T_c)$ likely reflects temperature-driven selection on the metabolic normalisation constant among taxa that has resulted in communities being locally adapted to their respective temperature. Our findings suggest that warm-adapted communities will have elevated carbon fixation at higher temperatures compared to cold-adapted communities due to the downregulation of $CR(T_c)$. This will reduce the predicted shift towards heterotrophy expected from the metabolic response to short-term warming alone (Figure 3.2). These results add to recent work that highlights the importance of the indirect effects of temperature on metabolic rates when predicting the response of the biosphere to warming (Michaletz *et al.* 2014; Yvon-Durocher *et al.* 2015; Padfield *et al.* 2016).

As well as changes in the metabolic normalisation constant, shifts in the size structure of communities may alter the metabolic balance of communities through changes in mass-corrected biomass. The metabolic scaling framework presented here estimates the size-scaling exponent of metabolic rate, α directly

from the complete size distribution of each community (Yvon-Durocher & Allen 2012). In line with previous work and predictions from metabolic theory, size-scaling exponents for both GPP and CR had 95% confidence intervals that overlapped both ¾ and isometric scaling and were not significantly different from each other (DeLong *et al.* 2010; Huete-ortega *et al.* 2017). There was no impact of long-term warming on the size-scaling of GPP and CR. Taken together, these results suggest that changes in the size structure of communities are unlikely to alter the metabolic balance of communities as gross photosynthesis and respiration scale similarly with changes in body size and are unaffected by warming.

Although our metabolic scaling theory found a significant effect of short-term warming and size structure on metabolic rates, community flux did not change as a result of short- or long-term warming. This is due to a trade-off between community properties. Increases in temperature and shifts in size structure between communities should be compensated for by changes in total community abundance. Under the same resource conditions, zero sum dynamics predict a trade-off between total abundance and average individual metabolic rate, meaning that communities with different size structures and at different temperatures can have similar metabolic rates (White *et al.* 2004; Ernest *et al.* 2008, 2009). In line with this prediction, across all the communities, microcosms with higher average individual metabolic rates had proportional lower total community abundance (Figure 3.4). This trade-off meant that shifts in the size structure and short-term warming that increased average individual metabolic rates were compensated for by changes in total abundance, resulting

in no overall change in community flux (Figure 3.2). This cross-community scaling is caused by an ultimate energetic constraint that sets an upper limit on community resource-use and metabolism. Thus, changes in nutrient concentrations with climate change may be a key predictor of the metabolism of phytoplankton communities, regardless of community size-structure (Behrenfeld *et al.* 2006).

Despite the large differences in size structure and community composition, rates of GPP and CR were significantly correlated with community size structure (Figure 3.3). This is because fluxes are ultimately driven by the abundance, temperature and body size distribution of the organisms that comprise each community. The success of the framework, in spite of large differences in other community properties, is encouraging, especially given that the parameters for the size-scaling and temperature-dependence of GPP and CR are similar to previous work and the values expected from metabolic theory. However, more work is needed if the framework is to be applicable to natural phytoplankton communities, including further testing to assess the generality of the parameter values reported here. For example, I have shown that long-term warming can decrease the metabolic normalisation constant of respiration, but this study cannot determine the timescales over which communities, and the functions they mediate, can change due to warming. Understanding whether changes that offset the direct impacts of warming on community rates can track the rate of climate warming will be essential for predicting future responses of phytoplankton to warming.

Predicting how temperature influences metabolism in the natural environment is further complicated by multiple abiotic drivers that often covary with temperature. These abiotic drivers often also influence metabolic rate and interactions between temperature, light and nutrient supply (Edwards *et al.* 2016; Thomas *et al.* 2017) are known to dampen the temperature sensitivity of phytoplankton growth rates. This may partially explain why the values for the activation energies of GPP and CR in this study are nearly double those previously reported in the natural setting (López-Urrutia *et al.* 2006; Yvon-Durocher *et al.* 2010; Regaudie-de-Gioux & Duarte 2012). Notwithstanding, this framework could help provide estimates of phytoplankton metabolism in the aquatic realm. As opposed to other methods, the application of the model is limited only by the number of samples of phytoplankton community size-structure across time and space. Such information on the size structure is becoming increasingly available due to the emergence of automated counting methods, such as flow cytometry, that makes characterising the size distribution of aquatic microbial communities easier and less resource-intensive.

Overall, this method, derived from metabolic scaling theory, can help estimate phytoplankton metabolism, which is critical to improve knowledge of ocean productivity and our ability to predict the feedbacks between the aquatic carbon cycle and climate change. The uncertainty surrounding the metabolic balance of large areas of the ocean currently limits the ability to parameterise ocean climate models and identify temporal and spatial variations in these parameterisations (del Giorgio & Duarte 2002; Kwiatkowski *et al.* 2017). I have

shown that applying metabolic theory and linking individual and community-level properties could drive progress in this fundamental area of research.

CONCLUSION

Phytoplankton fix ~50% of the carbon globally, but the extent to which this is remineralised by respiration is still uncertain. This chapter uses metabolic scaling theory to show that phytoplankton community metabolism can be predicted from the fundamental constraints of temperature and body size on individual metabolic rate and community size-structure. I propose that estimates of phytoplankton in the natural environment can be predicted from samples of phytoplankton size-structure alone. Short-term warming increased metabolic rates and long-term warming resulted in large shifts in the community composition. However, trade-offs between short- and long-term warming, that increased average individual metabolic rate, and total community abundance meant that community flux did not systematically change across communities. Long-term warming resulted in a downregulation of the respiratory community normalisation constant as a result of shifts in community composition. These results suggest that warming may influence the metabolic balance of phytoplankton communities in ways that are more complex than the short-term response to warming alone.

Chapter 4: Metabolic compensation constrains the temperature-dependence of gross primary production

ABSTRACT

Gross primary production (GPP) is the largest flux in the carbon cycle, yet its response to global warming is highly uncertain. The temperature sensitivity of GPP is directly linked to photosynthetic physiology, but the response of GPP to warming over longer timescales could also be shaped by ecological and evolutionary processes that drive variation in community structure and functional trait distributions. Here, I show that selection on photosynthetic traits within and across taxa dampen the effects of temperature on GPP across a catchment of geothermally heated streams. Autotrophs from cold streams had higher photosynthetic rates and after accounting for differences in biomass among sites, ecosystem-level, biomass-specific GPP was independent of temperature despite a 20 ºC thermal gradient. Our results suggest that temperature-compensation of photosynthetic rates constrains the long-term temperature-dependence of GPP, and highlights the importance of considering physiological, ecological and evolutionary mechanisms when predicting how ecosystem-level processes respond to warming.

INTRODUCTION

The carbon cycle is fundamentally metabolic (Falkowski *et al.* 2000). At the ecosystem level, gross primary production (GPP) represents the total amount of CO_2 fixed by photosynthesis into organic carbon and is the largest flux in the global carbon cycle (Beer *et al.* 2010), transferring CO_2 from the atmosphere to the biosphere, fuelling food webs and biological production (Field 1998). Understanding the mechanisms that shape how temperature influences rates of GPP across spatial, temporal and organisational scales is therefore an essential prerequisite to forecasting feedbacks between global warming and the carbon cycle.

Temperature can dictate rates of GPP over short timescales through its effects on photosynthetic physiology (Medlyn *et al.* 2002; Allen *et al.* 2005; Galmes *et al.* 2015). However, it is clear that over longer timescales (e.g. decades of gradual warming) ecological and evolutionary processes that mediate temperature-induced changes in biomass, community composition and local adaptation of metabolic traits could feedback to influence the emergent effects of warming on ecosystem properties (Allen *et al.* 2005; Enquist *et al.* 2007; Michaletz *et al.* 2014; Cross *et al.* 2015). Indeed a recent analysis demonstrated that most of the variation in terrestrial primary production along a latitudinal temperature gradient could be explained by changes in biomass, and after controlling for variation in biomass, rates were independent of temperature (Michaletz *et al.* 2014). Such temperature-invariance in biomass-specific rates of primary production is counterintuitive considering the well-known exponential effects of temperature on the biochemistry of metabolism (Gillooly *et al.* 2001).

Furthermore, it implies that selection on photosynthetic traits that compensate for the effects of temperature on physiological rates could play a fundamental role in mediating the effects of temperature on rates of primary production in the long-term (Kerkhoff *et al.* 2005; Enquist *et al.* 2007).

Here I investigate how rates of ecosystem-level gross primary production are influenced by the direct effects of temperature on the kinetics of photosynthesis, and indirect effects of temperature-driven selection on photosynthetic traits, and changes in community biomass. I do so by extending the general model for ecosystem metabolism from metabolic theory (Enquist *et al.* 2003, 2007; Allen *et al.* 2005; Kerkhoff *et al.* 2005; Michaletz *et al.* 2014) to account for changes in key traits that influence the thermal response of individual metabolism, as well as potential temperature effects on ecosystem biomass pools. I then test the model's predictions against empirical data collected from a catchment of naturally warmed Icelandic geothermal streams spanning a gradient of 20 ºC.

THEORY

The metabolic theory of ecology (MTE) provides a powerful framework for understanding how temperature affects GPP by linking the photosynthetic rates of an ecosystem's constituent individuals with the size and biomass structure of the community (Enquist *et al.* 2003, 2007; Allen *et al.* 2005; Kerkhoff *et al.* 2005; Yvon-Durocher & Allen 2012; Michaletz *et al.* 2014).

The temperature-dependence of whole organism metabolic rate

Organism-level metabolism, $b(T)$, responds predictably to temperature, increasing exponentially up to an optimum, followed by a more pronounced exponential decline (Figure 4.1). These thermal response curves can be quantified using a modification of the Sharpe-Schoolfield equation for high temperature inactivation (Schoolfield *et al.* 1981a):

$$b(T) = \frac{b(T_c) m^{\alpha} e^{E(\frac{1}{kT_c} - \frac{1}{kT})}}{1 + e^{E_h(\frac{1}{kT_h} - \frac{1}{kT})}} \quad (4.1)$$

where $b(T)$ is the rate of metabolism at temperature T, in Kelvin (K), k is Boltzmann's constant (8.62×10^{-5} eV K^{-1}), E is the activation energy (in eV), E_h characterises temperature-induced inactivation of enzyme kinetics above T_h, which is the temperature at which half the enzymes are inactivated. In this expression, $b(T_c)$ is the rate of metabolism normalised to a reference temperature (e.g. 10 ºC), where no low or high temperature inactivation occurs and m^{α} is the mass dependence of metabolic rate characterised by an exponent α, that ranges between ¾ and 1 across multicellular and unicellular autotrophs (Gillooly *et al.* 2001; DeLong *et al.* 2010). Equation 4.1 yields a maximum metabolic rate, $b(T_{opt})$, at an optimum temperature, T_{opt}.

$$T_{opt} = \frac{E_h T_h}{E_h + k T_h ln\left(\frac{E_h}{E} - 1\right)} \quad (4.2)$$

The parameters in equations 4.1 & 4.2, which govern the height and shape of the thermal response curve can be considered "metabolic traits" (Padfield *et al.* 2016) and have long been known to reflect adaptation to the prevailing thermal environment (Berry & Bjorkman 1980; Huey & Kingsolver 1989). Equation 4.1 can be simplified to the Arrhenius equation,

$$b(T) = b(T_c) m^{\alpha} e^{E(\frac{1}{kT_c} - \frac{1}{kT})} \quad (4.3)$$

which captures only the rising part of the thermal response curve, if the temperatures organisms experience in the environment are below T_{opt} (Savage *et al.* 2004; Dell *et al.* 2011; Sunday *et al.* 2012). I use this simpler, more tractable model of the temperature-dependence in the following theory, which attempts to explore the mechanisms driving the emergent temperature sensitivity of ecosystem-level gross primary production. At the organism-level, the size and temperature-dependence of gross photosynthesis can be characterised as:

$$gp(T) = gp(T_c)m^{\alpha}e^{E_{gp}\left(\frac{1}{kT_c}-\frac{1}{kT}\right)} \quad (4.4)$$

where $gp(T)$ is the rate of gross photosynthesis at temperature T, $gp(T_c)$ is the rate of gross photosynthesis normalised to a reference temperature and E_{gp} is the activation energy of gross photosynthesis. Net photosynthesis, np, which is the amount of photosynthate available for allocation to biomass production after accounting for autotroph respiration, is given by,

$$np(T) = gp(T_c)m^{\alpha}e^{E_{gp}\left(\frac{1}{kT_c}-\frac{1}{kT}\right)} - r(T_c)m^{\alpha}e^{E_r\left(\frac{1}{kT_c}-\frac{1}{kT}\right)} = np(T_c)m^{\alpha}e^{E_{np}\left(\frac{1}{kT_c}-\frac{1}{kT}\right)} \quad (4.5)$$

where $np(T)$ is the rate of net photosynthesis at temperature T, $r(T_c)$ is the rate of autotrophic respiration normalised to a reference temperature, T_c, and E_{np} and E_r are the activation energies of net photosynthesis and autotrophic respiration. The form of equation 4.5 implies that the temperature sensitivity of np will not strictly follow a simple Boltzmann-Arrhenius relation. Nevertheless, I can approximate the temperature sensitivity of net photosynthesis using an apparent activation energy, E_{np}, with a reasonable degree of accuracy (see supplementary methods for a derivation of E_{np} and Appendix Figure 13).

Scaling metabolism from organisms to ecosystems

Using Equation 4.4 and principles from MTE, the rate of gross primary productivity per-unit-area of an ecosystem, A, can be approximated by the sum of the photosynthetic rates of its constituent organisms (Figure 4.1c):

$$GPP_s(T) = GPP(T_c)e^{E_{GPP}(\frac{1}{kT_c}-\frac{1}{kT})} \quad (4.6)$$

where $GPP_s(T)$ is the rate of gross primary production in ecosystem s, at temperature T, $GPP(T_c) = \frac{1}{A}\sum_{i=1}^{J} gp_i(T_c)\, m_i^{\alpha}$, is the ecosystem-level metabolic normalisation constant, where J is the total number of individual organisms, i, which comprise all autotrophs in s. In equation 4.6, the apparent long-term temperature-dependence of ecosystem-level gross primary production, E_{GP}, is assumed to be equal to that of the average temperature-dependence for individual-level gross photosynthesis, E_{gp}, provided that the ecosystem-level normalisation constant, $GPP(T_c)$, is independent of temperature (Figure 4.1d). However, if $gp_i(T_c)$ or total autotrophic biomass, $M_s = \frac{1}{A}\sum_{i=1}^{J} m_i$, exhibit temperature-dependence, for example via acclimation or adaptation acting on $gp_i(T_c)$ or covariance between resource availability, temperature and M_s, then the scaling of the activation energy from individuals to ecosystems will no longer hold (e.g. $E_{GPP} \neq E_{gp}$). Thus, ecological processes that influence M_s and evolutionary dynamics which can shape variation in $gp_i(T_c)$ have the potential to play an integral, but as yet underappreciated role in mediating the response of ecosystem metabolism to temperature if they modify the metabolic capacity of ecosystem biomass pools (Kerkhoff *et al.* 2005; Davidson & Janssens 2006; Enquist *et al.* 2007; Michaletz *et al.* 2014).

Incorporating indirect effects of temperature on ecosystem metabolism

Previous work on aquatic and terrestrial autotrophs has shown that autotrophs can adjust their respiratory and photosynthetic normalisation constants; up-regulating rates at low temperatures and down-regulating at high temperature to compensate for the constraints of thermodynamics on enzyme kinetics (Atkin *et al.* 2015; Padfield *et al.* 2016; Reich *et al.* 2016; Scafaro *et al.* 2016). Such changes may be manifest in several ways. First, over relatively short time scales (e.g. within the generation time of an individual) acclimation of cellular physiology (a form of phenotypic plasticity) can result in adjustments to photosynthetic and respiratory capacity that partially compensate for the effects of changes in temperature (Atkin & Tjoelker 2003; Yamori *et al.* 2014). Second, over multiple generations, adaptive evolution driven by natural selection on traits that influence metabolism can also result in temperature-compensation of photosynthetic and respiratory capacity. Such evolutionary shifts in metabolic traits have been shown to occur both via rapid micro-evolutionary responses, resulting in warm- or cold-adapted genotypes of the same species (Padfield *et al.* 2016; Schaum *et al.* 2017) as well as macro-evolutionary divergence in metabolic traits among different species (Addo-Bediako *et al.* 2002; Deutsch *et al.* 2008; Sunday *et al.* 2012). Finally, when scaling up to an ecosystem, the distribution of metabolic traits across the constituent individuals will emerge from temperature-driven selection on trait variation arising both within and among species. When temperature imposes a strong selective force, and variation in temperatures are maintained over time scales that span multiple generations (e.g. over spatial thermal gradients or due to global warming), I

expect temperature-driven changes in $gp_i(T_c)$ along thermal gradients to reflect selection on trait variation within and among taxa that has arisen via adaptive evolution. In the absence of an explicit first principles derivation, we can approximate the effects of temperature-driven selection on $gp_i(T_c)$ as

$$gp_i(T_c) \approx e^{E_a(\frac{1}{kT_c}-\frac{1}{kT})} \quad (4.7)$$

where $E_a$characterises the change in $gp_i(T_c)$ with temperature owing to temperature-driven selection. Substituting the temperature-dependence for $gp_i(T_c)$ into Equation 4.6 and simplifying, yields the following expression for the temperature-dependence of gross primary production,

$$GPP_s(T) = GPP(T_c)e^{E_a+E_{gp}(\frac{1}{kT_c}-\frac{1}{kT})} \quad (4.8)$$

Under the "hotter-is-better" model of thermal adaptation (Figure 4.1a), where a single activation energy governs the temperature-dependence of metabolism within and across species (Gillooly *et al.* 2001; Savage *et al.* 2004; Angilletta *et al.* 2010) and $E_a = 0$, the ecosystem-level temperature-dependence would equal that of individual-level metabolism (i.e. $E_{GPP} = E_{gp}$; Figure 4.1d) – this is the typical assumption made in metabolic theory (Brown *et al.* 2004; Demars *et al.* 2016). However, when $E_a \neq 0$, $E_{GPP} = E_a + E_{gp}$, and the ecosystem-level temperature-dependence will deviate from the average organism-level temperature dependence owing to the effects of temperature-driven selection on $gp_i(T_c)$. If selection results in complete compensation (i.e. $E_a = -E_{gp}$; Figure 1b), and M_s does not covary with temperature, then ecosystem-level gross primary production will be independent of temperature (i.e. $E_{GPP} = 0$; Figure 4.1d (2)). Following the same reasoning, any temperature-dependence in M_s will also result in deviations from the average individual-level activation

energy. For example, recent experimental work has shown that covariance between temperature and rates of nutrient cycling can cause M_s to increase with temperature (Welter *et al.* 2015; Williamson *et al.* 2016), $M_s \approx e^{E_b(\frac{1}{kT_c}-\frac{1}{kT})}$, where E_b characterises the temperature-dependence of total autotrophic biomass. When $E_b > 0$, substituting in the temperature-dependence for M_s into Equation 4.8 leads to an increase in the ecosystem-level temperature-dependence regardless of the mode of thermal adaptation ($E_{GPP} = E_{gp} + E_b + E_a$; Figure 4.1d (1)). This model emphasises how different ecological and evolutionary mechanisms that drive temperature-dependent variation in organism-level metabolic traits and/or ecosystem biomass pools can influence the emergent long-term temperature sensitivity ecosystem metabolism (Figure 4.1c:d).

Using metabolic scaling theory (see Eqn's. 4.1 to 4.8), I can investigate alternative hypotheses on the effects of temperature-driven selection and covariance between biomass and temperature on the long-term temperature-dependence of gross primary production (GPP). I define the long-term temperature-dependence of GPP as that derived across ecosystems that differ in average temperature. To determine the GPP for any given ecosystem, I created an arbitrary number of taxa (in this case n = 30), and assigned them each a mass, m, activation energy, E, and individual normalisation constant, $b(T_c)$, each drawn from normal distributions that were constrained to return positive values ($gp(T_c)$: mean = 10, s.d. = 0.5; E: mean = 0.65 eV, s.d. = 0.2; m = 100 g, s.d. = 100). I then created abundance and biomass distributions consistent with the energetic equivalence rule (Damuth 1987; White *et al.* 2007)

in which the relationship between abundance and average body size of a taxa $N \propto m$, is the inverse of the relationship between average body size and metabolic rate. In this simulation, the size-scaling exponent of body size and metabolic rate is assumed to be 0.75, so the abundance of each taxa within the ecosystem is proportional to $N \propto m^{-0.75}$. Total biomass of each taxa was then calculated as the product of N and m which becomes invariant across taxa within each ecosystem. GPP is then the sum of the gross photosynthetic rates of all organisms comprising the biomass pool at a given temperature (Figure 4.1c).

To explore a range of hypotheses for the indirect effects of temperature-driven selection on the photosynthetic normalisation, E_a, and biomass-temperature covariance, E_b, on the long-term temperature-dependence of GPP, E_{GPP}, I simulated 30 ecosystems each consisting of 30 taxa along a gradient in temperature (10 to 50 ºC). In scenario 1, the photosynthetic normalisation, $gp(T_c)$, and biomass are independent of temperature (E_b & E_a = 0 eV). Under these circumstances the long-term temperature-dependence of GPP will be equal to the average temperature-dependence of organism-level gross photosynthesis ($E_{GPP} = E_{gp}$; Figure 4.1d (1)). In scenario 2, we simulate the effects of complete temperature-compensation of organism-level gross photosynthesis, by making the temperature-dependence of $gp(T_c)$ equal, but of opposite sign to that of E_{gp} ($E_a = -E_{gp}$), with biomass independent of temperature (E_b = 0 eV). Under this scenario, long-term GPP is independent of temperature (Figure 4.1d (2)). In scenario (3), we allow biomass to positively covary with temperature ($E_b = E_{gp}$), whilst making $gp(T_c)$ temperature-invariant

(E_a = 0 eV). In this case, the long-term temperature-dependence of GPP is amplified with respect to that of organism-level gross photosynthesis ($E_{GPP} > E_{gp}$; Figure 4.1d (1)).

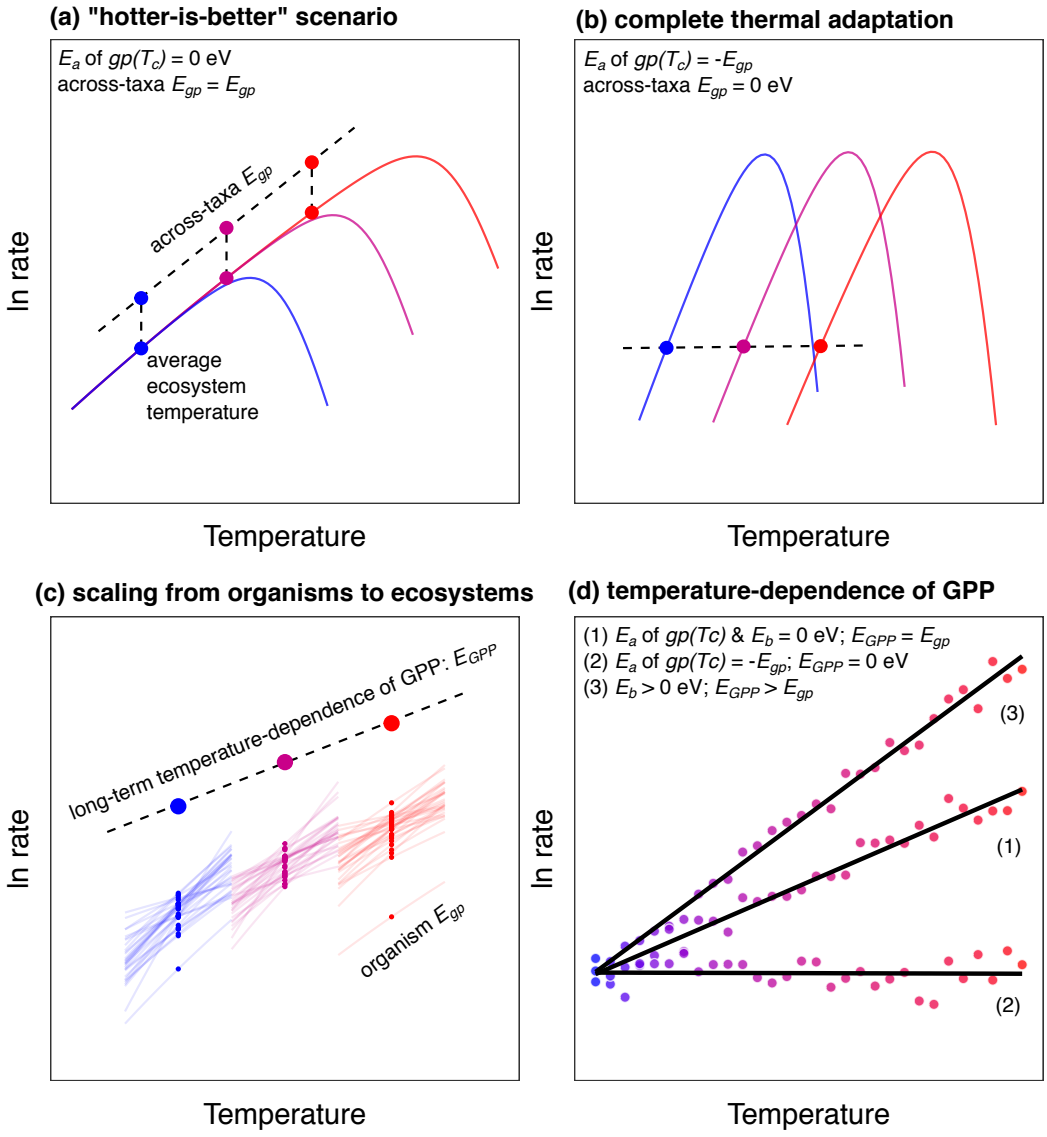

Figure 4.1. Scaling metabolism from organisms to ecosystems.
(a)In a "hotter-is-better" scenario, there is no temperature-driven selection on the photosynthetic normalisation, $gp(T_c)$. Thermal adaptation shifts optimum performance up and down an "across-taxa" thermal response curve, where the temperature-dependence within and across taxa is the same. (b) Under complete temperature-compensation, temperature-driven selection on $gp(T_c)$ is the inverse of the temperature-dependence of organism-level gross photosynthesis, E_{gp}, resulting in an equalisation of performance across average temperatures (filled circles in b). (c) The long-term temperature-dependence of GPP, E_{GPP}, across ecosystems varying in average temperature is an emergent property influenced by the thermal response of each organism in the ecosystem and the total biomass. (d) Metabolic theory assumes that E_{GPP} is equal to E_{gp} (1). However, if temperature-driven selection results in systematic trait variation in the photosynthetic normalisation ($E_a = -E_{gp}(2)$), or biomass is positively temperature-dependent ($E_b > 0$; (3)), E_{GPP} may deviate from E_{gp}. In (a:d) blue represents cold temperatures and red represents hot temperatures.

These simulations demonstrate how indirect effects of temperature-driven selection on the photosynthetic normalisation and covariance between biomass and temperature can have as large an effect on the emergent temperature-dependence of ecosystem metabolism as the direct effects of temperature on the kinetics of photosynthesis.

I now use measurements of the temperature-dependence of organism- and ecosystem-level photosynthesis from a catchment of naturally warmed geothermal streams to test the expectations of the model and investigate how ecological and evolutionary processes shape the long-term temperature sensitivity of GPP. Critically, this system allows me to measure photosynthetic responses to temperature at both organism and ecosystem scales from sites that are in close proximity, yet differ substantially in their thermal history (i.e. 20 ºC *in situ* temperature gradient among sites).

METHODS

Study site

The study was conducted in a geothermally active valley close to Hveragerði village, 45 km east of Reykjavík, Iceland (64.018350, -21.183433). The area contains a large number of mainly groundwater-fed streams that are subjected to differential natural geothermal warming from the bedrock (O'Gorman *et al.* 2014). Twelve streams have been mapped in the valley with average temperatures ranging from 7 – 27 ºC (Appendix Figure 7 & Appendix Table 6). We measured a number of physical (width, depth, velocity) and chemical (pH, conductivity, nitrate, nitrite, soluble reactive phosphate, ammonium) variables

across the catchment (Appendix Table 7) and none of these variables were significantly correlated with temperature (Appendix Table 8). The study was carried out during May and June in 2015 and 2016.

Inorganic nutrients

Water samples for measuring dissolved inorganic nutrient concentrations (NO_2^-, NO_3^-, NH_4^+ and PO_4^{3+}; μmol L^{-1}) were collected from each stream in 2016. Samples were filtered (Whatmann GF/F) and stored frozen at -20 ºC for subsequent analysis using a segmented flow auto-analyser (Appendix Table 7) (Kirkwood 1996).

Measuring the organism-level metabolic thermal response

I sampled 13 of the most abundant macroscopic cyanobacteria, filamentous eukaryotic algae, and bryophyte taxa from 8 streams spanning the catchment's full thermal gradient to characterise their metabolic thermal responses using an O_2 electrode system. Multiple taxa were sampled from four streams where more than one taxon was at high density (Appendix Table 9). Because I sampled macroscopic algae – e.g. crops of filamentous algae or bryophyte fronds – measurements of metabolic rate are assumed to be at the level of the focal organism. I acknowledge that commensal microbes (e.g. protists and bacteria) are likely to be associated with these samples, but I assume that these organisms contribute a tiny fraction of the total biomass relative to the focal organism. Given the sensitivity of the O_2 electrode, these commensal organisms likely make a negligible contribution to the measurements of metabolism. Rocks dominated by a focal alga were brought back to the

laboratory and maintained in water from their natal stream over the course of the metabolic measurements. Metabolic rates were measured via changes O_2 concentration in a Clark-type oxygen electrode (Hansatech Ltd, King's Lynn UK Chlorolab2). For each incubation, a fresh sample of the focal organism was suspended in stream water from the natal stream filtered at 0.7 μm and placed in a gas tight cuvette (2 mL) associated with the O_2 electrode. The cuvette was surrounded by a water-jacket, connected to a recirculating water bath, which maintained a constant temperature. A magnetic stirrer within the cuvette ensured homogeneity of O_2 concentration throughout the chamber. For each focal organism, measurements first entailed characterising a photosynthesis-irradiance (PI) curve from 0 – 2000 μmol m^{-2} s^{-1} at the average temperature of the stream from which it was sampled. Net photosynthesis (np) was measured as O_2 evolution. Light intensities were maintained for one minute and were increased in intervals of 50 μmol^{-1} m^{-2} s^{-1} up to 300 μmol^{-1} m^{-2} s^{-1}, and then in intervals of 100 μmol^{-1} m^{-2} s^{-1} up to 1000 μmol^{-1} m^{-2} s^{-1}, followed by 200 μmol steps up to 2000 μmol^{-1} m^{-2} s^{-1}. Rates of respiration (r) were always measured as O_2 consumption in the dark immediately after the light response. This yielded a photosynthesis-irradiance curve from which the optimal light intensity for net photosynthesis was estimated using a modification of Eilers' photoinhibition model (Eilers & Peeters 1988) fitted via non-linear least squares regression (Appendix Figure 8):

$$np(I) = \frac{np_{max} I}{(np_{max}/\alpha {I_{opt}}^2)\, I^2 + \left(1 - \left(\frac{2np_{max}}{\alpha I_{opt}}\right)\right) I + \frac{np_{max}}{\alpha}} - r \qquad (4.9)$$

where $np(I)$, is the rate of net photosynthesis at irradiance, I, np_{max} is the photosynthetic maximum that occurs at optimal light, I_{opt}, α controls the

gradient of the initial slope and r is respiration. The optimum light intensity (I_{opt}, μmol^{-1} m^{-2} s^{-1}) for each taxon was then used for measuring net photosynthesis at all other assay temperatures in the acute thermal gradient experiments. This makes the assumption that I_{opt} does not vary with instantaneous temperature (Schaum *et al.* 2017). Instantaneous rates of net photosynthesis (at I_{opt}) and respiration were then taken at temperatures ranging from 5 to 50 ºC. Rates of gross photosynthesis were calculated by summing rates of net photosynthesis and respiration.

Rates of photosynthesis and respiration were normalised to biomass by expressing each rate measurement per unit of chlorophyll *a*. Chlorophyll *a* extraction was achieved for each incubation by grinding the sample with methanol until all tissue had been broken down, centrifugation and measuring chlorophyll *a* extinction coefficients on a spectrophotometer. Total chlorophyll *a* (μg) was then calculated by measuring absorbance at 750 nm, 665 nm and 632 nm.

$$\text{Chl } a = (13.26(A_{665} - A_{750}) - 2.68(A_{665} - A_{750})) \times 10^{-3} \quad (4.10)$$

Acute temperature responses of chlorophyll-normalised gross and net photosynthesis and respiration were fitted to the modified Sharpe-Schoolfield equation for high temperature inactivation (Equation 4.1). Best fits for each thermal response curve were determined using non-linear least squares regression using the 'nlsLM' function in the 'minpack.lm' (Elzhov *et al.* 2009) package in R statistical software (R Core Team 2014; v3.2.2), following the methods outlined in *Chapter 1*.

I tested for temperature-driven selection on metabolic traits by assessing whether the parameters in eqns. 4.1 and 4.2 as well as the rate of gross photosynthesis at the average temperature of the natal stream of the focal organism, $gp(T_s)$, varied systematically with temperature across the catchment. I fitted the metabolic traits to a modified Boltzmann-Arrhenius function within a linear mixed effects modelling framework:

$$\ln z(T) = \ln z(T_c) + E_a \left(\frac{1}{kT_c} - \frac{1}{kT}\right) + \varepsilon^t \quad (4.11)$$

where z is the metabolic trait at stream temperature, T, $z(T_c)$ is the value of the trait at the mean temperature across all streams, T_c, and E_a is the activation energy that determines how much z changes as a function of T due to temperature-driven selection and ε^t is a random effect on the intercept accounting for multiple measurements of the same metabolic trait of each focal organism (i.e. one value each for gross and net photosynthesis and respiration). I fitted Eq. 4.11 to each metabolic trait with stream temperature, flux (3 level factor with 'gross' and 'net photosynthesis' and 'respiration') and their interaction as fixed effects (Appendix Table 9). Significance of the parameters were determined using likelihood ratio tests. Model selection was carried out on models fitted using maximum likelihood and the most parsimonious model was refitted using restricted maximum likelihood for parameter estimation.

Measuring *in situ* rates of ecosystem-level gross primary production

Ecosystem metabolism was calculated from measurements of dissolved oxygen over time in each stream using the single station method (Odum 1956). Sensors were deployed in all streams and at multiple sites within a stream

where temperature gradients existed within streams due to differential geothermal warming. Dissolved oxygen concentration and temperature were monitored at 1-minute intervals using miniDOT optical dissolved oxygen loggers (PME Inc) (Appendix Figure 9 & Appendix Figure 10). Light sensors **(**Licor LI-193 spherical quantum sensor**)** were deployed simultaneously at two sites in the centre of the catchment. Physical variables of each stream, including the depth (m), width (m), velocity (m s^{-1}, measured using Hatch FH950), were measured along horizontal transects at approximately 10 m intervals up to the source of the stream. Values for depth, width and velocity were averaged across the reach (Appendix Table 7).

The change in O_2 concentration at a single station between two subsequent measurements (ΔDO) can be approximated as:

$$\Delta\, DO = \frac{[O_2]_t - [O_2]_{t-1}}{\Delta t} \quad (4.12)$$

with $[O_2]_t$ the concentration of oxygen (mg L^{-1}) at time t and can be modelled using a framework based on Odum's O_2 change technique (Odum 1956):

$$\Delta\, DO = GPP - ER \pm G \quad (4.13)$$

where $\Delta\, DO$ is the composite of volumetric gross primary productivity, GPP (g m^{-3} min^{-1}), minus volumetric ecosystem respiration, ER (g m^{-3} min^{-1}) and G is the net exchange of oxygen with the atmosphere (g O_2 m^{-3}). The net exchange of oxygen with the atmosphere (G) is the product of the O_2 gas transfer velocity, K (m min^{-1}), and the O_2 concentration gradient between the water body and the atmosphere (temperature and atmosphere corrected DO concentration at 100% saturation minus $[O_2]_t$) over the measurement interval.

The gas transfer velocity, K, was calculated using the surface-renewal model and corrected for the stream temperature:

$$K = 50.8\, V^{0.67} \times D^{-0.85} \times 1.024^{(T-20)} \quad (4.14)$$

where V is velocity (cm s^{-1}), D is the mean stream depth (cm) adjusted for stream temperature, T (Bott 1996). This equation returns K in cm hr^{-1} which was subsequently converted into m min^{-1}. Estimated rates of reaeration, derived using the surface renewal model from measurements of velocity and depth, correspond well to reaeration rates measured experimentally using propane additions in an adjacent Icelandic catchment with comparable physico-chemical characteristics (Appendix Figure 13; Demars *et al.* 2011).

Measurements of dissolved oxygen concentration, light and temperature were averaged over 15 minute intervals for each 24-hour period. The net metabolic flux for a given measurement interval is equal to $\Delta\, DO - G$. During the night (where light < 5 μmol m^{-2} s^{-1}), GPP is zero, so the net metabolic flux is equal to ER. During the day, ER was determined by interpolating average ER over the defined night period. GPP for each daytime interval was the difference between net metabolism flux and interpolated ER. Daily volumetric rates of GPP (g O_2 m^{-3} day^{-1}) were calculated as the sum of the 15-minute rates over each 24-hour period. Volumetric rates were converted to areal units (g O_2 m^{-2} day^{-1}) by multiplying by the mean water depth of the stream reach. At the end of the two years of sampling, I had 39 daily estimates of GPP across the 15 sites (Appendix Table 11).

In 2016, I also measured autotrophic biomass density (g Chl *a* m^{-2}) across the catchment by taking measurements of chlorophyll *a*. Autotrophic biomass was estimated by removing all organic material from a 30 cm^2 template on 3 randomly chosen rocks from each stream. Biofilm and plant material was removed from within the sample area using forceps and a stiff bristled brush, rinsed with distilled water and the slurry decanted into a Falcon tube. Chlorophyll was then extracted and quantified using the protocol detailed above. The total autotrophic biomass, M_s, of each stream reach was estimated by multiplying average autotrophic biomass density by the total reach area, which was estimated from the mean width and the upstream distance the oxygen sensor integrated over (Chapra & Di Toro 1991; Demars *et al.* 2015),

$$d = \frac{3V \times depth}{K} \quad (4.15)$$

where three times the velocity of the stream (*V,* m min^{-1}), multiplied by stream depth (m) and divided by the gas transfer velocity (K; m min^{-1}) gives the approximation of the distance upstream integrated by the single station method (*d*; m) (Grace & Imberger 2006). Biomass-corrected rates of GPP per stream (g O_2 g Chl a^{-1} day^{-1}) were calculated by dividing areal rates of GPP by the total autotrophic biomass, M_s, in the upstream reach.

I used linear mixed-effects modelling to investigate the overall temperature-dependence of GPP across the catchment, allowing me to control for the hierarchical structure of the data (e.g. variance of days nested within years nested within streams). I characterised the temperature dependence of GPP with a linearised version of the Boltzmann-Arrhenius function in a linear mixed effects model:

$$\ln GPP_s(T) = E_{GPP}\left(\frac{1}{kT_c} - \frac{1}{kT}\right) + (\langle \ln GPP(T_c)\rangle + \varepsilon_P^{s/y/d}) \quad (4.16)$$

where $GPP_s(T)$ is the rate of gross primary production in stream *s* on year *y* on day *d* at temperature *T* (Kelvin), E_{GPP} is the activation energy (eV) which characterises the exponential temperature sensitivity of photosynthetic rates, $\langle \ln GPP(T_c) \rangle$ is the average rate of GPP across streams and days normalised to T_c = 283 K (10 ºC) and $\varepsilon_P^{s/y/d}$ is a nested random effect that characterises deviations from $\langle \ln GPP(T_c) \rangle$ at the level of *d* within *y* within *s*. Significance of the parameters and model selection was carried out as described above for the analysis of the population-level metabolic traits (Table 4.1).

I tested for the effect of total autotrophic biomass and temperature on *in situ* GPP across the catchment using the data from 2016 (where I also quantified autotroph biomass) by undertaking a multiple regression by expanding eq. 16 to include the effect the biomass on GPP:

$$\ln GPP_s(T) = E_{GP}\left(\frac{1}{kT_c} - \frac{1}{kT}\right) + \beta \ln M_s + (\langle \ln GPP(T_c)\rangle + \varepsilon_P^{s/d}) \quad (4.17)$$

where β characterises the power-law scaling of $GPP_s(T)$ with M_s and the random effects specification changed to account for deviation from $\langle \ln GP(T_c)\rangle$ between days nested within streams. Model selection was as described above (Table 4.1).

RESULTS

Temperature-driven selection on metabolic traits

Organism-level gross photosynthesis and respiration followed unimodal responses to acute temperature variation and were well fit by equation 4.1

(Figure 4.2a-b). I predicted exponential declines in the metabolic normalisation constants, moving from cold to warm environments, owing to the effects of temperature-driven selection. Consistent with this hypothesis, the log-transformed rates of gross photosynthesis, $(\ln gp(T_c))$ and respiration $(\ln r(T_c))$ normalised to a reference temperature, T_c = 10 ºC, declined linearly with increasing stream temperature with the same activation energy (E_a = -0.64 eV; 95% CI: -1.22 to -0.05 eV; Figure 4.2c). Since $np(T_c) = gp(T_c) - r(T_c)$, the normalisation for net photosynthesis also declined with increasing temperature with an E_a = -0.64 eV.

Because the dominant autotroph taxa varied across the streams (Appendix Table 10), the decline in the photosynthetic trait, $gp(T_c)$, with increasing stream temperature is likely influenced by selection operating on trait variation both within and among taxa. To explore the effects of temperature-driven selection within taxa, I analysed data from only the most common taxon, cyanobacteria from the genus *Nostoc* spp.*,* which were distributed across 5 streams spanning a gradient of 10.2 ºC. $gp(T_c)$, $np(T_c)$ and $r(T_c)$ also decreased with increasing stream temperature in *Nostoc* with the thermal sensitivity not significantly different from that of all the autotroph taxa together (Appendix Figure 12). An important consequence of the decrease in $gp(T_c)$ with increasing stream temperature was that rates of gross photosynthesis at the average temperature of each stream, $gp(T_s)$, were independent of temperature across the catchment's thermal gradient (Figure 4.2d), suggesting that temperature-driven selection on photosynthetic traits led to complete temperature-compensation of organism-level metabolism.

Both the optimum temperature, T_{opt}, and T_h, which is the temperature at which half the enzymes are inactivated, were positively correlated with average stream temperature (Appendix Table 10) providing further evidence that each taxon was locally adapted to its natal thermal regime. I found no evidence for systematic variation in the activation or inactivation energies (E or E_h) across the thermal gradient suggesting these traits are unlikely to be under strong selection (Appendix Table 10). Previous work has shown that photosynthesis has a lower activation energy than respiration (Allen *et al.* 2005; López-Urrutia *et al.* 2006; Padfield *et al.* 2016). In contrast, I found that the average activation energies of gross photosynthesis and respiration were not significantly different and could be characterised by a common activation energy (E = 0.87 eV; 95% CI = 0.77 to 0.97 eV). Similarly, E_h, which characterises inactivation of kinetics past the optimum was not significantly different between fluxes and could be characterised by a common value for respiration and photosynthesis (E_h = 4.91 eV; 95% CI: 3.95 – 5.97 eV).

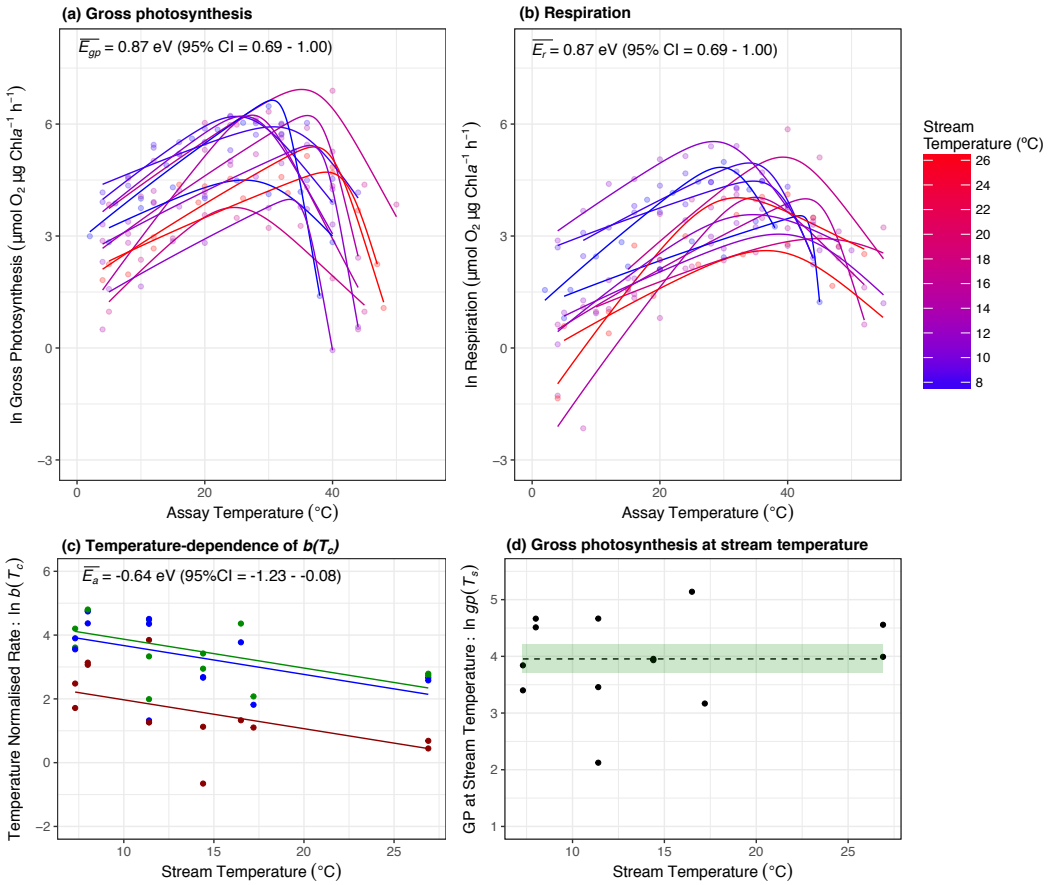

Figure 4.2. Temperature-driven shifts in metabolic traits.
(a,b) Acute thermal response curves for gross photosynthesis and respiration were measured for each isolated autotroph from streams spanning average temperatures from 7 ºC (blue) to 27 ºC (red). Fitted lines are based on the best-fit parameters from non-linear least squares regression using the modified Sharpe-Schoolfield model (see Methods). (c) Metabolic rates normalised to 10 ºC, $b(T_c)$, decrease exponentially with increasing stream temperature for gross photosynthesis (green), net photosynthesis (blue) and respiration (red) (d) Rates of gross photosynthesis at the average stream temperature showed no temperature dependence. Fitted lines in (c) and (d) and coloured bands in (d) represent the best fit and the uncertainty of the fixed effects of the best linear mixed effect model.

Ecosystem level gross primary productivity

Based on the observation that the activation energies of gross photosynthesis (E_{gp}) and the parameter describing the temperature-driven changes in $gp(T_c)$, (E_a), were similar, but of opposite sign, the model for the scaling of metabolism from organisms to ecosystems (Eq. 4.8) predicts that rates of *in situ* gross

primary production (GPP) should be independent of temperature across the catchment (e.g. $E_{GPP} = E_{gp} + E_a \approx 0$), provided that biomass does not covary with temperature. Rates of GPP increased with temperature and the long-term temperature sensitivity of GPP yielded an activation energy of E_{GPP}= 0.57 eV (95% CI: 0.10 – 1.04 eV; Figure 4.3a).

To investigate potential covariance between temperature and biomass, M_s, and its impact on the temperature-dependence of GPP, in 2016 I also quantified total autotrophic biomass, M_s. Autotroph biomass density increased systematically with temperature across the catchment with a temperature sensitivity of E_b = 0.68 eV (95% CI: 0.24 – 1.12 eV; Figure 4.3b). The similarity between E_{GPP} and E_b – they have 95% confidence intervals that overlap – indicates that covariance between autotrophic biomass and temperature could be the main driver of the temperature-dependence of GPP across the catchment.

I quantified the effects of both temperature and M_s on GPP using multiple regression in a mixed effects modelling framework for data collected in 2016 (see Methods). The best fitting model included only $\ln(M_s)$ as a predictor (Table 4.1; Figure 4.3c) and after controlling for variation in $\ln(M_s)$, rates of biomass-specific GPP were independent of temperature across the catchment (Table 4.1; Figure 4.3d). These findings are consistent with predictions from our model and provide evidence that systematic variation in the photosynthetic normalisation constant owing to temperature-driven selection results in

complete compensation of biomass-specific metabolic rates at organism and ecosystem scales.

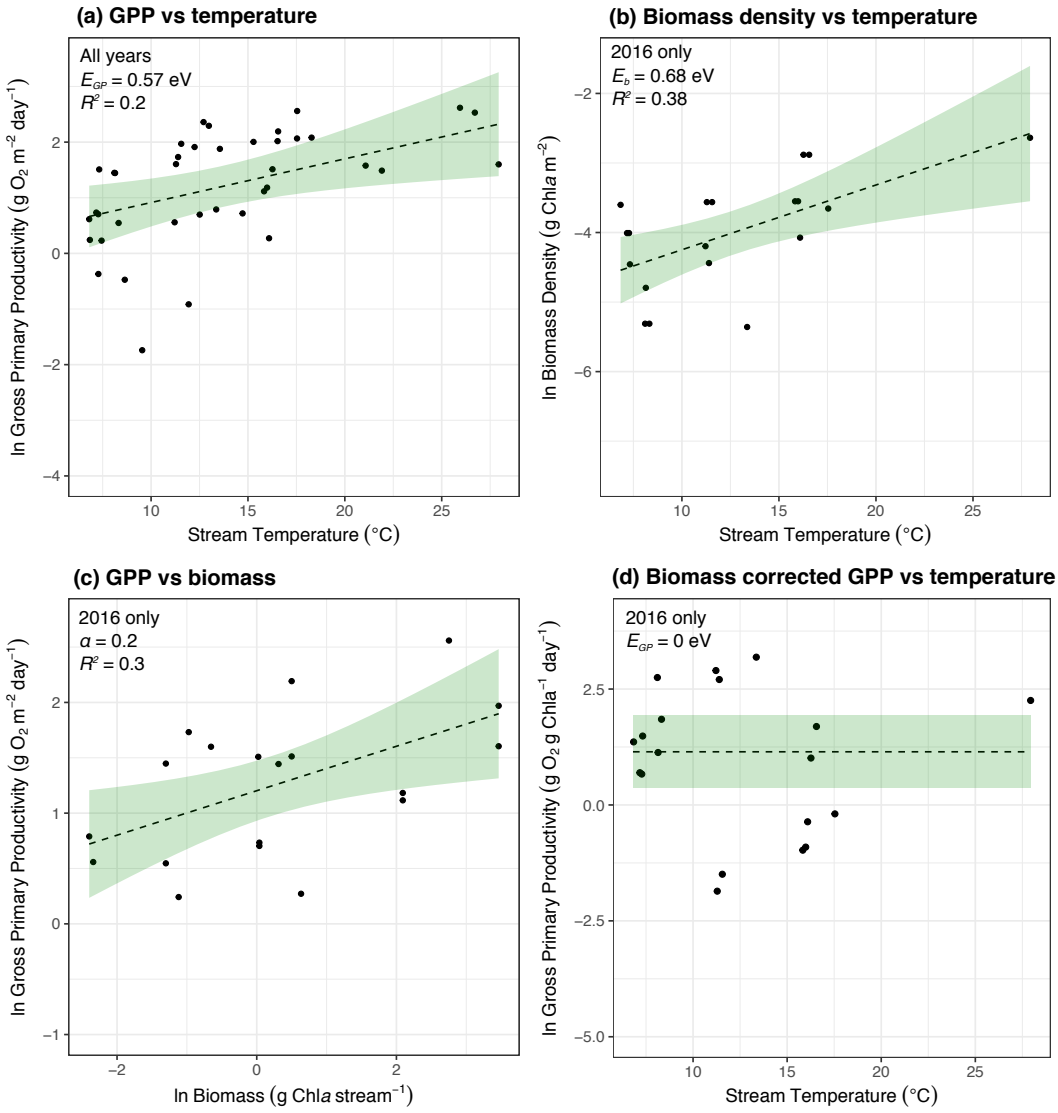

Figure 4.3. The effects of temperature and autotrophic biomass on gross primary productivity.

Gross primary productivity (a) and autotrophic biomass density (b) increase with temperature across the catchment. (c) A multiple regression shows that variation in in situ GPP is driven primarily by changes in autotroph biomass. (d) After accounting for biomass, rates of biomass-corrected GPP are invariant with respect to temperature across the catchment. Fitted lines in (a, c, d) represent the best fit and the uncertainty of the fixed effects of the best linear mixed effect model (Table 1). In (b) the lines represent the fitted line and associated confidence interval of a linear regression.

Table 4.1. Results of the linear mixed effects model analysis for gross primary productivity (GPP) for all years and 2016 only.
The results of the model selection procedure on the fixed effect terms are given and the most parsimonious models are highlighted in bold. Analyses reveal that in situ GPP increased significantly with stream temperature. The analyses for 2016 show that the observed temperature response was driven by covariance between biomass and temperature rather than the direct effects of temperature on rates of photosynthesis per se.

Model	d.f.	AICc	log Lik	L-ratio	P
All years :					
random effects structure random = 1 | stream/year/day					
fixed effects structure					
1. ln GPP ~ 1 + stream temperature	**6**	**82.9**	**-34.0**		
2. ln GPP ~ 1	5	85.8	-36.9	5.80	**0.016**
2016 only :					
random effects structure random = 1 | stream/day					
fixed effects structure					
1. ln GPP ~ 1 + stream temperature + ln biomass	6	48.8	-14.9		
2. ln GPP ~ 1 + ln biomass	**5**	**45.3**	**-15.3**	0.87	0.35
3. ln GPP ~ 1	4	45.8	-17.4	4.25	**0.04**

DISCUSSION

Understanding how ecosystem-level properties like gross primary production (GPP) will respond to global warming is of central importance to predicting the response of the carbon cycle and contributing biogeochemical and food web processes to climate change. It is however a major challenge that requires an integration of physiological, ecological and evolutionary processes that together shape the emergent response of ecosystem metabolism to long-term changes in temperature. I have addressed this key problem by extending the general model of ecosystem metabolism from metabolic theory (Enquist *et al.* 2003,

2007; Allen *et al.* 2005; Kerkhoff *et al.* 2005) and testing its predictions at organism and ecosystem scales in a catchment of naturally warmed geothermal streams. The model and analyses presented here demonstrate that temperature-driven selection on metabolic traits and shifts in ecosystem biomass can be as important as the direct effects of temperature on metabolism in shaping the temperature-dependence of GPP.

The model predicted that when the temperature-dependence of the metabolic normalisation constant across taxa inhabiting environments with different thermal histories is the inverse of organism-level metabolism, the two temperature sensitivities cancel, rendering biomass-specific metabolic rates independent of temperature. Measurements of the thermal response curves for photosynthesis and respiration from the autotrophs isolated across the 20 ºC *in situ* gradient provided strong support for this prediction with rates of gross photosynthesis independent of temperature across the catchment's thermal gradient. In addition, activation energies characterising the temperature-dependence of organism-level gross photosynthesis and the photosynthetic normalisation, $gp(T_c)$, were similar, but of opposite sign.

The exponential decline in $gp(T_c)$ along the *in situ* thermal gradient primarily reflected turnover in the composition of the dominant autotroph taxa across the streams resulting from temperature-driven selection on trait variation among taxa (e.g. species sorting). This result is in line with work demonstrating declines in the metabolic normalisation constant across vascular plant species along broad-scale latitudinal gradients in terrestrial ecosystems (Atkin *et al.*

2015). However, I also found a comparable negative temperature-dependence of $gp(T_c)$ within the most common and widely distributed genus, *Nostoc* spp., indicating that temperature-driven selection within taxa was also an important determinant of variation in this key trait among sites in our study. This finding is consistent with work demonstrating down-regulation of the metabolic normalisation constant in a unicellular alga via rapid (e.g. over 100 generations or 45 days) evolutionary adaptation to an experimental thermal gradient in the laboratory (Padfield *et al.* 2016). Collectively, this work highlights that changes in the metabolic normalisation constant result from temperature-driven selection both within and across taxa and can give rise to complete temperature compensation of metabolic capacity over broad thermal gradients (Figure 4.1b).

Our work shows that temperature-driven selection, in driving complete temperature compensation of organism-level metabolism, had important implications for understanding the temperature dependence of ecosystem-level GPP across the catchment. GPP increased with temperature across the catchment (Figure 4.3a), but it did so because biomass also positively covaried with temperature (Figure 4.3b), likely driven by a shift in algal community composition, with warmer streams being dominated by cyanobacteria capable of fixing nitrogen, alleviating the constraints imposed by the limiting concentrations of inorganic nitrogen observed in these streams (Appendix Table 7) (Welter *et al.* 2015; Williamson *et al.* 2016). After accounting for biomass, biomass-specific GPP was independent of temperature (Figure 4.3c), consistent with the effects of temperature-compensation of organism-level metabolism. These findings confirm the predictions of our model and previous

suggestions (Kerkhoff *et al.* 2005; Enquist *et al.* 2007) that local adaptation and species sorting can yield the paradoxical phenomenon that rates of biomass-specific ecosystem metabolism are independent of temperature over thermal gradients that have been maintained over long timescales.

A great deal of empirical and theoretical work is still required to develop a complete, general theory that predicts how ecosystem properties emerge from evolutionary and community processes. Our work adds to recent efforts to this end (Enquist *et al.* 2007; Yvon-Durocher & Allen 2012; Smith & Dukes 2013; Daines *et al.* 2014; Schramski *et al.* 2015; Smith *et al.* 2016) by showing how the temperature-dependence of ecosystem biomass and the organism-level photosynthetic normalisation alter the emergent temperature sensitivity of ecosystem-level GPP. One important gap in the theory presented here is a mechanistic model for the temperature-dependence of the metabolic normalisation constant owing to temperature-driven selection. Our representation in Equation 4.7 is merely a statistical description of an empirical phenomenon. The metabolic cold adaptation hypothesis seeks to explain the observation that species from cold environments often have higher mass-specific metabolic rates compared to counterparts from warmer regions as an evolutionary adaptation to compensate for lower biochemical reaction rates (Addo-Bediako *et al.* 2002). However, a quantitative, first principles derivation of this pattern remains elusive. Recent work on autotrophs has proposed that down-regulation of respiration rates as organisms adapt to warmer environments is driven by selection to maintain the carbon-use efficiency above a threshold when rates of respiration are more sensitive to temperature than

those of photosynthesis (Padfield *et al.* 2016). Yet, as I have shown here, the assumption that the activation energy of respiration is always larger than that of photosynthesis does not always hold.

A better understanding of the mechanisms that give rise to the emergence of ecosystem properties is central to improving predictions of how global warming will alter the feedbacks between the biosphere on the carbon cycle (Levin 1998; Ziehn *et al.* 2011; Booth *et al.* 2012). Incorporating ecological changes in community biomass and evolutionary shifts in metabolic traits into earth system and ecosystem models should be considered as a priority (Smith & Dukes 2013; Daines *et al.* 2014; Smith *et al.* 2016), especially in light of these findings that the indirect effects of temperature can be of similar magnitude to the direct effects of temperature on physiological rates.

I capitalised on a 'natural experiment' using a geothermally heated stream catchment to show that temperature-driven selection on photosynthetic traits results in an equivalence in biomass normalised GPP over a 20 ºC *in situ* temperature gradient. My results suggest that temperature-driven selection on metabolic traits within and among taxa plays a key role in determining how metabolic rates scale from populations to ecosystems and questions the assumption that the effects of temperature on enzyme kinetics can be applied directly to assess the long-term effects of temperature on ecosystem metabolism (Demars *et al.* 2016). They also shed light on the way in which the interplay between ecological and evolutionary processes could influence the

response of the carbon cycle, and hence constituent food web and biogeochemical processes, to future environmental change.

CONCLUSION

I set out a theory that predicts how the indirect effects of temperature may influence the temperature-dependence of gross primary production. This metabolic scaling theory is then tested empirically in a set of geothermal streams that differ in thermal history. The temperature-dependence of gross primary production is similar to that of the average population-level activation energy. However, this is a result of covariance between biomass and temperature, that increases rates of GPP at higher stream temperatures, and selection on photosynthetic traits within and across taxa that dampens the effects of temperature on GPP. This chapter highlights the importance of considering physiological, ecological and evolutionary processes when predicting how ecosystem respond to warming.

Chapter 5: Discussion

Each chapter of this thesis contained its own detailed discussion; the purpose of this chapter is to highlight the main findings and discuss unifying themes and wider implications.

Synopsis of each chapter:

Chapter 2:

- The model phytoplankton, *Chlorella vulgaris*, rapidly adapted to warming after ~ 45 days (~ 100 generations).
- The temperature-dependence of gross photosynthesis (E_{gp}~ 0.62 eV) was substantially lower than that of respiration (E_r~ 1.26 eV), meaning that as growth temperatures increased, the carbon-use efficiency (CUE) decreased, and this was limiting at 33 ºC.
- Rapid evolution of the metabolic normalisation constant, $b(T_c)$, meant that rates of respiration decreased at higher temperatures, relative to rates of gross photosynthesis. Thus, increased growth rate at 33 ºC was facilitated by increased CUE after 100 generations of growth.
- Maximising CUE could be a potential universal metabolic adaptation to warming.

Chapter 3:

- Gross primary production and community respiration could be predicted simply from the size- and temperature-dependence of individual physiology and the size-structure of phytoplankton communities.

- The temperature-dependence of community gross primary production (E_{GPP}~ 0.74 eV) was lower than that of community respiration (E_{CR}~ 1.42 eV).
- The metabolic normalisation constant of respiration decreased due to long-term warming.
- Trade-offs between increases in average metabolic rate and total community abundance meant that short- and long-term warming did not alter total community metabolism.

Chapter 4:

- Rates of population-level gross photosynthesis at a common temperature decreased as stream temperature increased. This decrease was similar in magnitude, but of opposite sign, to the activation energy of population-level photosynthesis such that gross photosynthesis was independent of stream temperature.
- At the ecosystem-level, rates of gross primary productivity increased with stream temperature, but this was driven by increases in autotrophic biomass with temperature. After correcting for differences in biomass across streams, gross primary productivity per-unit-biomass was independent of stream temperature due to temperature-driven changes in the photosynthetic normalisation constant.
- Indirect effects of temperature are capable of influencing emergent ecosystem-level metabolism as much as the direct effect of temperature on metabolic rate.

General remarks

"Ecosystems are prototypical examples of complex adaptive systems, in which patterns at higher levels emerge from localised interactions and selection processes acting at lower levels"

Simon Levin, 1992

Understanding how ecological patterns and mechanisms link across organisational and spatiotemporal scales is a key question in ecology. Most ecological disciplines study a set of specific research questions in isolation, arbitrarily setting the scales at which they view ecological phenomena. However, almost all ecological phenomena are inextricably linked. It is the organisms within an ecosystem that define its structure and dictate its functioning. And it is the selection processes on those organisms that define their function and ability to persist in any given ecosystem. The necessity to link across ecological scales is of increased importance as a result of recent and projected climate warming. Warming will have profound effects on all levels of biological organisation. Species level responses have been described for many different taxa and include reductions in body size (Gardner *et al.* 2011), shifts in distribution (Parmesan 2006) and changes in physiology and phenology (Walther *et al.* 2002). However, attempts to predict changes of entire communities has proven difficult due to alterations in species interactions that can cause complex and non-linear responses at the community-level (Tylianakis *et al.* 2008; Montoya & Raffaelli 2010; Walther 2010). We need a far more complete understanding of the relationships between community

structure and ecosystem function if we are going to successfully predict the response of the biosphere to warming.

The metabolic theory of ecology (MTE) views metabolism as a key trait that controls ecological phenomena of organisms (e.g. growth rate (Savage *et al.* 2004), abundance, mortality and interspecific interactions (Dell *et al.* 2013)), communities (e.g. body size-abundance scaling (White *et al.* 2007; Yvon-Durocher *et al.* 2010)) and ecosystems (e.g gross primary production and community respiration). Extensions of MTE have successfully predicted ecosystem properties from the constraints of body size and temperature on individual physiology and community structure (Enquist *et al.* 2003; Schramski *et al.* 2015). Such approaches rely on the collection biological data simultaneously over multiple levels of organisation, but this remains an immense challenge.

Throughout this thesis, I investigated the consequences of warming on metabolism from organisms to ecosystems. This has provided novel insights into the impact of warming at these levels in isolation, but critically has allowed me to improve links between patterns observed at different scales. I first investigated the metabolic mechanisms which facilitate thermal adaptation to warming in a species of aquatic phytoplankton. Evolutionary shifts in metabolic traits resulted in increased thermal tolerance after just 45 days of growth at a sub-optimal temperature. Previous work had concentrated on the ability of phytoplankton adapt to environmental change (Lohbeck *et al.* 2012; Schaum &

Collins 2014; Schlüter *et al.* 2014), rather than the mechanism through which it occurred.

Then in *Chapter 3* and *Chapter 4*, I use metabolic scaling theory (MST) to explore how individual physiology and community structure influence ecosystem metabolism. In *Chapter 3*, I demonstrate how phytoplankton community metabolism can be predicted from the size structure and the size- and temperature-dependence of individual physiology. This represents one of the first empirical validations of MST, and may be useful for the wider scientific community as it allows phytoplankton community metabolism to be estimated from the complete size distribution alone. Previous work looking at the size-scaling of phytoplankton metabolism has measured rates of size-fractionated communities (García *et al.* 2015; Huete-ortega *et al.* 2017). I demonstrated that only a single metabolic rate measurement is needed to estimate the size- and temperature-dependence of community metabolism.

Finally, in *Chapter 4*, I explored the links between population- and ecosystem-level metabolism and emphasised the importance of both direct and indirect effects of temperature on ecosystem metabolism. This study measured metabolism at both the population- and ecosystem-level in a set of geothermal streams and extends metabolic scaling theory to incorporate the indirect effects of temperature on ecosystem metabolism. In doing so, I show how temperature-driven selection on population-level photosynthesis constrains the temperature response of ecosystem-level gross primary production. I now

expand on some of these research highlights and identify pathways and considerations for future research.

The importance of the indirect effect of temperature on metabolic rates

The metabolic theory of ecology (MTE) provided a theoretical framework to link cellular and ecosystem processes and gave a set of explicit, quantitative predictions for each experiment. Although the seminal paper on MTE is now more than a decade old, controversies about the theoretical foundations and empirical validity of MTE remain. Validating the assumptions, performance and applicability of MTE will help improve and revise its models and further our understanding of complex ecological phenomena (Price *et al.* 2012).

One of the weaknesses of MTE has been its previous inability to incorporate and account for the indirect effects of temperature on metabolism. Previous work on MTE reported similar temperature sensitivities of metabolism (photosynthesis and respiration) across spatial, temporal and organisational scales (Yvon-Durocher *et al.* 2012). This led some to the assumption that a single mechanism, the thermodynamic constraints of temperature on enzyme kinetics, controls metabolic rates from organisms to ecosystems (Gillooly *et al.* 2001; Allen *et al.* 2005; Demars *et al.* 2016). Furthermore, recent work implied a direct mapping of the temperature-dependence at the enzymatic level to the temperature-dependence of gross primary production (Demars *et al.* 2016). In contrast, numerous studies have shown that changes in the metabolic normalisation constant, $b(T_c)$, after long-term warming can dampen the response of metabolism in the long-term (Bradford *et al.* 2008; Scafaro *et al.*

2016), and over broad spatial scales, biomass corrected rates of ecosystem net primary productivity are invariant across a latitudinal gradient in temperature (Michaletz *et al.* 2014). Aspects community structure (e.g. community composition, size structure and biodiversity) that are known to influence metabolic rates are also likely to change due to warming (Lewandowska *et al.* 2014; Yvon-Durocher *et al.* 2015). However, direct evidence of the indirect effects of temperature on metabolism, using a metabolic theory framework, remains scarce.

The work presented here highlights the importance of indirect effects of temperature on the metabolic rates of individuals, communities and ecosystems. At the population-level, the respiratory normalisation constant decreased relative to photosynthesis after long-term warming. This decrease had a temperature-dependence similar magnitude, but of opposite sign, to that of the activation energy. This is in direct conflict with MTE, which predicts that the downregulation of the metabolic normalisation constant has little impact on metabolic rates, relative to the direct effect of temperature on enzyme kinetics (Gillooly *et al.* 2001). If true, the temperature response of metabolism should be the same across and within populations (Fig. 1.2). I tested this by calculating the rate of gross photosynthesis and respiration at growth temperature for cultures after 100 generations (long-term warming). I then fitted a regression between rate at growth temperature and standardised temperature, $\frac{1}{kT_c} - \frac{1}{kT}$, to both metabolic fluxes and compared them to the average temperature-dependence of gross photosynthesis (0.62 eV) and respiration (1.26 eV) from the thermal response curves (short-term warming). Thermal adaptation

decreased the long-term temperature-dependence compared to the average within-population activation energy for both gross photosynthesis and respiration (Figure 5.1). The temperature-dependence of gross photosynthesis across-populations was 0.37 eV (95% credible intervals = 0.11 – 0.64 eV) and that of respiration was 0.85 eV (95% credible intervals 0.49 -1.21 eV).

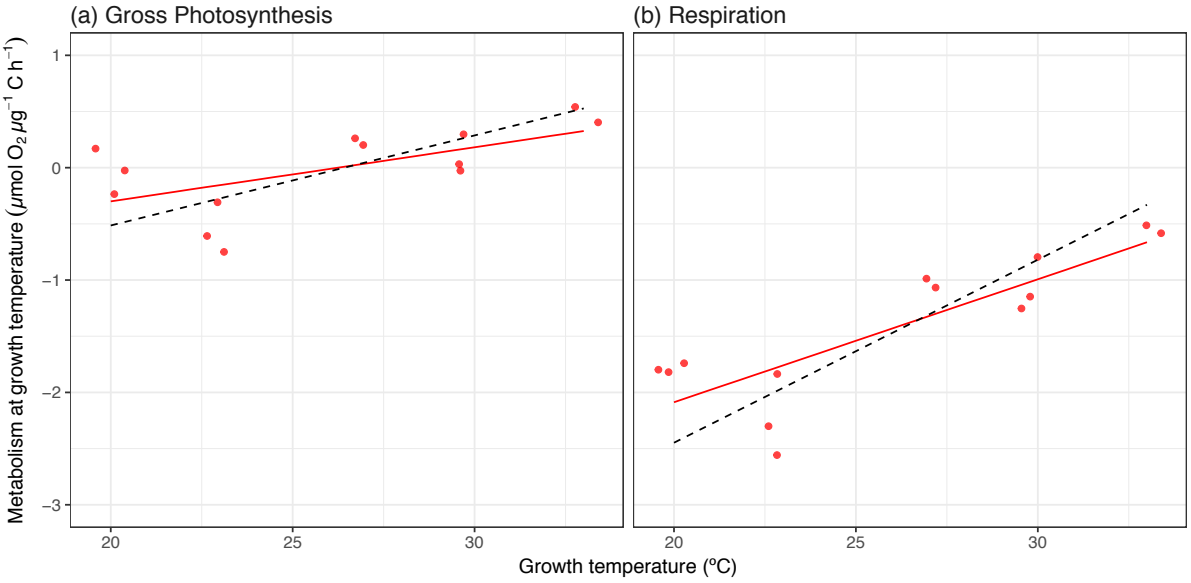

Figure 5.1. The long-term temperature-dependence of metabolism of Chlorella vulgaris after 100 generations.
The long-term (across population) temperature-dependence of (a) gross photosynthesis and (b) respiration of Chlorella vulgaris is shallower than the average within-population activation energy (black dashed line) after long-term warming (100 generations; red points and line). This is a result of thermal adaptation reducing the metabolic normalisation of both photosynthesis and respiration at higher growth temperatures. The fitted lines are the result of a bayesian linear regression and the dashed lines are the predicted relationships based on the population-level activation energy of gross photosynthesis and respiration respectively.

A similar metabolic response occurred in phytoplankton communities, where the respiratory normalisation constant decreased after long-term warming. In this instance, however, the shift in the normalisation constant was due to temperature-driven selection across species resulting in shifts in community

composition between ambient and warm mesocosms. I also observed trade-offs in community properties as a result of an ultimate resource constraint that limited the ability for community metabolism to increase under warming. In *Chapter 4*, temperature-driven selection on population-level photosynthesis and changes in biomass across the thermal gradient alter the temperature-dependence of gross primary production. Although the observed temperature-dependence of ecosystem-level GPP was similar to that of population-level gross photosynthesis, the mechanisms which controlled this temperature response were very different.

These findings highlight how the indirect effects of temperature can have large impacts on the metabolic response of organisms and ecosystems. MTE, like all theory, is not meant to encompass all ecological phenomena, but we need to acknowledge these limitations when attempting to apply causal mechanisms to ecological phenomena measured at vastly different scales. We need to be increasingly aware of the indirect effects of temperature on metabolic rate, especially as they can be as important as the direct effect of temperature on enzyme activity. Predictions that extrapolate from the direct effects of warming on metabolic rate alone may usefully be revisited.

Reconciling the temperature-dependence of metabolism across scales

As MTE assumes the temperature-dependence of metabolic rate is governed by instantaneous changes in enzyme activity, it is somewhat surprising that very little work using MTE has measured metabolism over very short timescales across temperatures within species of autotrophs. The closest I achieved to

these scales was population-level metabolism over minutely intervals. At these scales, phytoplankton photosynthesis was often less sensitive to temperature than respiration, but at values that were often close to double those previously reported. For example, in *Chapter 2*, the population-level activation energies for gross photosynthesis and respiration were 0.62 eV and 1.26 eV respectively, with similar values for the temperature-dependence of both metabolic fluxes at the community-level in *Chapter 3* (E_{GPP} = 0.74 eV and E_{CR}= 1.42 eV). There is a need to reconcile these differences in temperature-dependence to understand the applicability of these rapid rate measurements to responses in the natural environment.

Previous work on the temperature-dependence of phytoplankton metabolism has generally analysed long-term responses to warming, analysing data across species (López-Urrutia *et al.* 2006) or over seasonal and annual temperature variation (Yvon-Durocher & Allen 2012). At these longer timescales, the direct effect of temperature on metabolic rates can be confounded with other mechanisms that influence metabolism such as local adaptation. For example, the activation energy for across-population gross photosynthesis of *Chlorella vulgaris* after 100 generations was 0.37 eV, similar to the values previously found at longer timescales (Allen *et al.* 2005; López-Urrutia *et al.* 2006).

Throughout this thesis, instantaneous rates of respiration and photosynthesis were always measured at nutrient and light-saturating conditions to isolate the effect of temperature on metabolism across scales. However, phytoplankton growth and metabolism are also strongly influenced by nutrients and light

availability. Below light saturating conditions, photosynthesis is often less sensitive to temperature due to limited photon absorption at low irradiance (Raven & Geider 1988; Davison *et al.* 1991; Nicklisch *et al.* 2008). A recent data compilation that examined the interaction between phytoplankton growth, temperature and light, found that light limitation constrained the temperature-dependence of whole community phytoplankton growth (Edwards *et al.* 2016). Nutrient concentration also impacts phytoplankton growth and metabolism, decreasing the temperature-dependence of metabolism and increasing the sensitivity of phytoplankton to warming through reductions in the optimum temperature of growth (Thomas *et al.* 2017).

The increased importance of indirect effects of warming on metabolism through time and the presence of interacting abiotic drivers in the natural environment likely explains the higher values of the activation energy for photosynthesis and respiration reported here. More studies are needed to determine whether these changes in the temperature response of growth and metabolism, due to changes in light availability and nutrient limitation, occur in a predictable manner, especially given that climate change is likely to increase nutrient limitation in the upper ocean (Behrenfeld *et al.* 2006, 2015). Exploring variation in the temperature-dependence of both photosynthesis and respiration will be critical to understand how the acute temperature sensitivity (characterising the rate at which individual metabolic rates change) relates to the long-term ecosystem-level temperature response (the scale at which we need global estimates of productivity).

Downregulation of metabolic rates: A universal response to warming?

Across all levels organisation, I found temperature-driven shifts in the metabolic-normalisation constant. These downregulations were due to rapid evolution within a single species of phytoplankton and selection on trait variation across species in phytoplankton and biofilm communities. As similar responses also occur in bacteria (Bradford *et al.* 2008), terrestrial autotrophs (Atkin *et al.* 2015; Scafaro *et al.* 2016) and ectotherms (Addo-Bediako *et al.* 2002), downregulation of metabolic rates may be a general evolutionary and ecological response to warming.

This downregulation of metabolic rates is thought to allow organisms to maintain a "healthy" carbon-use efficiency (CUE). This ensures that a maximal proportion of organic carbon is available for biomass production and growth. However, a "healthy" CUE can be maintained through alternate shifts in metabolic traits. A recent study found that another aquatic alga, *Chlamydomonas reinhardtii*, adapted to a 4 ºC temperature difference (Schaum *et al.* 2017) by maintaining a "healthy" CUE. However, this was achieved by upregulating rates of photosynthesis at higher temperatures with little change in respiration rates. Consequently, maintaining a "healthy" CUE may be the universal response to warming in phytoplankton, irrespective of how it is achieved. The mechanism through which a "healthy" CUE is maintained likely reflects a combination of the strength of selection on each metabolic trait and the capacity for each trait to change. Deepening our understanding of the biochemical and molecular mechanisms that control the response of metabolic

traits and their generality across phytoplankton and other autotrophs should be a priority for future research.

Scaling individual responses to community properties

In *Chapter 3*, metabolic scaling theory successfully linked individual physiology and size structure to community metabolism, then in *Chapter 4* I incorporated the indirect effects of temperature into MST. These steps forward may improve predictions of the feedbacks between the aquatic carbon cycle and climate change. However, the data collected here on the physiology of phytoplankton and other aquatic autotrophs could be useful for other approaches to predicting community-level phenomena. Biological traits measured in the laboratory can be aggregated to predict community-level responses to climate change. The increased use of trait-based approaches in community ecology (Mcgill *et al.* 2006), using fundamental traits to understand the distributions of species and emergent community-level properties, increases the applications of laboratory based data that measures responses of organisms to abiotic drivers (Litchman *et al.* 2007; Sinclair *et al.* 2016).

Phytoplankton are particularly amenable to trait-based approaches as their fundamental niche is mainly defined by the key metabolic processes of growth, photosynthesis and respiration and acquisition of key resources (light and nutrients) (Litchman & Klausmeier 2008). Trait-based approaches have successfully demonstrated how phytoplankton community composition and abundance change with changes in light availability (Edwards *et al.* 2013b) and nutrients (Edwards *et al.* 2013a). In addition, parameters taken from laboratory

cultures have been used to predict primary production in lake ecosystems (Zwart *et al.* 2015). Further examples include biogeographical studies that incorporated experimental data on the thermal response curves of growth to demonstrate global patterns of thermal adaptation and to predict potential future distributions of phytoplankton under warming (Thomas *et al.* 2012, 2015). To enhance these approaches, there needs to be increased communication across ecological disciplines to identify globally important phytoplankton species to use in experimental evolution approaches and to define key traits to measure.

All of these methods currently use fixed values of the functional traits for each species and therefore ignore thermal adaptation and trait variation within species. Previous work has shown that phytoplankton can adapt to modest changes in temperature and irradiance in the ocean (Irwin *et al.* 2015). This work furthers this by showing how metabolic traits can adapt to increase thermal tolerance after just 45 days, albeit under laboratory conditions. As well as metabolic traits varying through time, local adaptation may result in trait differences due to current spatial variation in temperature. For example, local adaptation to different oceanic pH levels results in increased variation of key traits within species that decreases the sensitivity of oceanic species to future ocean acidification (Calosi *et al.* 2017). As thermal variation is likely to increase with climate warming, local adaptation to current temperature variation may play an important role in determining the ability of phytoplankton species to cope in future environments. Understanding the extent to which key traits vary

in time and space, within and across phytoplankton species, is paramount to improve predictions on how communities will respond to climate change.

Thermal adaptation and the global carbon cycle

A variety of ocean biogeochemistry models of varying levels of complexity have been developed in an attempt to predict the impact of climate change on ocean productivity. These are now integral to earth system models (ESMs) that assimilate the interactions between atmosphere, ocean, land and the biosphere and model the movement of carbon amongst these different pools. Different greenhouse gas emission scenarios can then be used to simulate the future climate and feedbacks between different pools. However, the uncertainty related to the estimates of the biosphere component of ESMs has hindered meaningful climate change policy. The current uncertainty associated with future changes in ocean productivity is larger across different ESM models within the same gas emission scenario than it is across different scenarios (Kwiatkowski *et al.* 2017). Constraining estimates of ocean productivity and reducing this uncertainty is essential for improving the ability for these ESMs to advise future climate change policy.

Linking information from fine spatial scales and individual responses to broad spatial scales could be one way of improving predictions. Ecosystem models are often designed to simulate processes well at small scales and concentrate on modelling short-term responses to temperature change, whereas long-term changes to temperature and mechanisms driving carbon exchange responses over broad spatial scales are rarely represented (Smith & Dukes 2013). In

terrestrial autotrophs, temperature acclimation parameterisations have been developed for both photosynthesis and respiration by allowing parameters to shift with mean air temperature over the previous 30 days (Kattge & Knorr 2007; Atkin *et al.* 2008). Incorporating these into earth system models can improve predictions of carbon uptake in terrestrial ecosystems (Smith *et al.* 2016), although the magnitude of improvement depends on the process, region and time period evaluated.

This work shows that similar responses that constrain the effect of short-term warming on metabolic rates also occur in phytoplankton. The effects of thermal adaptation on rates of photosynthesis and respiration could be incorporated into ecosystem models in the aquatic world (especially as the patterns I observe are conserved at the population and community level), at the very least to observe the sensitivity of the predictions of biogeochemical cycles to evolutionary and ecological responses of metabolic traits. However, the rates of adaptation observed here occurred in nutrient replete conditions in a vastly simplified selection environment in the laboratory. Rates of evolution to temperature in the natural environment may be limited by nutrient limitation that increases phytoplankton generation times. Consequently, understanding whether evolutionary and ecological changes that offset the direct impacts of warming on metabolic rates can track the rate of climate warming will be essential for predicting future responses of the aquatic carbon cycle.

Concluding remarks

Examining patterns and developing concepts that help assimilate observations and mechanisms across scales is key to developing a predictive theory for ecology. This was one of the take home messages of Simon Levin's influential paper 25 years ago, and remains a fundamental aim of ecology. Metabolic theory and the research, discussions and disagreements it has inspired, has resulted in significant progress in linking theory and observations across ecological scales. I have contributed to this endeavour by linking evolutionary, physiological and ecological processes to show how warming impacts metabolism across scales. By spanning multiple levels of organisation, my work contributes to the considerable progress that metabolic scaling theory has already made in understanding how community structure and individual physiology link to emergent ecosystem processes. However, developing a predictive theory of ecology remains an immense challenge. If we are to combat the multifarious nature of climate change, we need to widen the arbitrary scales at which we view our own research, to increasingly collaborate and link ideas and data across ecological disciplines. We are all ecologists, first and foremost.

Appendix

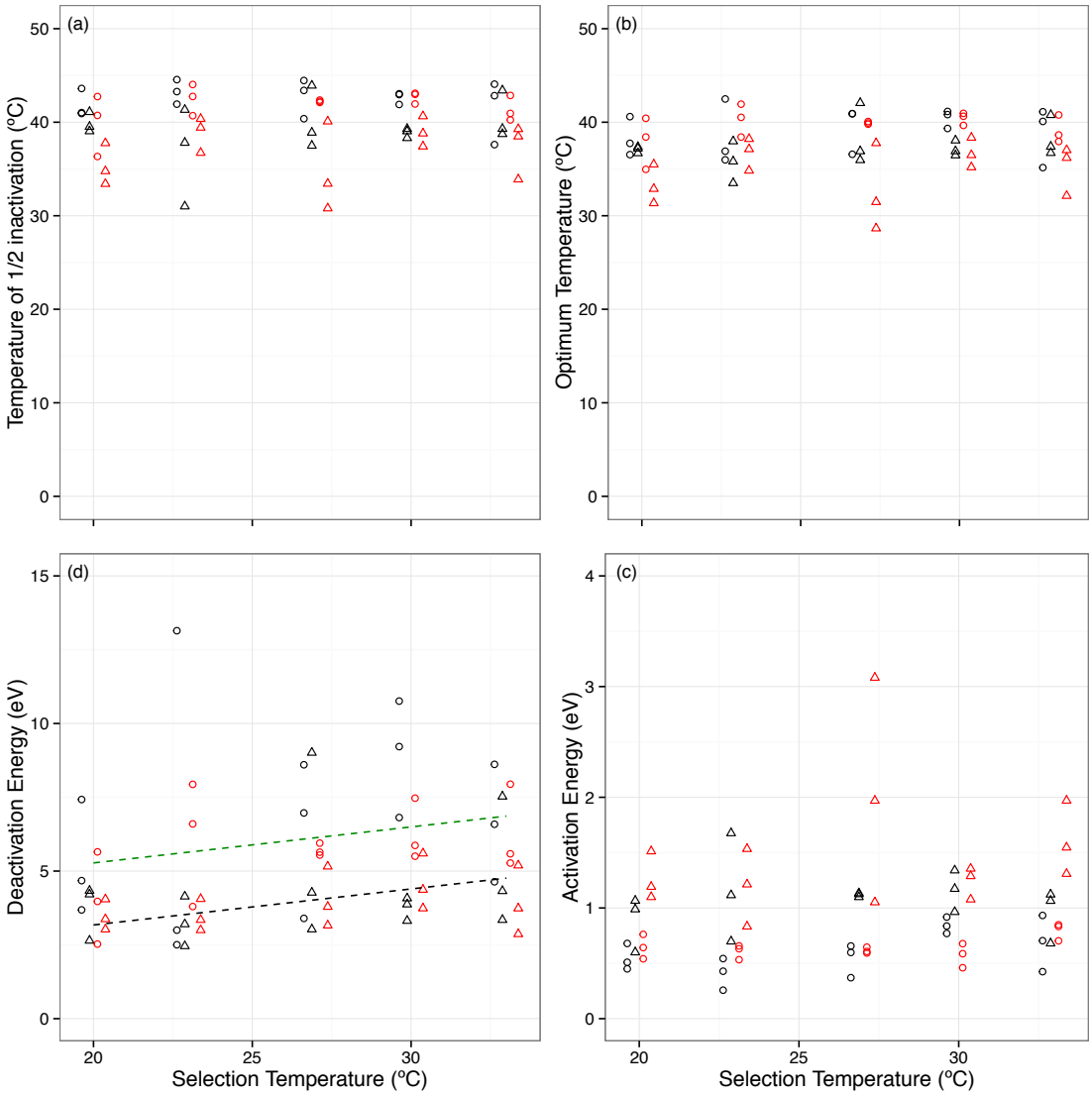

Appendix Figure 1. Effects of selection temperature on metabolic traits.
In (a-d) circles show the metabolic traits of photosynthesis and triangles those of respiration after exposure to different selection temperatures for ~10 (black) and ~100 generations (red). In (c) fitted broken lines show the significant linear relationship between the deactivation energy and selection temperature for photosynthesis (green) and respiration (black) (see Appendix Table 2).

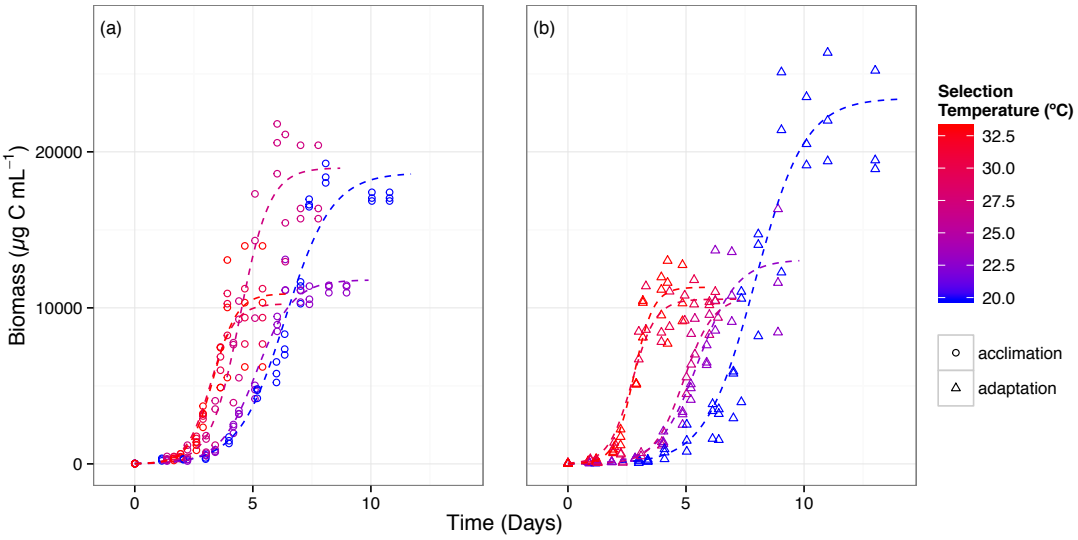

Appendix Figure 2. Effects of temperature on population dynamics. Sigmoid growth curves were measured for populations following short-term (10 generations; a) and long-term warming (100 generations; b) at 20 ºC (blue), through to 33 ºC (red). Analyses reveal that at 33 ºC, growth rates (r) are higher after long-term warming. Fitted lines are based on mean parameters at each growth temperature of non-linear least squares regression using a sigmoid growth curve equation (n = 3) (see Eq. 2.5).

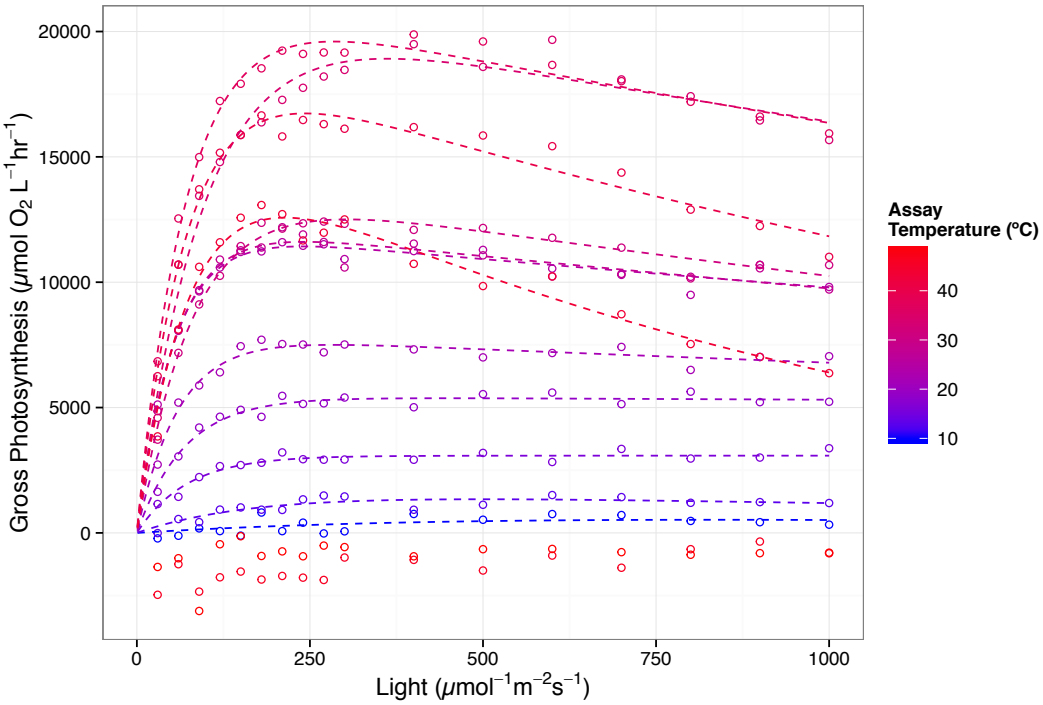

Appendix Figure 3. Photosynthesis irradiance curves used to characterise the acute temperature response of photosynthesis.

Rates of gross photosynthesis (P) were measured at various light intensities across the full range of acute temperatures (10 – 49 °C), characterising the metabolic thermal niche of Chlorella vulgaris. Here data are presented for one replicate at the long-term ancestral temperature regime (20 ºC). Lines represent the best fit to the photoinhibition model using non-linear least squares regression (see Methods Eq. 2.6).

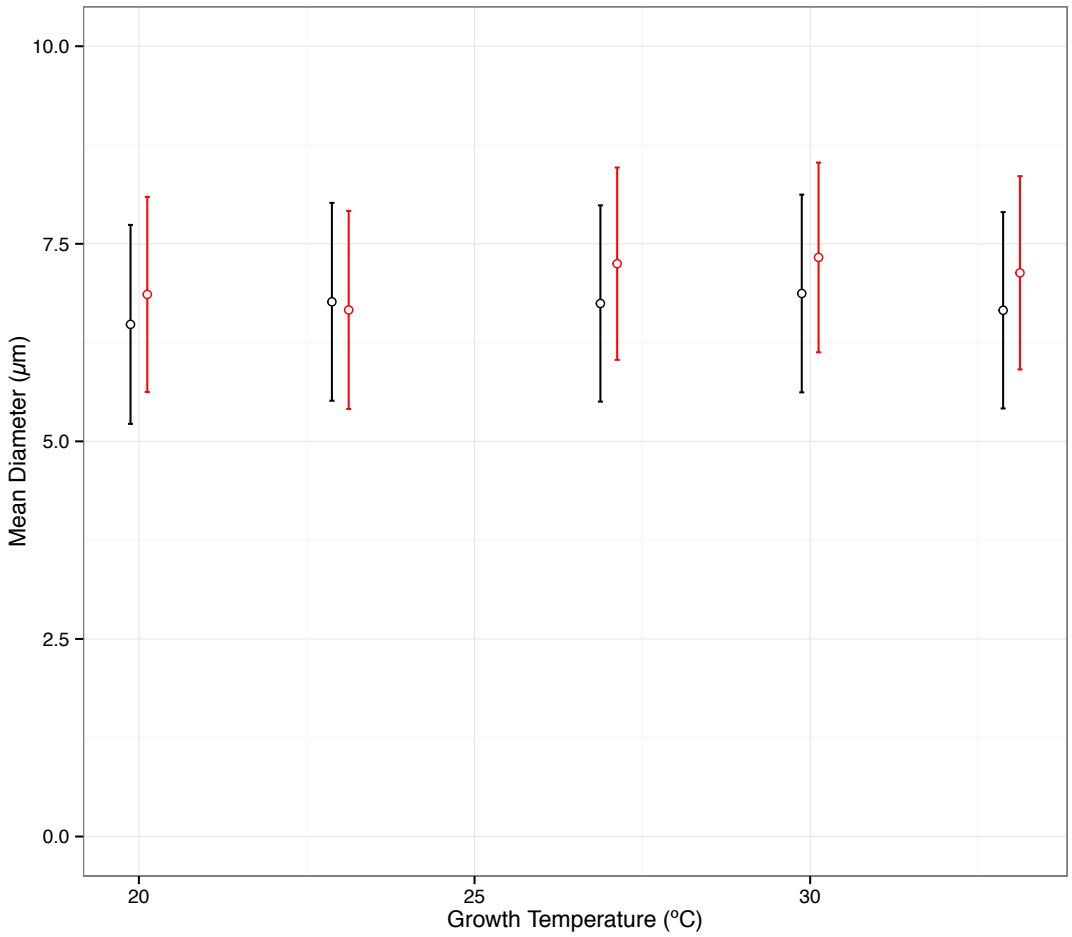

Appendix Figure 4. Effects of selection temperature on cell size.
Equivalent spherical diameter was measured for each replicate after short-term (black circles) and long-term (red circles) exposure to each selection temperature. Mean cell diameter was estimated for each replicate population as the anti-log of the average log_{10} cell diameter. Body size did not vary between selection temperatures or between long-term versus short-term warming. Error bars represent 1 standard deviation from the mean.

Appendix Table 1. Trajectory of exponential growth rate at the various selection temperatures.

Parameters are estimated from a mixed effects model (see Chapter 2 Methods and Appendix Table 1) and treatment contrasts were made using Tukey's least significant difference tests. Contrasts significant at the 0.05 level for the slope of the growth trajectory are 20 ºC vs 27 ºC, 20 ºC vs 30 ºC, 20 ºC vs 33 ºC, 23 ºC vs 27 ºC, 23 ºC vs 30 ºC, 23 ºC vs 33 ºC, 27 ºC vs 33 ºC and 30 ºC vs 33 ºC. Significant contrasts for the intercept at 0.05 significance are 20 ºC vs 27 ºC, 20 ºC vs 30 ºC, 20 ºC vs 33 ºC, 23 ºC vs 27 ºC, 23 ºC vs 30 ºC and 23 ºC vs 33 ºC.

Growth Temperature	Slope (95% CI)	Intercept (95% CI)
20 ºC	0.000152 (-0.000260 – 0.000566)	0.87 (0.85 – 0.89)
23 ºC	0.00122 (-0.000288 – 0.00274)	1.14 (1.08 – 1.19)
27 ºC	0.00452 (0.00239 – 0.00665)	1.42 (1.34 – 1.49)
30 ºC	0.00556 (0.00329 – 0.00783)	1.58 (1.49 – 1.66)
33 ºC	0.0130 (0. 00929 – 0.0168)	1.48 (1.36 – 1.60)

Appendix Table 2. Parameter estimates for the metabolic traits governing the thermal response curves for Chlorella.

Selection Temperature	Replicate	Exposure	Flux	$b(T_c)$ (µmol O_2 µg C^{-1} h^{-1} @ 25ºC)	E_a (eV)	E_h (eV)	T_h (ºC)	T_{opt} (ºC)	R^2
20	1	short-term	R	0.5	0.99	4.33	39.04	36.69	0.46
20	2	short-term	R	0.53	1.07	4.21	39.51	37.36	0.9
20	3	short-term	R	0.32	0.6	2.64	41.09	37.19	0.58
23	1	short-term	R	0.38	0.7	3.2	41.33	37.96	0.43
23	2	short-term	R	0.41	1.68	2.46	31	33.49	0.79
23	3	short-term	R	0.34	1.12	4.14	37.8	35.81	0.78
27	1	short-term	R	0.41	1.1	3.03	37.49	35.95	0.87
27	2	short-term	R	0.36	1.12	9.01	43.92	42.06	0.76
27	3	short-term	R	0.39	1.13	4.27	38.89	36.9	0.73
30	1	short-term	R	0.3	1.34	3.31	39.04	38.05	0.86
30	2	short-term	R	0.39	1.17	4.08	38.31	36.46	0.73
30	3	short-term	R	0.65	0.96	3.87	39.28	36.9	0.88
33	1	short-term	R	0.26	1.06	3.35	39.29	37.38	0.93
33	2	short-term	R	0.3	1.12	4.32	38.74	36.72	0.18
33	3	short-term	R	0.79	0.68	7.53	43.4	40.77	0.88
20	1	short-term	P	1.88	0.51	7.42	43.61	40.6	0.91
20	2	short-term	P	1.95	0.68	4.68	40.93	37.74	0.88
20	3	short-term	P	0.93	0.45	3.68	41.03	36.54	0.51
23	1	short-term	P	1.18	0.54	13.14	44.55	42.49	0.85
23	2	short-term	P	1.51	0.26	2.5	43.27	35.97	0.54
23	3	short-term	P	1.54	0.43	3	41.93	36.9	0.69
27	1	short-term	P	1.55	0.6	3.4	40.37	36.57	0.95
27	2	short-term	P	1.75	0.66	8.6	43.4	40.92	0.87
27	3	short-term	P	1.78	0.37	6.97	44.46	40.9	0.89
30	1	short-term	P	1.03	0.84	9.22	42.95	40.82	0.91
30	2	short-term	P	0.78	0.92	10.76	43.04	41.15	0.94
30	3	short-term	P	1.62	0.77	6.81	41.9	39.33	0.91
33	1	short-term	P	0.75	0.7	6.59	42.84	40.09	0.89
33	2	short-term	P	1.25	0.93	4.64	37.61	35.15	0.56
33	3	short-term	P	2.33	0.42	8.61	44.07	41.12	0.73
20	1	long-term	R	0.4	1.19	3.02	34.77	32.88	0.6
20	2	long-term	R	0.59	1.51	3.37	33.41	31.35	0.84
20	3	long-term	R	0.49	1.1	4.04	37.76	35.49	0.76
23	1	long-term	R	0.15	1.21	4.05	39.43	37.12	0.87
23	2	long-term	R	0.24	0.83	3.35	40.36	38.21	0.95
23	3	long-term	R	0.17	1.53	3	36.73	34.83	0.92
27	1	long-term	R	0.12	3.08	3.79	30.79	28.65	0.95
27	2	long-term	R	0.2	1.97	3.16	33.43	31.47	0.92
27	3	long-term	R	0.21	1.05	5.16	40.09	37.77	0.92
30	1	long-term	R	0.2	1.29	3.74	37.41	35.19	0.75
30	2	long-term	R	0.18	1.08	5.6	40.64	38.34	0.86
30	3	long-term	R	0.13	1.36	4.37	38.8	36.49	0.9
33	1	long-term	R	0.15	1.55	5.19	38.48	36.19	0.86
33	2	long-term	R	0.19	1.31	3.74	39.27	37.02	0.84
33	3	long-term	R	0.14	1.97	2.87	33.89	32.13	0.9
20	1	long-term	P	1.22	0.54	5.65	42.74	40.42	0.82
20	2	long-term	P	2.05	0.76	2.53	36.34	34.96	0.93
20	3	long-term	P	1.7	0.64	3.97	40.73	38.42	0.94
23	1	long-term	P	0.73	0.63	6.6	42.75	40.52	0.94
23	2	long-term	P	0.79	0.66	3.8	40.7	38.41	0.96
23	3	long-term	P	0.75	0.53	7.94	44.03	41.93	0.97
27	1	long-term	P	0.93	0.61	5.95	42.37	40.08	0.91
27	2	long-term	P	0.97	0.59	5.54	42.11	39.79	0.93
27	3	long-term	P	0.89	0.65	5.64	42.23	39.92	0.98
30	1	long-term	P	0.84	0.59	7.47	43.09	40.95	0.88
30	2	long-term	P	0.81	0.46	5.5	42.98	40.64	0.83
30	3	long-term	P	0.64	0.68	5.87	41.95	39.66	0.95
33	1	long-term	P	0.7	0.83	5.58	40.94	38.64	0.95
33	2	long-term	P	0.89	0.7	7.94	42.86	40.78	0.93
33	3	long-term	P	0.81	0.85	5.27	40.25	37.93	0.86

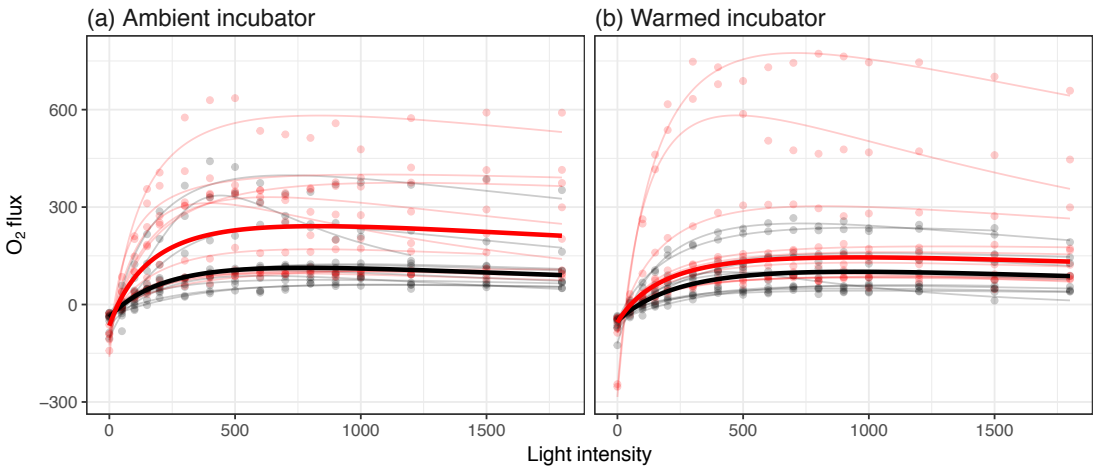

Appendix Figure 5. Photosynthesis irradiance curves of heated-ancestral (red) and ambient-ancestral (black) communities in the (a) ambient and (b) warmed incubators.

Value for the photosynthetic maximum were used as the metabolic rate data to which Eq 3.2 was fitted. Faded points and lines represent the raw measurements and individual fits to each photosynthesis irradiance curve. The bold, thicker lines represent the fit of the average parameter values from all of the individual parameter values.

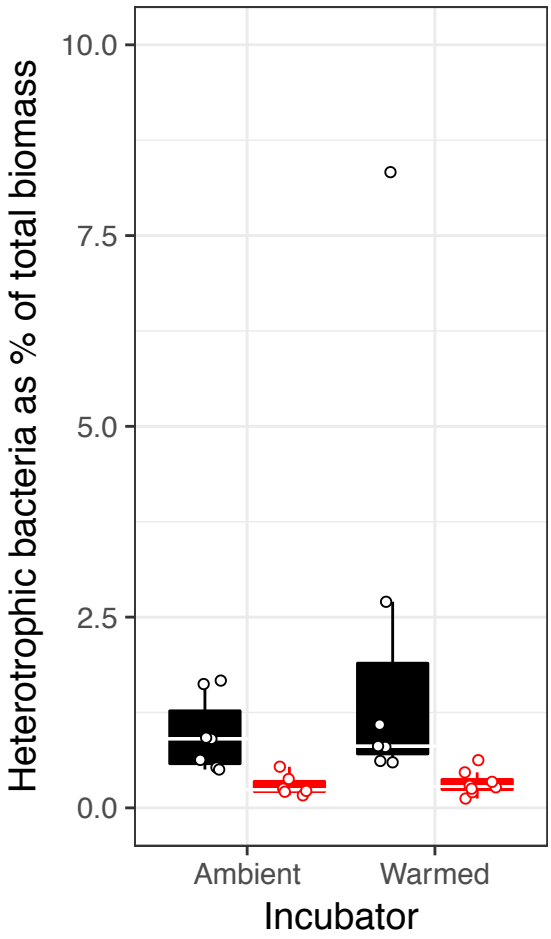

Appendix Figure 6. Proportion of heterotrophic bacteria of total biomass.
The proportion of heterotrophic bacteria of total biomass is less than 3% in both heated-ancestral and ambient-ancestral communities in all but a single community. Consequently, all analyses only used the size distributions from the autotrophic communities. Each point represents one community; tops and bottoms of box-whisker plots represent the 75th and 25th percentiles and the white horizontal line represents the median.

Appendix Table 3. Results of mixed effects model analysis for the effects of short- and long-term warming on community metabolic rate.
Analyse reveal that community metabolism is not significantly altered by either short- or long-term warming.

flux	model	d.f.	AIC	Log Lik	χ^2	P
gross primary production	Random effects structure ~ 1|mesocosm					
	Fixed effects structure					
	1. ~ 1 + short-term warming * long-term warming	6	84.59	-36.29		
	2. ~ 1 + short-term warming + long-term warming	5	82.61	-36.30	0.021	0.88
	3. ~ 1 + long-term warming	4	80.95	-36.47	0.34	0.55
	4. ~ 1	3	82.661	-38.33	3.71	0.054
community respiration	Random effects structure ~ 1|mesocosm					
	Fixed effects structure					
	1. ~ 1 + short-term warming * long-term warming	6	71.35	-29.67		
	2. ~ 1 + short-term warming + long-term warming	5	69.35	-29.68	0.0071	0.93
	3. ~ 1 + long-term warming	4	68.73	-30.37	1.38	0.24
	4. ~ 1	3	69.71	-31.86	2.98	0.08

Appendix Table 4. Results of the maximum likelihood modelling for simultaneously estimating parameters in Eq. 3.2.
Analyses reveal that the only effect of long-term warming is a reduction in the normalisation of community respiration.

flux	model	d.f	AIC	Deviance	χ^2	P
gross primary production	1. long-term warming * E_{GPP} + long-term warming * α_{GPP} + long-term warming * $GPP(T_c)$	6	52.93	40.93		
	2. E_{GPP} + long-term warming * α_{GPP} + long-term warming * $GPP(T_c)$	5	52.09	42.09	1.15	0.28
	3. E_{GPP} + α_{GPP} + long-term warming * $GPP(T_c)$	4	49.24	41.24	0.85	0.36
	4. $\boldsymbol{E_{GPP} + \alpha_{GPP} + GPP(T_c)}$	3	47.24	41.24	0.001	0.97
community respiration	1. long-term warming * E_{CR} + long-term warming * α_{CR} + long-term warming * $CR(T_c)$	6	54.51	42.51		
	2. E_{CR} + long-term warming * α_{CR} + long-term warming * $CR(T_c)$	5	52.52	42.52	0.004	0.95
	3. $\boldsymbol{E_{CR}}$ + $\boldsymbol{\alpha_{CR}}$ + long-term warming * $\boldsymbol{CR(T_c)}$	**4**	**51.64**	**43.64**	**1.12**	**0.29**
	4. E_{CR} + α_{CR} + $CR(T_c)$	3	54.3	48.3	4.66	**0.031**

Appendix Table 5. Parameters used in the formulation of the metabolic scaling theory of metabolism from organisms to ecosystems.

Notation	Formulation	Description	Unit
Organism-level:			
E_{gp}		Activation energy of gross photosynthesis	eV
E_{np}		Activation energy of net photosynthesis	eV
E_r		Activation energy of respiration	eV
E_h		Deactivation energy	eV
$gp(T_c)$		Temperature normalised rate of gross photosynthesis	μmol O_2 μg $Chla^{-1}$ h^{-1}
$np(T_c)$		Temperature normalised rate of net photosynthesis	μmol O_2 μg $Chla^{-1}$ h^{-1}
$r(T_c)$		Temperature normalised rate of respiration	μmol O_2 μg $Chla^{-1}$ h^{-1}
T_{opt}		Optimum temperature	ºC
T_h		Temperature where half of enzymes are inactivated	ºC
m^a		Mass dependence of metabolic rate	μg $Chla^{-1}$
Ecosystem-level:			
$GPP(T_c)$	$\frac{1}{A}\sum_{i=1}^{J} gp_i(T_c)\, m_i^{\alpha}$	Temperature normalised rate of gross primary productivity	g O_2 g $Chla^{-1}$ day^{-1}
E_{GPP}	$E_{gp} + E_a + E_b$	Activation energy of gross primary productivity	eV
M_s	$\frac{1}{A}\sum_{i=1}^{J} m_i$	Total biomass	g Chla m^{-2}
E_a		Activation energy of adaptation of $gp(T_c)$	eV
E_b		Activation energy for temperature dependence of biomass	eV

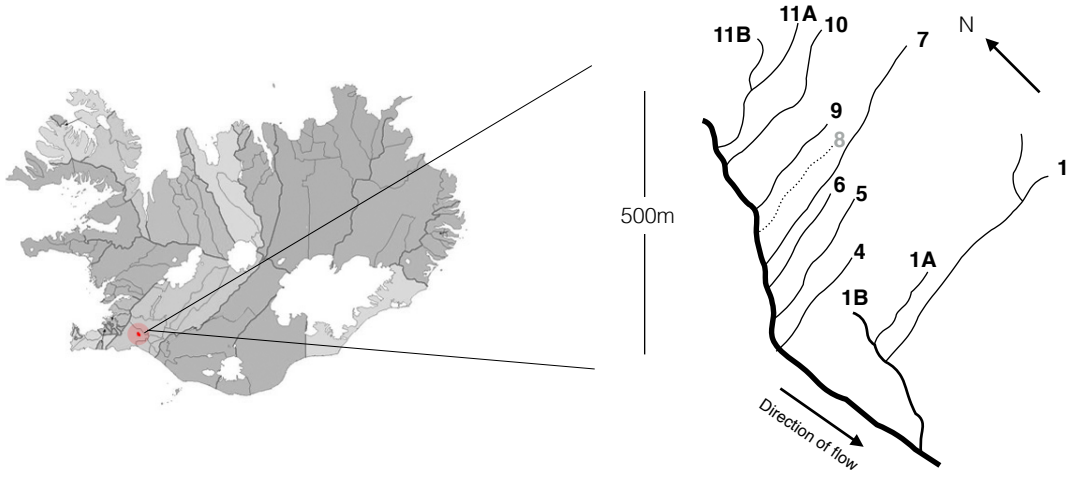

Appendix Figure 7. Map of the geothermal stream system in a valley near Hveragerdi, SW Iceland (64.018350, -21.183433).

Appendix Table 6. Mean, minimum and maximum temperature values averaged across days and years (May 2015, May 2016) in the 15 sites. Values are based on a temperature estimates taken at 1 minute intervals. The sites are listed with increasing mean temperature.

	Temperature (ºC)		
Site	Mean	Minimum	Maximum
S9	6.8	5.3	7.9
S7 : high	7.1	6.7	7.9
S4	7.3	5.1	8.9
S1A	8	4.5	11.8
S1B	8.2	7.1	9.7
S6	11	7.3	14.1
S7 : low	11.4	10.4	12.1
S1 : low	12.1	9.7	16.3
S5 : low	13.2	12.1	14.8
S10	14.4	10.4	16.9
S11A	14.4	12.4	16.6
S1 : high	16.5	13.3	18.8
S11B : high	17.2	14.7	19.6
S11B : low	21.5	19.8	23.4
S5 : high	26.9	24.8	28.6

Appendix Table 7. Key physical and chemical features of the 15 sites investigated

Site	width (m)	depth (m)	velocity ($m\ s^{-1}$)	integrated upstream estimate (m)	pH	conductivity ($\mu S\ m^{-1}$)	nutrients ($\mu mol\ L^{-1}$)			
							NO_2	NO_3	NH_4	PO_4
S9	0.41	0.027	0.11	29	7.57	173.3	0.29	0.23	0.27	0.86
S7 : high	0.4	0.053	0.3	237	7.43	359.1	0.22	0.44	0.28	0.7
S4	0.46	0.06	0.36	191	7.27	204.6	0.2	0.08	0.22	0.14
S1A	0.59	0.07	0.5	561	7.40	230.9	0.25	0.4	0.7	0.54
S1B	0.42	0.058	0.14	131	7.50	462.4	0.28	0.25	0.18	0.17
S6	0.19	0.029	0.12	302	7.43	289.6	0.22	0.4	0.21	1.02
S7 : low	0.3	0.043	0.4	107	7.43	304.7	0.22	0.44	0.28	0.7
S1 : low	1.1	0.13	0.81	917	7.36	305.2	0.26	0.26	0.48	0.35
S5 : low	0.32	0.041	0.09	60	7.63	273.6	0.22	0.57	0.17	0.14
S10	0.22	0.109	0.24	552	7.53	167.0	0.35	-	0.24	0.74
S11A	0.71	0.078	0.77	405	7.17	235.7	0.24	0.29	0.19	0.55
S1 : high	0.74	0.12	0.61	884	7.20	321.7	0.26	0.26	0.48	0.35
S11B : high	0.31	0.042	0.33	222	7.33	407.9	0.25	0.25	0.27	1.25
S11B : low	0.4	0.042	0.33	370	7.33	407.9	0.25	0.25	0.27	1.25
S5 : high	0.17	0.037	0.06	109	7.63	319.2	0.22	0.57	0.17	0.27

Appendix Table 8. Pearson correlation coefficients between temperature and physical and chemical variables

Variable	*r*	P value
width	-0.14	0.56
depth	0.07	0.77
velocity	0.04	0.87
pH	-0.03	0.91
conductivity	-0.02	0.92
NO_2	-0.001	0.47
NO_3	0.18	0.47
NH_4	-0.19	0.44
PO_4	0.07	0.77

Appendix Table 9. The photosynthetic traits governing the thermal response curves for the dominant biofilms of each site.

			Net photosynthesis					Respiration					Gross photosynthesis				
Site	Year	Taxon	ln $np(T_c)$ (µmol O_2 µg Chla^{-1} h^{-1} @ 10ºC)	E_{np} (eV)	E_h (eV)	T_h (ºC)	T_{opt} (ºC)	ln $r(T_c)$ (µmol O_2 µg Chla^{-1} h^{-1} @ 10ºC)	E_r (eV)	E_h (eV)	T_h (ºC)	T_{opt} (ºC)	ln $gp(T_c)$ (µmol O_2 µg Chla^{-1} h^{-1} @ 10ºC)	E_{gp} (eV)	E_h (eV)	T_h (ºC)	T_{opt} (ºC)
S4	2016	Cladophora	3.9	1.03	4.39	30.6	28.48	2.48	1.01	3.78	31.66	29.53	4.2	0.92	9.19	32.49	30.57
S1A	2016	Cladophora	4.74	0.79	2.58	28.33	25.88	3.07	0.64	4.36	37.28	33.97	4.77	0.89	2.71	26.98	24.95
S1A	2016	Nostoc	4.37	0.52	8.77	36.87	34.28	3.14	0.44	4.26	38.83	34.63	4.8	0.47	2.72	35.36	30.71
S4	2015	Cladophora	3.55	0.87	1.78	21.67	21.52	1.71	0.45	17.21	43.78	41.97	3.61	0.53	2.18	30.18	26.1
S7 : high	2016	Cladophora	4.35	0.73	7.04	31.77	29.33	3.85	0.8	2.94	31.06	28.42	4.48	0.93	3.51	28.24	25.99
S7 : high	2016	Nostoc	2.67	0.98	3.57	34.32	32.1	1.27	0.93	1.77	34.12	34.59	3.33	0.62	9.05	38.83	36.43
S7 : high	2015	Feathermoss	1.32	0.77	4.99	34.19	31.44	1.26	0.55	2.13	42.8	38.64	1.99	0.66	8.81	35.6	33.28
S11A	2016	Nostoc	2.67	1.91	5.29	28.47	27.62	1.13	0.71	5.85	45.74	42.79	2.95	1.57	4.37	28.46	27.43
S10	2016	Nostoc	2.68	1.08	9.9	38.53	36.76	-0.66	1.64	3.15	34.74	34.94	3.42	0.85	7.12	38.39	36.06
S1 : high	2016	Nostoc	3.77	1.03	8.87	39.61	37.69	1.33	1.09	3.23	41.01	39.26	4.36	0.85	3.66	37.86	35.15
S11b : high	2015	Feathermoss	1.82	1.12	2.64	24.53	23.64	1.1	0.48	1.64	49.7	45	2.08	1.14	2.5	25.19	24.64
S5 : high	2015	Anabaena	2.58	0.54	5.9	42.5	39.19	0.68	0.66	2.04	39.71	36.65	2.73	0.55	5.69	42.37	39.02
S5 : high	2016	Anabaena	2.66	0.85	4.02	37.4	34.71	0.45	1.58	2.35	29.63	32.12	2.79	0.77	5.63	39.89	37.14

Appendix Table 10. Results of a linear effects model analysis for each metabolic trait with fixed effects of stream temperature and metabolic flux. Significant models are highlighted in bold.

Metabolic Trait	Effect	d.f.	AIC	Log Lik	L-ratio	P value
$b(T_c)$	~ 1 + stream temperature * metabolic flux	8	96.94	-40.47		
	~ 1 + stream temperature + metabolic flux	6	94.89	-41.43	1.93	0.37
	~ 1 + metabolic flux	5	98.28	-44.14	5.41	**0.02**
E	~ 1 + stream temperature * metabolic flux	8	37.03	-10.51		
	~ 1 + stream temperature + metabolic flux	6	36.36	-12.18	3.33	0.189
	~ 1 + stream temperature	4	34.41	-13.21	2.05	0.36
	~ 1	3	32.92	-13.46	0.51	0.48
E_h	~ 1 + stream temperature * metabolic flux	8	72.92	-28.46		
	~ 1 + stream temperature + metabolic flux	6	73.83	-30.91	4.91	0.09
	~ 1 + metabolic flux	5	72.07	-31.04	0.24	0.62
	~ 1	3	71.37	-32.68	3.30	0.19
T_h	~ 1 + stream temperature * metabolic flux	8	-192.08	104.04		
	~ 1 + stream temperature + metabolic flux	6	-192.92	102.46	3.15	0.206
	~ 1 + metabolic flux	5	-190.32	100.16	4.60	**0.032**
T_{opt}	~ 1 + stream temperature * metabolic flux	8	-27.21	21.61		
	~ 1 + stream temperature + metabolic flux	6	-28.72	20.36	2.49	0.29
	~ 1 + metabolic flux	5	-24.54	17.27	6.18	**0.013**
$b(T_s)$	~ 1 + stream temperature * metabolic flux	8	48.64	-16.32		
	~ 1 + stream temperature + metabolic flux	6	44.68	-16.34	0.05	0.98
	~ 1 + metabolic flux	5	42.99	-16.49	0.31	0.58
	~ 1	4	64.21	-29.10	25.22	**<0.0001**

Appendix Table 11. The number of days of stream gross primary productivity measured from each site across years.
Sites are ordered by increasing average stream temperature

	Number of days of site GPP measurements		
Site	2015	2016	Total
S9	0	1	1
S7 : high	2	2	4
S4	0	1	1
S1A	2	1	3
S1B	0	2	2
S6	2	1	3
S7 : low	0	1	1
S1 : low	2	2	4
S5 : low	0	1	1
S10	2	1	3
S11A	2	2	4
S1 : high	2	1	3
S11B : high	2	2	4
S11B : low	2	0	2
S5 : high	2	1	3

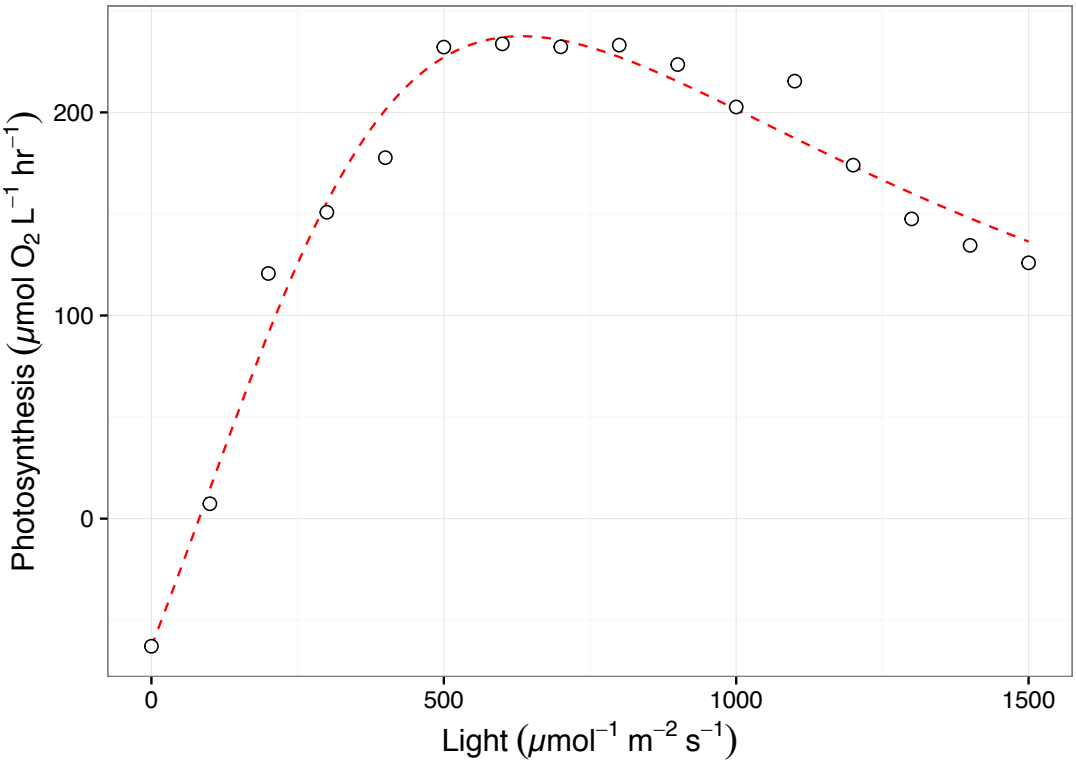

Appendix Figure 8. Photosynthesis irradiance curve used to determine optimal light for the acute temperature response of gross photosynthesis.
Rates of net photosynthesis were measured at various light intensities at the average stream temperature of each biofilm. Here data are presented for Nostoc spp. in stream 7 (high) at 7.1 ºC. Lines represent the best fit to the modified Eiler's model using non-linear least squares regression (see Chapter 4 methods).

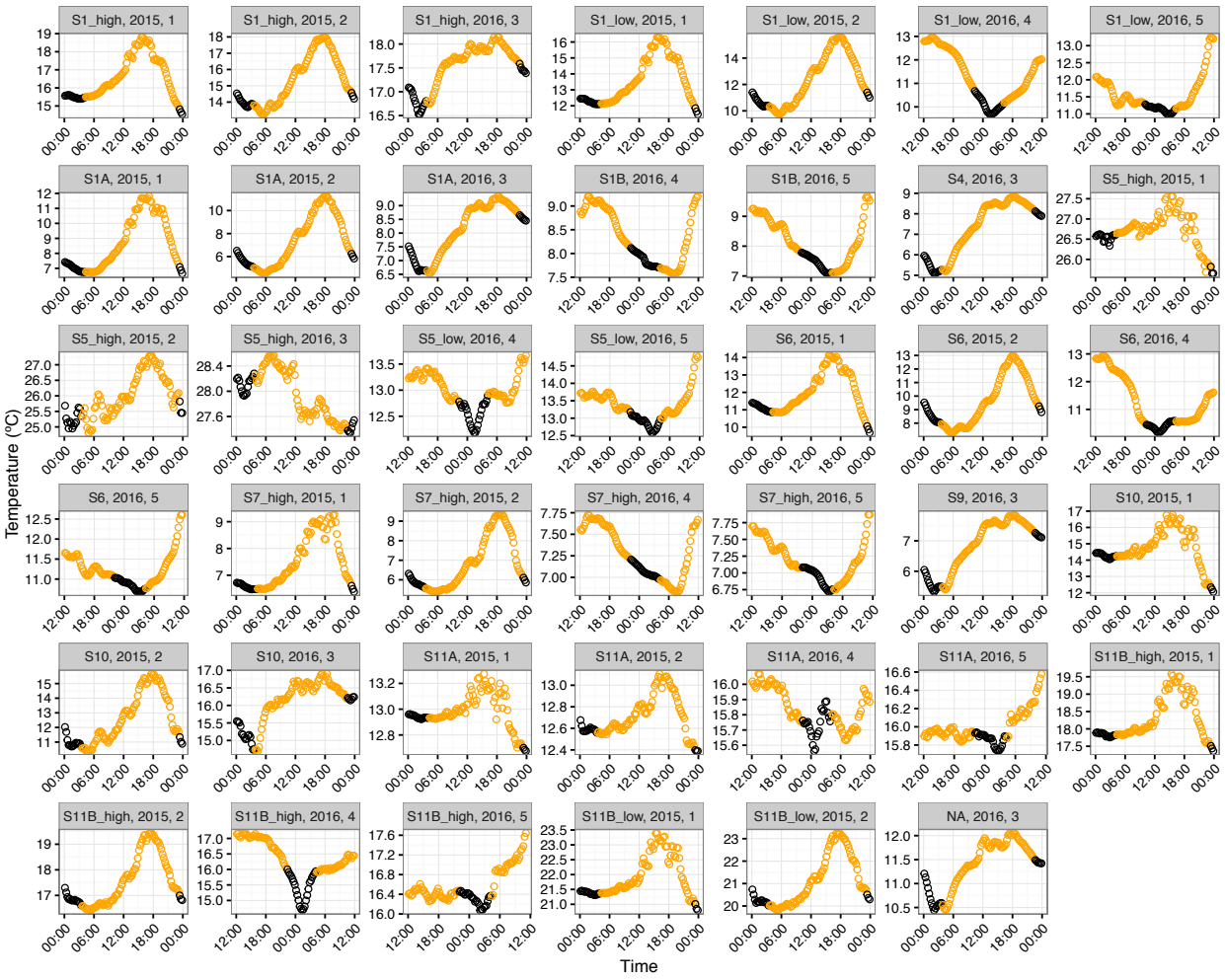

Appendix Figure 9. Daily cycles in temperature from each stream across days and years.

Each panel is a single day of temperature variation split by each unique stream and across years (2015 or 2016). The data is split into "night" (black points) and "day" (yellow points) by defining night as < 5μmol m^{-2} s^{-1} (see Chapter 4 methods).

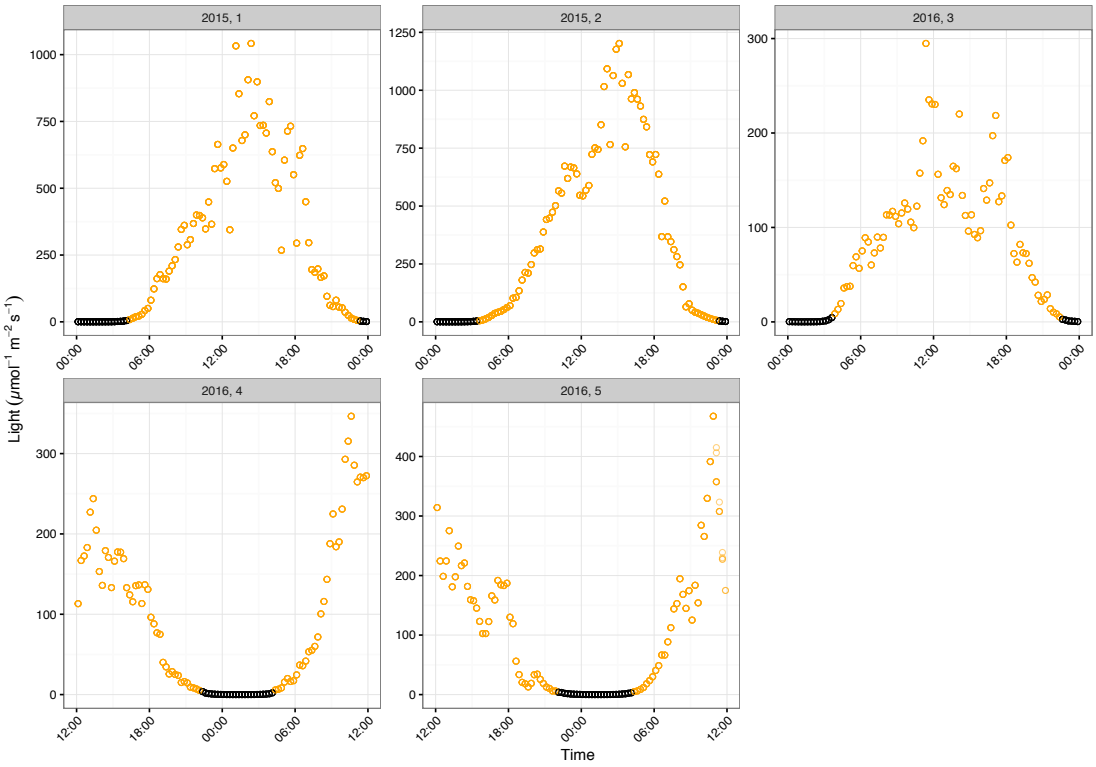

Appendix Figure 10. Daily cycles in light from across days and years. Each panel is a single day of light variation split by each unique stream and across years (2015 or 2016). The data is split into "night" (black points) and "day" (yellow points) by defining night as < 5μmol m^{-2} s^{-1} (see Chapter 4 methods).

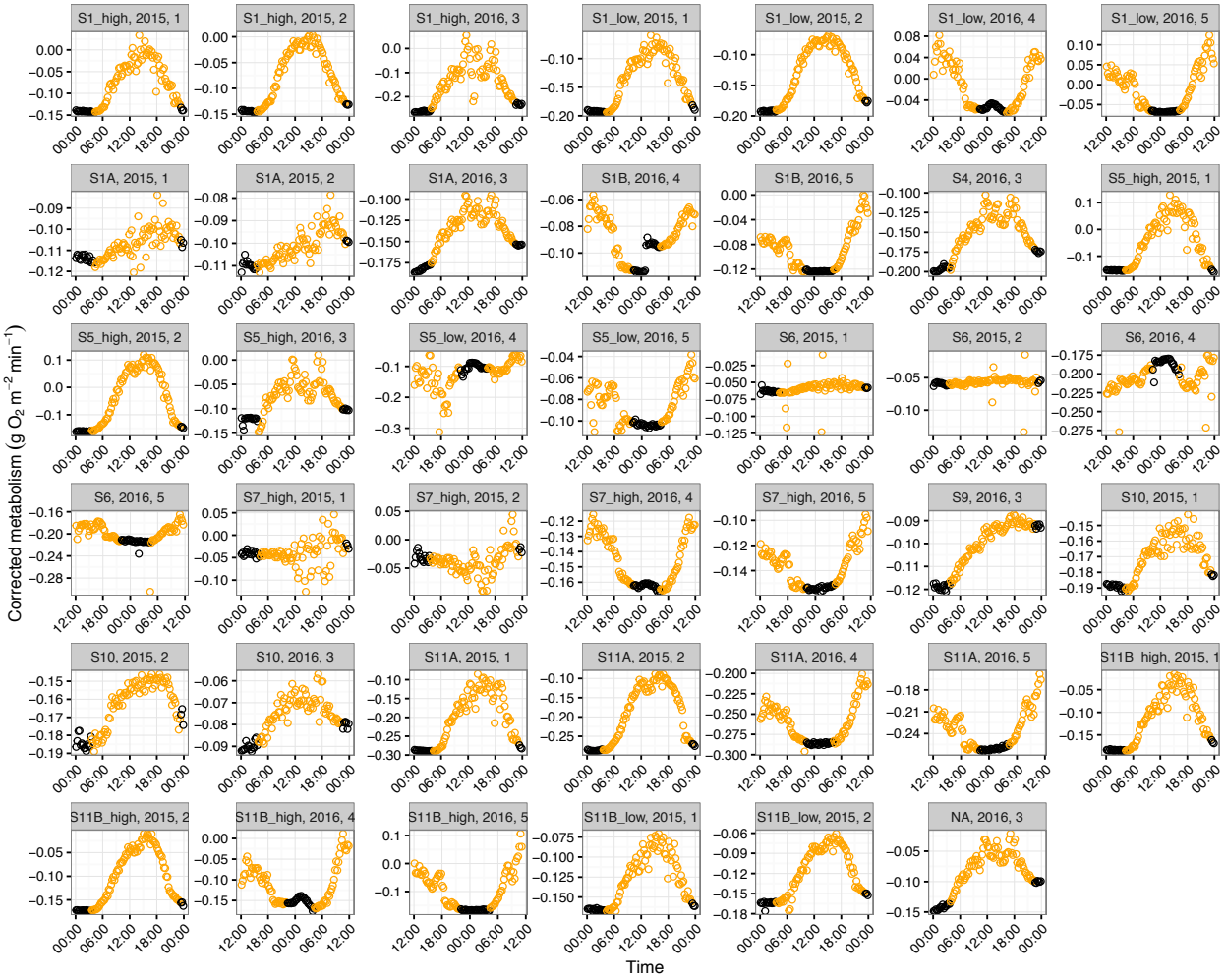

Appendix Figure 11. Daily cycles in metabolic flux from each site across days and years.

Each panel is a single day of metabolic rate after accounting for reaeration (ΔDO – K; see Methods) split by each unique stream and across years (2015 or 2016). The data is split into "night" (black points) and "day" (yellow points) by defining night as < 5μmol m^{-2} s^{-1} (see Chapter 4 methods).

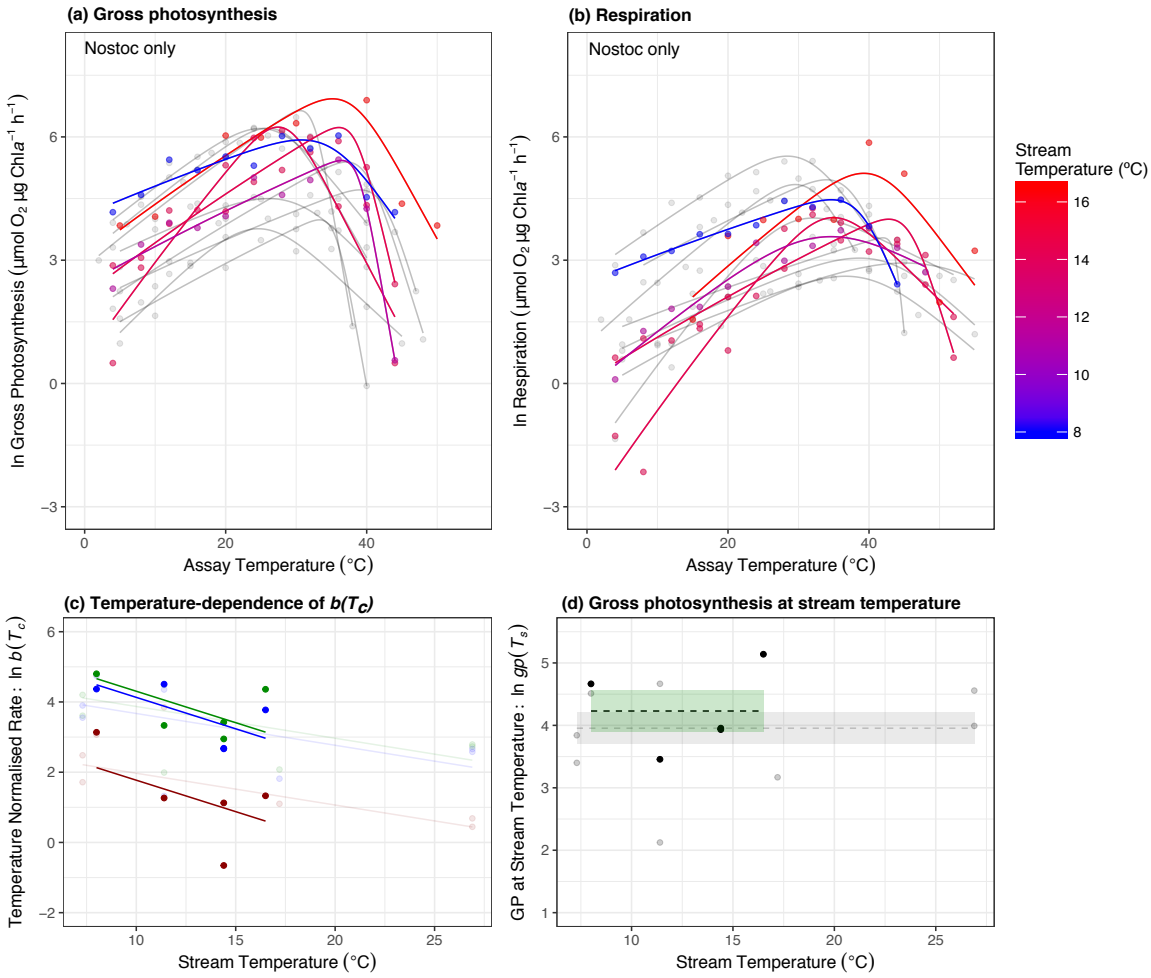

Appendix Figure 12. Patterns of thermal adaptation in Nostoc spp. only. (a) (a,b) Acute thermal response curves for gross photosynthesis and respiration were measured for each isolated autotroph from streams spanning average temperatures from 7 ºC (blue) to 17 ºC (red) for stream biofilms dominated by Nostoc spp. (c) Optimum temperatures were consistently higher than the average stream temperature. (c) Metabolic rates normalised to 10 ºC, $b(T_c)$, decrease exponentially with increasing stream temperature for gross photosynthesis (green), net photosynthesis (blue) and respiration (red). (d) Rates of gross photosynthesis at the average stream temperature showed no temperature dependence. Grey points and lines highlight the other taxa to facilitate direct comparison to the relationship for Nostoc spp.

Appendix Methods

Derivation of the activation energy of net photosynthesis.

The rate of net photosynthesis, $np(T)$, at temperature, T, is equal to the difference between the rates of gross photosynthesis, $gp(T)$, and respiration, $r(T)$. Equation 4.5 implies that the temperature sensitivity of net photosynthesis will not follow a simple Boltzmann-Arrhenius relationship. Instead, the apparent activation energy of net photosynthesis, E_{np}, can be approximated in the vicinity of T_c as (Yvon-Durocher *et al.* 2014),

$$E_{np} \equiv \frac{dln(np(T))}{d\left(\frac{1}{kT}\right)}_{T=T_c} = \frac{E_{gp}\, gp(T_c) + E_r r(T_c)}{gp(T_c) + r(T_c)} \quad \text{(A1)}$$

which is equal to an average of the activation energies of E_{gp} and E_r, weighted by their respective normalisations, $gp(T_c)$ and $r(T_c)$. Using this approximation, I can express the temperature dependence of np as

$$np(T) = np(T_c) m^{\alpha} e^{E_{np}\left(\frac{1}{kT_c} - \frac{1}{kT}\right)} \quad \text{(A2)}$$

where $np(T_c) = gp(T_c) - r(T_c)$. I quantified the accuracy of this approximation by comparing E_{np} derived using Eq. A1 to the apparent activation energy of net photosynthesis measured by fitting Eq. 4.1 to the net photosynthesis data (see Chapter 4 Methods). The derived and measured estimates of E_{np}were positively correlated with a slope that had confidence intervals which overlapped unity (slope = 1.22, 95% CI: 0.78 – 1.65) and R^2 = 0.75 (Fig. S7).

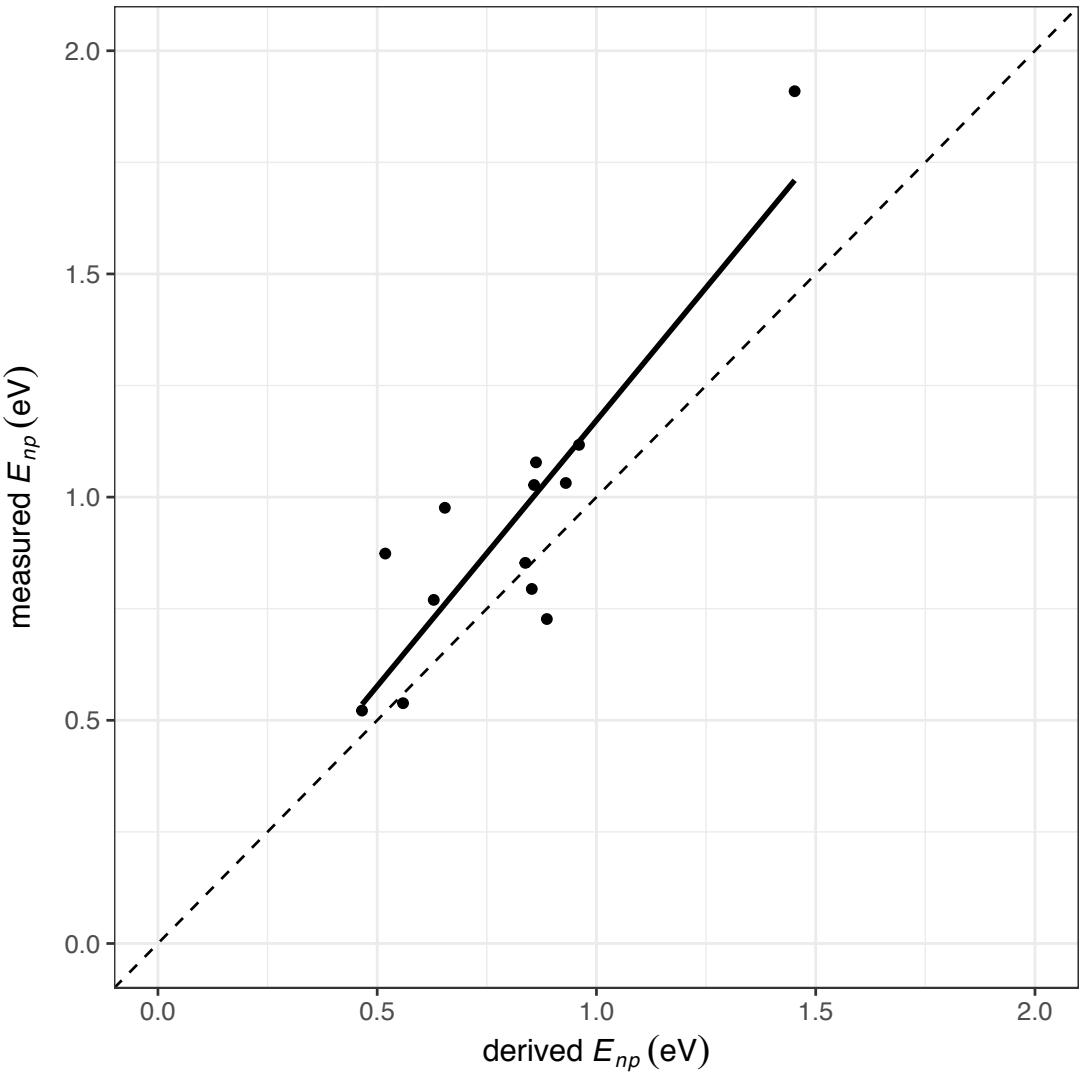

Appendix Figure 13. Comparison between measured and derived activation energies for net photosynthesis.
Activation energies of net photosynthesis measured from fitting the rate data to the modified Sharpe-Schoolfield equation (Eq. 4.1) correlate well with the derived activation energy of net photosynthesis calculated using equation A1. The fitted line is the best fit of a linear model and the 1:1 line is shown for comparison.

Comparison of measured and modelled reaeration rates

To assess the robustness of our modelled values of reaeration, I compared measurements of the reaeration rate made in nearby streams in Iceland with comparable physical characteristics using propane additions (from Demars *et al.* 2011), to values estimated using the surface renewal model (eq. 4.14). In Demars *et al.* (2011), the reaeration rate was measured using a tracer study, where propane was bubbled continuously across the width of the stream at an upstream station. Water samples were taken at a downstream station and analysed by gas chromatography back in the laboratory. The change in propane concentration the over the reach and the travel time were used to estimate the reaaeration rate, K (min^{-1}).

I compared the measured values of reaeration, K (min^{-1}), from Demars *et al.* (2011) to estimated values of K derived Eq. 14 (see Chapter 4) and measurements of velocity, depth and temperature for those streams. I found a strong correlation between modelled and measured values of K with 95% confidence intervals on the slope that included unity (slope = 1.13, 95% CI: 0.76 – 1.50) and an R^2 = 0.61 (Appendix Figure 14). In addition, I examined potential biases by plotting the residuals of the ln-ln plot of modelled *vs.* measured reaeration against stream temperature (Appendix Figure 15). This analysis demonstrates that the model residuals do not vary systematically with stream temperature. Consequently, I am confident that estimates of reaeration derived from the surface renewal model are robust for the streams included in this experiment.

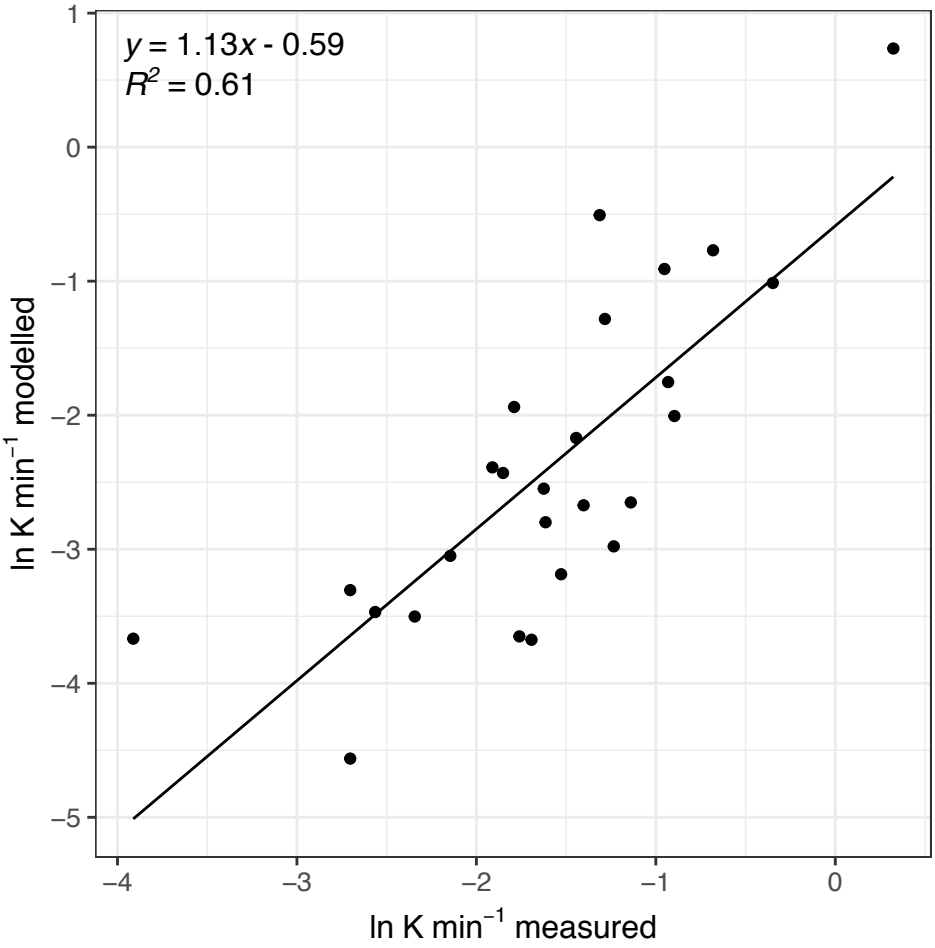

Appendix Figure 14. Comparison of modelled and measured rates of reaeration. Rates of measured reaeration using a propane tracer study are positively correlated with those derived using the surface renewal model (Eq. 4.14) with a slope that was statistically indistinguishable from unity.

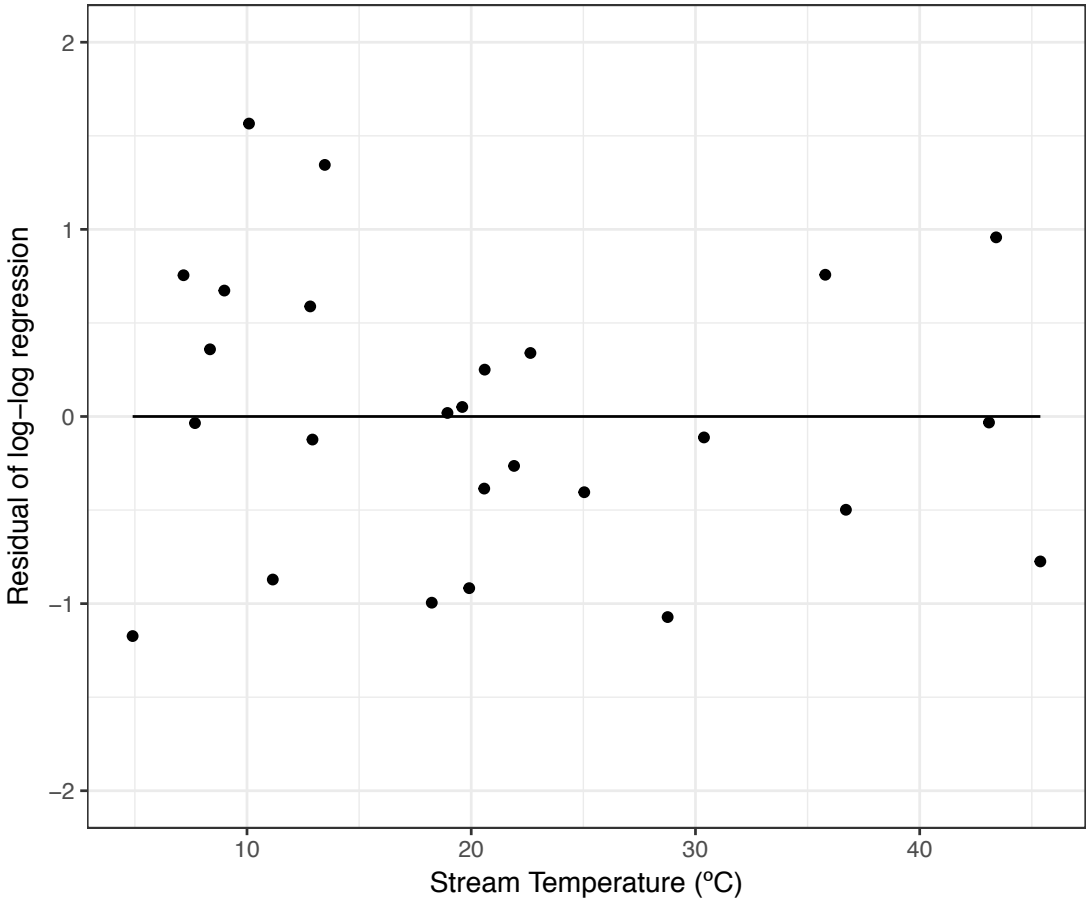

Appendix Figure 15. The relationship between the residuals of modelled vs measured reaeration and stream temperature.
Although there is uncertainty in the modelling of reaeration, there is no systematic bias in the modelled residuals.

BIBLIOGRAPHY

1.Addo-Bediako, A., Chown, S.L. & Gaston, K.J. (2002). Metabolic cold adaptation in insects : a large-scale perspective. *Funct. Ecol.*, 332–338

2.Allen, A.P., Brown, J.H. & Gillooly, J.F. (2002). Global biodiversity, biochemical kinetics, and the energetic-equivalence rule. *Science*, 297, 1545–8

3.Allen, A.P. & Gillooly, J.F. (2009). Towards an integration of ecological stoichiometry and the metabolic theory of ecology to better understand nutrient cycling. *Ecol. Lett.*, 12, 369–84

4.Allen, A.P., Gillooly, J.F. & Brown, J.H. (2005). Linking the global carbon cycle to individual metabolism. *Funct. Ecol.*, 19, 202–213

5.Allison, S.D. (2014). Modeling adaptation of carbon use efficiency in microbial communities. *Front. Microbiol.*, 5, 1–9

6.Allison, S.D., Wallenstein, M.D. & Bradford, M.A. (2010). Soil-carbon response to warming dependent on microbial physiology. *Nat. Geosci.*, 3, 336–340

7.Anderson-Teixeira, K.J., Delong, J.P., Fox, A.M., Brese, D. A. & Litvak, M.E. (2011). Differential responses of production and respiration to temperature and moisture drive the carbon balance across a climatic gradient in New Mexico. *Glob. Chang. Biol.*, 17, 410–424

8.Anderson, T.R. (2005). Plankton functional type modelling: Running before we can walk? *J. Plankton Res.*, 27, 1073–1081

9.Angilletta, M. (2009). *Thermal adaptation: a theoretical and empirical synthesis*. Oxford University Press, 2009

10.Angilletta, M.J. (2006). Estimating and comparing thermal performance curves. *J. Therm. Biol.*, 31, 541–545

11.Angilletta, M.J., Huey, R.B. & Frazier, M.R. (2010). Thermodynamic effects on organismal performance: is hotter better? *Physiol. Biochem. Zool.*, 83, 197–206

12.Atkin, O.K., Atkinson, L.J., Fisher, R.A., Campbell, C.D., Zaragoza-Castells, J., Pitchford, J.W., *et al.* (2008). Using temperature-dependent changes in leaf scaling relationships to quantitatively account for thermal acclimation of respiration in a coupled global climate-vegetation model. *Glob. Chang. Biol.*, 14, 2709–2726

13.Atkin, O.K., Bloomfield, K.J., Reich, P.B., Tjoelker, M.G., Asner, G.P., Bonal, D., *et al.* (2015). Global variability in leaf respiration in relation to climate , plant functional types and leaf traits. *New Phytol.*, 206, 614–636

14.Atkin, O.K., Evans, J.R., Ball, M.C., Lambers, H. & Pons, T.L. (2000). Leaf respiration of snow gum in the light and dark. Interactions between temperature and irradiance. *Plant Physiol.*, 122, 915–923

15.Atkin, O.K., Scheurwater, I. & Pons, T.L. (2007). Respiration as a percentage of daily photosynthesis in whole plants is homeostatic at moderate, but not high, growth temperatures. *New Phytol.*, 174, 367–80

16.Atkin, O.K. & Tjoelker, M.G. (2003). Thermal acclimation and the dynamic response of plant respiration to temperature. *Trends Plant Sci.*, 8, 343–51

17.Atkinson, D. (1994). Temperature and Organism Size-A Law for Ectotherms? *Adv. in Eco. Res.*, 25, 1–58

18.Banavar, J.R., Moses, M.E., Brown, J.H., Damuth, J., Rinaldo, A., Sibly, R.M., *et al.* (2010). A general basis for quarter-power scaling in animals. *Proc. Natl. Acad. Sci. U. S. A.*, 107, 15816–20

19.Barneche, D.R., Kulbicki, M., Floeter, S.R., Friedlander, A. M., Maina, J. & Allen, A. P. (2014). Scaling metabolism from individuals to reef-fish communities at broad spatial scales. *Ecol. Lett.*, 17(9), 1067-1076

20.Base, A. (2015). Chlorella vulgaris Beyerinck [Beijerinck] [WWW Document]. URL http://www.algaebase.org/search/species/detail/?species_id=Cd1da6b97f340f66e&sk=0&from=results

21.Beer, C., Reichstein, M., Tomelleri, E., Ciais, P., Jung, M. & Carvalhais, N. (2010). Terrestrial gross carbon dioxide uptake: Global distribution and covariation with climate. *Science.*, 329, 834–839

22.Behrenfeld, M.J., O'Malley, R.T., Boss, E.S., Westberry, T.K., Graff, J.R., Halsey, K.H., *et al.* (2015). Revaluating ocean warming impacts on global phytoplankton. *Nat. Clim. Chang.,* 323-330

23.Behrenfeld, M.J., O'Malley, R.T., Siegel, D. A, McClain, C.R., Sarmiento, J.L., Feldman, G.C., *et al.* (2006). Climate-driven trends in contemporary ocean productivity. *Nature*, 444, 752–5

24.Bennett, A.F. & Lenski, R.E. (2007). An experimental test of evolutionary trade-offs during temperature adaptation. *Proc. Natl. Acad. Sci. U. S. A.*, 104, 8649–8654

25.Bernacchi, C.J., Singsaas, E.L., Pimentel, C., Portis Jr, a. R. & Long, S.P. (2001). Improved temperature response functions for models of Rubisco-limited photosynthesis. *Plant, Cell Environ.*, 24, 253–259

26.Bernstein, L., Bosch, P., Canziani, O., Chen, Z. & Christ, R. (2008). *IPCC, 2007: climate change 2007: synthesis report*

27.Berry, J. & Bjorkman, O. (1980). Photosynthetic response and adaptation to temperature in higher plants. *Annu. Rev. Plant Physiol.*, 31, 491–543

28.Bolker, B. & Team, R. (2010). bbmle: Tools for general maximum likelihood estimation. *R Package version 0.9*

29.Bond-Lamberty, B. & Thomson, A. (2010). Temperature-associated increases in the global soil respiration record. *Nature*, 464, 579–582

30.Booth, B.B.B., Jones, C.D., Collins, M., Totterdell, I.J., Cox, P.M., Sitch, S., *et al.* (2012). High sensitivity of future global warming to land carbon cycle processes. *Environ. Res. Lett.*, 7, 24002

31.Bopp, L., Aumont, O., Cadule, P., Alvain, S. & Gehlen, M. (2005). Response of diatoms distribution to global warming and potential implications: A global model study. *Geophys. Res. Lett.*, 32, L19606

32.Bott, T. (1996). Primary productivity and community respiration. In: *Methods stream Ecol. Elsevier Acad. Press*. San Diego

33.Bradford, M.A., Davies, C.A., Frey, S.D., Maddox, T.R., Melillo, J.M., Mohan, J.E., *et al.* (2008). Thermal adaptation of soil microbial respiration to elevated temperature. *Ecol. Lett.*, 11, 1316–1327

34.Bradford, M.A., Watts, B.W. & Davies, C.A. (2010). Thermal adaptation of heterotrophic soil respiration in laboratory microcosms. *Glob. Chang. Biol.*, 16, 1576–1588

35.Bradford, M.A. (2013). Thermal adaptation of decomposer communities in warming soils. *Front. Microbiol.*, 4, 1–16

36.Bradshaw, W.E. & Holzapfel, C.M. (2010). Light, time, and the physiology of biotic response to rapid climate change in animals. *Annu. Rev. Physiol.*, 72, 147–166

37.Brown, J., Gillooly, J., Allen, A., Savage, V. & West, G. (2004). Toward a metabolic theory of ecology. *Ecology*, 85(7), 1771–1789

38.Buckling, A., Craig Maclean, R., Brockhurst, M.A. & Colegrave, N. (2009). The Beagle in a bottle. *Nature*, 457, 824–9

39.Callahan, B.J., Mcmurdie, P.J., Rosen, M.J., Han, A.W., Johnson, A.J. & Holmes, S.P. (2015). DADA2 : High resolution sample inference from amplicon data. *bioRxiv*, 13, 0–14

40.Callahan, B.J., Sankaran, K., Fukuyama, J.A., McMurdie, P.J. & Holmes, S.P. (2016). Bioconductor workflow for microbiome data analysis: from raw reads to community analyses. *F1000Research*, 5, 1492

41.Calosi, P., Melatunan, S., Turner, L.M., Artioli, Y., Davidson, R.L., Byrne, J.J., *et al.* (2017). Regional adaptation defines sensitivity to future ocean acidification. *Nat. Commun.*, 8, 13994

42.Carey, J.C., Tang, J., Templer, P.H., Kroeger, K.D., Crowther, T.W., Burton,

A.J., *et al.* (2016). Temperature response of soil respiration largely unaltered with experimental warming. *PNAS*, 2–7

43.Chamberlain, S.A. & Szöcs, E. (2013). taxize: taxonomic search and retrieval in R. *F1000Research*, 2

44.Chapra, S. & Di Toro, D. (1991). Delta method for estimating primary production, respiration, and reaeration in streams. *J. Environ. Eng.*, 117, 640–655

45.Chust, G., Allen, J.I., Bopp, L., Schrum, C., Holt, J., Tsiaras, K., *et al.* (2014). Biomass changes and trophic amplification of plankton in a warmer ocean. *Glob. Chang. Biol.*, 20, 2124–2139

46.Clarke, A. (2004). Is there a Universal Temperature Dependence of metabolism? *Funct. Ecol.*, 18, 252–256

47.Cole, J.R., Wang, Q., Fish, J.A., Chai, B., McGarrell, D.M., Sun, Y., *et al.* (2014). Ribosomal Database Project: Data and tools for high throughput rRNA analysis. *Nucleic Acids Res.*, 42, 633–642

48.Coleman, J.R. & Colman, B. (1980). Effect of oxygen and temperature on the efficiency of photosynthetic carbon assimilation in two microscopic algae. *Plant Physiol.*, 65, 980–3

49.Collins, S. (2011). Many possible worlds: expanding the ecological scenarios in experimental evolution. *Evol. Biol.*, 38, 3–14

50.Collins, S. & Bell, G. (2004). Phenotypic consequences of 1,000 generations of selection at elevated CO_2 in a green alga. *Nature*, 431, 566–9

51.Collins, S., Rost, B. & Rynearson, T.A. (2013). Evolutionary potential of marine phytoplankton under ocean acidification. *Evol. Appl.*, 7, 140–155

52.Connor, M.I.O., Piehler, M.F., Leech, D.M., Anton, A. & Bruno, J.F. (2009). Warming and resource availability shift food web structure and metabolism, *PLoS Biology,* 7, 3–8

53.Cox, P.M., Betts, R.A, Jones, C.D., Spall, S.A & Totterdell, I.J. (2000). Acceleration of global warming due to carbon-cycle feedbacks in a coupled climate model. *Nature*, 408, 184–7

54.Cross, W.F., Hood, J.M., Benstead, J.P., Huryn, A.D. & Nelson, D. (2015). Interactions between temperature and nutrients across levels of ecological organisation. *Glob. Chang. Biol.*, 21, 1025–1040

55.Daines, S., Clark, J. & Lenton, T. (2014). Multiple environmental controls on phytoplankton growth strategies determine adaptive responses of the N : P ratio. *Ecol. Lett.*, 17, 414–425

56.Damuth, J. (1987). Interspecific allometry of population density in mammals and other animals: the independence of body mass and population energy-use.

Biol. J. Linn. Soc., 31, 193–246

57.Daufresne, M., Lengfellner, K. & Sommer, U. (2009). Global warming benefits the small in aquatic ecosystems. *Proc. Natl. Acad. Sci. U. S. A.*, 106, 12788–12793

58.Davidson, E.A. & Janssens, I.A. (2006). Temperature sensitivity of soil carbon decomposition and feedbacks to climate change. *Nature*, 440, 165–173

59.Davison, I., Greene, R. & Podolak, E. (1991). Temperature acclimation of respiration and photosynthesis in the brown alga *Laminaria saccharina*. *Mar. Biol.*, 110, 449–454

60.Decelle, J., Romac, S., Stern, R.F. & Bendif, E.L.M. (2015). PhytoREF : a reference database of the plastidial 16S rRNA gene of photosynthetic eukaryotes with curated taxonomy, 1435–1445

61.Dell, A.I., Pawar, S. & Savage, V.M. (2011). Systematic variation in the temperature-dependence of physiological and ecological traits. *Proc. Natl. Acad. Sci. U. S. A.*, 108, 10591–6

62.Dell, A.I., Pawar, S. & Savage, V.M. (2013). Temperature-dependence of trophic interactions are driven by asymmetry of species responses and foraging strategy. *J. Anim. Ecol.,* 83, 70-84

63.DeLong, J.P., Gibert, J.P., Luhring, T.M., Bachman, G., Reed, B., Neyer, A., *et al.* (2017). The combined effects of reactant kinetics and enzyme stability explain the temperature dependence of metabolic rates. *Ecol. Evol.*, 1–11

64.DeLong, J.P., Okie, J.G., Moses, M.E., Sibly, R.M. & Brown, J.H. (2010). Shifts in metabolic scaling, production, and efficiency across major evolutionary transitions of life. *Proc. Natl. Acad. Sci. U. S. A.*, 107, 12941–5

65.Demars, B.O.L., Gíslason, G.M., Ólafsson, J.S., Manson, J.R., Friberg, N., Hood, J.M., *et al.* (2016). Impact of warming on CO_2 emissions from streams countered by aquatic photosynthesis. *Nat. Geosci.*, 9, 758–761

66.Demars, B.O.L., Russell Manson, J., Ólafsson, J.S., Gíslason, G.M., Gudmundsdóttir, R., Woodward, G., *et al.* (2011). Temperature and the metabolic balance of streams. *Freshw. Biol.*, 56, 1106–1121

67.Demars, B.O.L., Thompson, J. & Manson, J.R. (2015). Stream metabolism and the open diel oxygen method: Principles, practice, and perspectives. *Limnol. Oceanogr. Methods*, 13, 356–374

68.Deutsch, C. a, Tewksbury, J.J., Huey, R.B., Sheldon, K.S., Ghalambor, C.K., Haak, D.C., *et al.* (2008). Impacts of climate warming on terrestrial ectotherms across latitude. *Proc. Natl. Acad. Sci. U. S. A.*, 105, 6668–6672

69.Dewar, R.C., Medlyn, B.E. & McMurtrie, R.E. (1999). Acclimation of the respiration photosynthesis ratio to temperature: insights from a model. *Glob. Chang. Biol.*, 5, 615–622

70.Dossena, M., Yvon-Durocher, G., Grey, J., Montoya, J.M., Perkins, D.M., Trimmer, M., *et al.* (2012). Warming alters community size structure and ecosystem functioning. *Proc. Biol. Sci.*, 279, 3011–3019

71.Duarte, C.M., Regaudie-de-Gioux, A., Arrieta, J.M., Delgado-Huertas, A. & Agustí, S. (2013). The oligotrophic ocean is heterotrophic. *Ann. Rev. Mar. Sci.*, 5, 551–69

72.Edwards, K.F., Litchman, E. & Klausmeier, C.A. (2013a). Functional traits explain phytoplankton responses to environmental gradients accross lakes of the United States. *Ecology*, 94, 1626–1635

73.Edwards, K.F., Litchman, E. & Klausmeier, C.A. (2013b). Functional traits explain phytoplankton community structure and seasonal dynamics in a marine ecosystem. *Ecol. Lett.*, 16, 56–63

74.Edwards, K.F., Thomas, M.K., Klausmeier, C.A. & Litchman, E. (2016). Phytoplankton growth and the interaction of light and temperature : A synthesis at the species and community level. *Limnol. Oceanogr.,* 1232-1244

75.Eilers, P.H. & Peeters, J.C. (1988). A model for the relationship between light intensity and the rate of photosynthesis in phytoplankton. *Ecol. Modell.*, 42, 199–215

76.Elzhov, T., Mullen, K. & Bolker, B. (2009). minpack. lm: R Interface to the Levenberg-Marquardt Nonlinear Least-Squares Algorithm

77.Enquist, B.J., Brown, J.H. & West, G.B. (1998). Allometric scaling of plan energetics and population density. *Nature*, 395, 163–165

78.Enquist, B.J., Economo, E.P., Huxman, T.E., Allen, A.P., Ignace, D.D. & Gillooly, J.F. (2003). Scaling metabolism from organisms to ecosystems. *Nature*, 423, 639–42

79.Enquist, B.J., Kerkhoff, A.J., Huxman, T.E. & Economo, E.P. (2007). Adaptive differences in plant physiology and ecosystem paradoxes: Insights from metabolic scaling theory. *Glob. Chang. Biol.*, 13, 591–609

80.Enquist, B.J., Michaletz, S., Enquist, B.J., Michaletz, S.T. & Kerkhoff, A.J. (2016). Toward a general scaling theory for linking traits , stoichiometry , and body size to ecosystem function Toward a General Scaling Theory for Linking Traits , Stoichiometry , and Body Size to Ecosystem Function

81.Eppley, R. (1972). Temperature and Phytoplankton Growth in the Sea. *Fish. Bull.*, 70, 1063-1085

82.Ernest, S.K.M., Brown, J.H., Thibault, K.M., White, E.P. & Goheen, J.R. (2008). Zero Sum , the Niche , and Metacommunities : Long-Term Dynamics of Community Assembly, *Am. Nat.,* 172, E257-E269

83.Ernest, S.K.M., White, E.P. & Brown, J.H. (2009). Changes in a tropical

forest support metabolic zero-sum dynamics. *Ecol. Lett.*, 12, 507–515

84.Falkowski, P., Scholes, R.J., Boyle, E., Canadell, J., Canfield, D., Elser, J., *et al.* (2000). The global carbon cycle : A test of our knowledge of earth as a system. *Science*, 290, 291–297

85.Falkowski, P.G. (1994). The role of phytoplankton photosynthesis in global biogeochemical cycles. *Photosynth. Res.,* 39.3, 235–258

86.Falkowski, P.G. (1998). Biogeochemical Controls and Feedbacks on Ocean Primary Production. *Science.*, 281, 200–206

87.Falkowski, P.G., Fenchel, T. & Delong, E.F. (2008). The microbial engines that drive Earth's biogeochemical cycles. *Science*, 320, 1034–1039

88.Field, C.B. (1998). Primary production of the biosphere: Integrating terrestrial and oceanic components. *Science.*, 281, 237–240

89.Finkel, Z. V, Katz, M.E., Wright, J.D., Schofield, O.M.E. & Falkowski, P.G. (2005). Climatically driven macroevolutionary patterns in the size of marine diatoms over the Cenozoic. *Proc. Natl. Acad. Sci. U. S. A.*, 102, 8927–32

90.Frazier, M.R., Huey, R.B. & Berrigan, D. (2006). Thermodynamics constrains the evolution of insect population growth rates: "warmer is better". *Am. Nat.*, 168, 512–520

91.De Frenne, P., Graae, B.J., Rodríguez-Sánchez, F., Kolb, A., Chabrerie, O., Decocq, G., *et al.* (2013). Latitudinal gradients as natural laboratories to infer species' responses to temperature. *J. Ecol.*, 101, 784–795

92.Fukami, T. & Wardle, D.A. (2005). Long-term ecological dynamics: reciprocal insights from natural and anthropogenic gradients. *Proc. Biol. Sci.*, 272, 2105–15

93.Galmes, J., Kapralov, M., Copolovici, L., Hermida-Carrera, C. & Niinemets, U. (2015). Temperature responses of the Rubisco maximum carboxylase activity across domains of life : phylogenetic signals , trade-offs , and importance for carbon gain. *Photosynth. Res.*, 123, 183–201

94.García, F.C., García-Martín, E.E., Taboada, F.G., Sal, S., Serret, P. & López-Urrutia, Á. (2015). The allometry of the smallest: superlinear scaling of microbial metabolic rates in the Atlantic Ocean. *ISME J.*, 1–8

95.Gardner, J.L., Peters, A., Kearney, M.R., Joseph, L. & Heinsohn, R. (2011). Declining body size: a third universal response to warming? *Trends Ecol. Evol.*, 26, 285–91

96.Geerts, A.N., Vanoverbeke, J., Vanschoenwinkel, B., Van Doorslaer, W., Feuchtmayr, H., Atkinson, D., *et al.* (2015). Rapid evolution of thermal tolerance in the water flea Daphnia. *Nat. Clim. Chang.*, 5, 1–5

97.Gifford, R.M. (1995). Whole plant respiration and photosynthesis of wheat

under increased CO_2 concentration and temperature: long-term vs. short-term distinctions for modelling. *Glob. Chang. Biol.*, 1, 385–396

98.Gifford, R.M. (2003). Plant respiration in productivity models: conceptualisation, representation and issues for global terrestrial carbon-cycle research. *Funct. Plant Biol.*, 30, 171

99.Gilchrist, G.W. (2017). Specialists and generalists in changing environments . I . Fitness landscapes of thermal sensitivity. *Am. Nat.*, 146, 252–270

100.Gillooly, J.F. (2006). Response to Clarke and Fraser : effects of temperature on metabolic rate. *Func. Ecol.* 400–404

101.Gillooly, J.F., Brown, J.H., West, G.B., Savage, V.M. & Charnov, E.L. (2001). Effects of size and temperature on metabolic rate. *Science*, 293, 2248–51

102.Giordano, M., Beardall, J. & Raven, J.A. (2005). CO_2 concentrating mechanisms in algae: mechanisms, environmental modulation, and evolution. *Annu. Rev. Plant Biol.*, 56, 99–131

103.del Giorgio, P.A. & Duarte, C.M. (2002). Respiration in the open ocean. *Nature*, 420, 379–384

104.del Giorgio, P., Cole, J.J. & Cimbleris, A. (1997). Respiration rates in bacteria exceed phytoplankton production in unproductive aquatic systems. *Nature*, 385, 148

105.Grace, M.R. & Imberger, S.J. (2006). *Stream metabolism : Performing and interpreting measurements*

106.Hansell, D.A., Ducklow, H.W., Macdonald, A.M. & Baringer, M.O. (2004). Metabolic poise in the North Atlantic Ocean diagnosed from organic matter transports. *Limnol. Oceanogr.*, 49, 1084–1094

107.Hillebrand, H., Burgmer, T. & Biermann, E. (2011). Running to stand still: temperature effects on species richness, species turnover, and functional community dynamics. *Mar. Biol.*, 159, 2415–2422

108.Huete-Ortega, A.M., Cermeño, P., Calvo-Díaz, A., Marañón, E. *et al.* (2017). Isometric size-scaling of metabolic rate and the size abundance distribution of phytoplankton, 279, 1815–1823

109.Huete-Ortega, M., Rodríguez-Ramos, T., López-Sandoval, D., Cermeño, P., Blanco, J., Palomino, R., *et al.* (2014). Distinct patterns in the size-scaling of abundance and metabolism in coastal and open-ocean phytoplankton communities. *Mar. Ecol. Prog. Ser.*, 515, 61–71

110.Huey, R.B. & Kingsolver, J.G. (1989). Evolution of thermal sensitivity of ectotherm performance. *Trends Ecol. Evol.*, 4, 131–135

111.Huey, R.B. & Kingsolver, J.G. (2011). Variation in universal temperature

dependence of biological rates. *Proc. Natl. Acad. Sci. U. S. A.*, 108, 10377–8

112.Irwin, A.J., Finkel, Z. V., Müller-Karger, F.E. & Troccoli Ghinaglia, L. (2015). Phytoplankton adapt to changing ocean environments. *Proc. Natl. Acad. Sci.*, 201414752

113.Isaac, N.J.B. & Carbone, C. (2010). Why are metabolic scaling exponents so controversial? Quantifying variance and testing hypotheses. *Ecol. Lett.*, 13, 728–35

114.Kattge, J. & Knorr, W. (2007). Temperature acclimation in a biochemical model of photosynthesis: A reanalysis of data from 36 species. *Plant, Cell Environ.*, 30, 1176–1190

115.Kearney, M., Porter, W.P., Williams, C., Ritchie, S. & Hoffmann, A.A. (2009). Integrating biophysical models and evolutionary theory to predict climatic impacts on species' ranges: The dengue mosquito Aedes aegypti in Australia. *Funct. Ecol.*, 23, 528–538

116.Kerkhoff, A.J., Enquist, B.J., Elser, J.J. & Fagan, W.F. (2005). Plant allometry, stoichiometry and the temperature-dependence of primary productivity. *Glob. Ecol. Biogeogr.*, 14, 585-598

117.Kirkwood, D. (1996). Nutrients: practical notes on their determination in seawater. *ICES Tech. Mar. Environ. Sci.*

118.Kleiber, M. (1932). Body size and metabolism. *Hilgardia*, 6, 315–351

119.Knies, J.L., Kingsolver, J.G. & Burch, C.L. (2009). Hotter is better and broader: thermal sensitivity of fitness in a population of bacteriophages. *Am. Nat.*, 173, 419–30

120.Kordas, R.L., Harley, C.D.G. & Connor, M.I.O. (2011). Community ecology in a warming world : The influence of temperature on interspecific interactions in marine systems. Exp. Mar. Bio. Eco. 400, 218–226

121.Kwiatkowski, L., Bopp, L., Aumont, O., Ciais, P., Cox, P.M., Laufkötter, C., *et al.* (2017). Emergent constraints on projections of declining primary production in the tropical oceans, 7

122.Lawrence, D., Fiegna, F., Behrends, V., Bundy, J.G., Phillimore, A.B., Bell, T., *et al.* (2012). Species interactions alter evolutionary responses to a novel environment. *PLoS Biol.*, 10, e1001330

123.Lee, C., Wakeham, S. & Arnosti, C. (2004). Particulate Organic Matter in the Sea : The Composition Conundrum. *Ambio*, 33, 565–575

124.Leibold, M.A., Holyoak, M., Mouquet, N., Amarasekare, P., Chase, J.M., Hoopes, M.F., *et al.* (2004). The metacommunity concept: A framework for multi-scale community ecology. *Ecol. Lett.*, 7, 601–613

125.Levin, S.A. (1992). The problem of pattern and scale in ecology. *Ecology*,

73, 1943–1967

126.Levin, S.A. (1998). Ecosystems and the biosphere as complex adaptive systems. *Ecosystems*, 1, 431–436

127.Lewandowska, A.M., Breithaupt, P., Hillebrand, H., Hoppe, H., Jürgens, K. & Sommer, U. (2011). Responses of primary productivity to increased temperature and phytoplankton diversity. *J. Sea Res.* 72, 87-93

128.Lewandowska, A.M., Hillebrand, H., Lengfellner, K. & Sommer, U. (2014). Temperature effects on phytoplankton diversity — The zooplankton link. *J. Sea Res.*, 85, 359–364

129.Lewis H. Ziska, J. a B. (1998). The influence of increasing growth temperature and CO_2 concentration on the ratio of respiration to photosynthesis in soybean seedlings. *Glob. Chang. Biol.*, 4, 637–643

130.Li, W. & Godzik, A. (2006). Cd-hit: a fast program for clustering and comparing large sets of protein or nucleotide sequences. *Bioinformatics*

131.Listmann, L., LeRoch, M., Schlüter, L., Thomas, M.K. & Reusch, T.B.H. (2016). Swift thermal reaction norm evolution in a key marine phytoplankton species. *Evol. Appl.*, 9, 1156-1164

132.Litchman, E. & Klausmeier, C.A. (2008). Trait-Based Community Ecology of Phytoplankton. *Annu. Rev. Ecol. Evol. Syst.*, 39, 615–639

133.Litchman, E., Klausmeier, C.A., Schofield, O.M.E. & Falkowski, P.G. (2007). The role of functional traits and trade-offs in structuring phytoplankton communities : scaling from cellular to ecosystem level. *Ecol. Lett.*, 10, 1170–1181

134.Lloyd, J. & Taylor, J.A. (1994). On the temperature dependence of soil respiration. *Funct. Ecol.*, 315–323

135.Lohbeck, K.T., Riebesell, U. & Reusch, T.B.H. (2012). Adaptive evolution of a key phytoplankton species to ocean acidification. *Nat. Geosci.*, 5, 346–351

136.López-Urrutia, Á. & Morán, X.A.G. (2015). Temperature affects the size-structure of phytoplankton communities in the ocean. *Limnol. Oceanogr60, 733-738*

137.López-Urrutia, A., San Martin, E., Harris, R.P. & Irigoien, X. (2006). Scaling the metabolic balance of the oceans. *Proc. Natl. Acad. Sci. U. S. A.*, 103, 8739–8744

138.Loveys, B.R., Atkinson, L., Sherlock, D., Roberts, R., Fitter, A. & Atkin, O.K. (2003). Thermal acclimation of leaf and root respiration: an investigation comparing inherently fast-and slow-growing plant species. *Glob. Chang. Biol.*, 9, 895–910

139.Magozzi, S. & Calosi, P. (2014). Integrating metabolic performance,

thermal tolerance, and plasticity enables for more accurate predictions on species vulnerability to acute and chronic effects of global warming. *Glob. Chang. Biol.*, 1–14

140.Marañón, E. (2008). Inter-specific scaling of phytoplankton production and cell size in the field. *J. Plankton Res.*, 30, 157–163

141.Markensten, H., Moore, K. & Persson, I. (2010). Simulated lake phytoplankton composition shifts toward cyanobacteria dominance in a future warmer climate. *Ecol. Appl.*, 20, 752–767

142.Marquet, P. a., Allen, A.P., Brown, J.H., Dunne, J. a., Enquist, B.J., Gillooly, J.F., *et al.* (2015). On the importance of first principles in ecological theory development. *Bioscience*, 1–2

143.Mcgill, B.J., Enquist, B.J., Weiher, E. & Westoby, M. (2006). Rebuilding community ecology from functional traits, *TREE,* 21, 178-185

144.McLean, M.A., Jr, M.J.A. & Williams, K.S. (2005). If you can't stand the heat, stay out of the city : Thermal reaction norms of chitinolytic fungi in an urban heat island. *J. Therm. Biol.*, 30, 384–391

145.Medlyn, B.E., Dreyer, E., Ellsworth, D., Forstreuter, M., Harley, P.C., Kirschbaum, M.U.F., *et al.* (2002). Temperature response of parameters of a biochemically based model of photosynthesis . II . A review of experimental data. *Plant Cell & Environ.,* 61, 1167–1179

146.Michaletz, S.T., Cheng, D., Kerkhoff, A.J. & Enquist, B.J. (2014). Convergence of terrestrial plant production across global climate gradients. *Nature*, 512, 39–43

147.Montagnes, D.J.S. & Berges, J.A. (1994). Estimating carbon, nitrogen, protein, and chlorophyll a from volume in marine phytoplankton. *Limnol. Oceanogr.*, 39, 1044–1060

148.Montoya, J.M. & Raffaelli, D. (2010). Climate change, biotic interactions and ecosystem services. *Philos. Trans. R. Soc. Lond. B. Biol. Sci.*, 365, 2013–8

149.Moorthi, S.D., Schmitt, J.A., Ryabov, A., Tsakalakis, I., Blasius, B., Prelle, L., *et al.* (2016). Unifying ecological stoichiometry and metabolic theory to predict production and trophic transfer in a marine planktonic food web. *Phil. Trans. R. Soc. B. Biol. Sci.,* 371, 20150270

150.Moran, X.A., Lopez-Urrutia, A., Calvo-Diaz, A. & LI, W.K. (2010). Increasing importance of small phytoplankton in a warmer ocean. *Glob. Chang. Biol.*, 16, 1137–1144

151.Munday, P.L., Warner, R.R., Monro, K., Pandolfi, J.M. & Marshall, D. (2013). Predicting evolutionary responses to climate change in the sea. *Ecol. Lett.*, 16, 1488–1500

152.Nicklisch, A., Shatwell, T.O.M. & Ko, J.A.N. (2008). Analysis and modelling

of the interactive effects of temperature and light on phytoplankton growth and relevance for the spring bloom. *J. Plank. Res.*, 30, 75-91

153.NOAA. (2017). Global Climate Report - Annual 2016 | State of the Climate | National Centers for Environmental Information (NCEI) [WWW Document]. URL https://www.ncdc.noaa.gov/sotc/global/201613

154.O'Connor, M.I., Gilbert, B. & Brown, C.J. (2011). Theoretical predictions for how temperature affects the dynamics of interacting herbivores and plants. *Am. Nat.*, 178, 626–38

155.O'Gorman, E.J., Benstead, J.P., Cross, W.F., Friberg, N., Hood, J.M., Johnson, P.W., *et al.* (2014). Climate change and geothermal ecosystems: Natural laboratories, sentinel systems, and future refugia. *Glob. Chang. Biol.*, 20, 3291–3299

156.O'Gorman, E.J., Pichler, D.E., Adams, G., Benstead, J.P., Cohen, H., Craig, N., *et al.* (2012). *Impacts of Warming on the Structure and Functioning of Aquatic Communities : Individual- to Ecosystem-Level Responses*

157.Odum, H.T. (1956). Primary production in flowing waters. *Limnol. Oceanogr.*, 1, 102–117

158.Oksanen, J., Kindt, R., Legendre, P. & O'Hara, B. (2007). The vegan package. *Community Ecol.*

159.Padfield, D., Yvon-durocher, G., Buckling, A., Jennings, S. & Yvon-durocher, G. (2016). Rapid evolution of metabolic traits explains thermal adaptation in phytoplankton. *Ecol. Lett.*, 19, 133–142

160.Parmesan, C. (2006). Ecological and evolutionary responses to recent climate change. *Annu. Rev. Ecol. Evol. Syst.*, 37, 637–669

161.Pawar, S., Dell, A.I. & Savage, V.M. (2012). Dimensionality of consumer search space drives trophic interaction strengths. *Nature*, 486, 485–9

162.Pawar, S., Dell, A.I., Savage, V.M. & Knies, J.L. (2016). Real versus artificial variation in the thermal sensitivity of biological traits. *Am. Nat.*, 187,

163.Peter, K.H. & Sommer, U. (2012). Phytoplankton cell size: intra- and interspecific effects of warming and grazing. *PLoS One*, 7

164.Petit, R.J., Raynaud, D., Basile, I., Chappellaz, J., Ritz, C., Delmotte, M., *et al.* (1999). Climate and atmospheric history of the past 420,000 years from the Vostok ice core, Antarctica. *Nature*, 399, 429–413

165.Pinheiro, J. & Bates, D. (2006). *Mixed-effects models in S and S-PLUS*. Springer Science & Business Media

166.Platt, T., Sathyendranath, S. & Ravindran, P. (1990). Primary production by phytoplankton : analytic solutions for daily rates per unit area of water surface. *Proc. Biol. Sci.*, 241, 101–111

167.Pörtner, H.O. & Knust, R. (2007). Climate change affects marine fishes through the oxygen limitation of thermal tolerance. *Science*, 20–23

168.Price, C.A., Weitz, J.S., Savage, V.M., Stegen, J.C., Clarke, A., Coomes, D.A., *et al.* (2012). Testing the metabolic theory of ecology. *Ecol. Lett.*, 15, 1465–1474

169.Pörtner; & Farrell, A.P. (2008). Physiology and Climate Change. *Science.*, 322, 690–692

170.Raich, J.. & Schlesinger, W.. (1992). The global carbon dioxide flux in soil respiration and its relationship to vegetation and climate. *Tellus*, 44B, 81–99

171.Rall, B.C., Brose, U., Hartvig, M., Kalinkat, G., Schwarzmuller, F., Vucic-Pestic, O., *et al.* (2012). Universal temperature and body-mass scaling of feeding rates. *Philos. Trans. R. Soc. B Biol. Sci.*, 367, 2923–2934

172.Raven, J.A. & Geider, R.J. (1988). Temperature and algal growth. *New Phytol.*, 110, 441–461

173.Raven, J.A., Giordano, M., Beardall, J. & Maberly, S.C. (2011). Algal and aquatic plant carbon concentrating mechanisms in relation to environmental change. *Photosynth. Res.*, 109, 281–296

174.Regaudie-de-Gioux, A. & Duarte, C.M. (2012). Temperature dependence of planktonic metabolism in the ocean. *Global Biogeochem. Cycles*, 26

175.Reich, P.B., Sendall, K.M., Stefanski, A., Wei, X., Rich, R.L. & Montgomery, R.A. (2016). Boreal and temperate trees show strong acclimation of respiration to warming. *Nature*, 531, 633–636

176.Reusch, T.B.H. & Boyd, P.W. (2013). Experimental evolution meets marine phytoplankton. *Evolution*, 67, 1849–1859

177.Robinson, C. & Williams, P.J. l. B. (2005). Respiration and its measurement in surface marine waters. In: *Respir. Aquat. Ecosyst.* pp. 147–180

178.Romero-Olivares, A.L., Allison, S.D. & Treseder, K.K. (2017). Soil microbes and their response to experimental warming over time: a meta-analysis of field studies. *Soil Biol. Biochem.*, 107, 32–40

179.Savage, V.M. (2004). Improved approximations to scaling relationships for species, populations, and ecosystems across latitudinal and elevational gradients. *J. Theor. Biol.*, 227, 525–34

180.Savage, V.M. & Allen, A.P. (2004). The predominance of quarter-power scaling in biology. *Func. Ecol.*, 18, 257–282

181.Savage, V.M., Gillooly, J.F., Brown, J.H. & Charnov, E.L. (2004). Effects of body size and temperature on population growth. *Am. Nat.*, 163, 429–41

182.Scafaro, A.P., Xiang, S., Long, B.M., Bahar, N.H.A., Weerasinghe, L.K., Creek, D., *et al.* (2017). Strong thermal acclimation of photosynthesis in tropical and temperate wet-forest tree species: the importance of altered Rubisco content. *Glob. Chang. Biol.*

183.Schaum, C.E., Barton, S., Bestion, E., Buckling, A., Garcia-Carreras, B., Lopez, P., *et al.* (2017). Adaptation of phytoplankton to a decade of experimental warming linked to increased photosynthesis. *Nat. Ecol. Evol.*, 1, 94

184.Schaum, E. & Collins, S. (2014). Plasticity predicts evolution in marine alga. *Proc. Biol. Sci.*, 281

185.Schaum, E., Rost, B., Millar, A.J. & Collins, S. (2013). Variation in plastic responses of a globally distributed picoplankton species to ocean acidification. *Nat. Clim. Chang.*, 3, 298–302

186.Schlüter, L., Lohbeck, K.T., Gröger, J.P., Riebesell, U. & Reusch, T.B.H. (2016). Long-term dynamics of adaptive evolution in a globally important phytoplankton species to ocean acidification. *Sc. Advances.,* 1–9

187.Schlüter, L., Lohbeck, K.T., Gutowska, M.A., Gröger, J.P., Riebesell, U. & Reusch, T.B.H. (2014). Adaptation of a globally important coccolithophore to ocean warming and acidification. *Nat. Clim. Chang.*, 4, 1024–1030

188.Schneider, B., Bopp, L., Gehlen, M., Segschneider, J., Frölicher, T.L., Joos, F., *et al.* (2008). Climate induced interannual variability of marine primary and export production in three global coupled climate carbon cycle models. *Biogeosciences Discuss.*, 4, 1877–1921

189.Schoolfield, R.M., Sharpe, P.J. & Magnuson, C.E. (1981a). Non-linear regression of biological temperature-dependent rate models based on absolute reaction-rate theory. *J. Theor. Biol.*, 88, 719–31

190.Schoolfield, R.M., Sharpe, P.J. & Magnuson, C.E. (1981b). Non-linear regression of biological temperature-dependent rate models based on absolute reaction-rate theory. *J. Theor. Biol.*, 88, 719–731

191.Schramski, J.R., Dell, A.I., Grady, J.M., Silby, R.M. & Brown, J.H. (2015). Metabolic theory predicts whole-ecosystem properties. *PNAS*, 112, 2617–2622

192.Schulte, P.M., Healy, T.M. & Fangue, N. a. (2011). Thermal performance curves, phenotypic plasticity, and the time scales of temperature exposure. *Integr. Comp. Biol.*, 51, 691–702

193.Serret, P., Robinson, C., Aranguren-Gassis, M., García-Martín, E.E., Gist, N., Kitidis, V., *et al.* (2015). Both respiration and photosynthesis determine the scaling of plankton metabolism in the oligotrophic ocean. *Nat. Commun.*, 6, 6961

194.Sinclair, B.J., Marshall, K.E., Sewell, M.A., Levesque, D.L., Willett, C.S., Slotsbo, S., *et al.* (2016). Can we predict ectotherm responses to climate

change using thermal performance curves and body temperatures? *Ecol. Lett.*, 19, 1372–1385

195.Smith, N.G. & Dukes, J.S. (2013). Plant respiration and photosynthesis in global-scale models: incorporating acclimation to temperature and CO2. *Glob. Chang. Biol.*, 19, 45–63

196.Smith, N.G., Malyshev, S.L., Shevliakova, E., Kattge, J. & Dukes, J.S. (2016). Foliar temperature acclimation reduces simulated carbon sensitivity to climate. *Nat. Clim. Chang.*, 6, 407–411

197.Spiess, A.N. & Neumeyer, N. (2010). An evaluation of R^2 as an inadequate measure for nonlinear models in pharmacological and biochemical research: a Monte Carlo approach. *BMC Pharmacol.*, 10, 6

198.Staehr, P.A. & Birkeland, M.J. (2006). Temperature acclimation of growth, photosynthesis and respiration in two mesophilic phytoplankton species. *Phycologia*, 45, 648–656

199.Stillman, J.H. (2003). Acclimation capacity underlies susceptibility to climate change. *Science.*, 301, 65

200.Stow, C.A., Jolliff, J., McGillicuddy, D.J., Doney, S.C., Allen, J.I., Friedrichs, M.A.M., *et al.* (2009). Skill assessment for coupled biological/physical models of marine systems. *J. Mar. Syst.*, 76, 4–15

201.Sunday, J.M., Bates, A.E. & Dulvy, N.K. (2011). Global analysis of thermal tolerance and latitude in ectotherms. *Proc. Biol. Sci.*, 278, 1823–30

202.Sunday, J.M., Bates, A.E. & Dulvy, N.K. (2012). Thermal tolerance and the global redistribution of animals. *Nat. Clim. Chang.*, 2, 1–5

203.Sutton, R., Suckling, E. & Hawkins, E. (2015). What does global mean temperature tell us about local climate? *Philos. Trans. R. Soc. A Math. Phys. Eng. Sci.*, 373, 20140426

204.Team, R.C. (2014). R: A language and environment for statistical computing. R Foundation for Statistical Computing, Vienna, Austria, 2012

205.Thomas, M.K., Arangguren-Gassis, M., Kremer, C.T., Gould, M.R., Anderson, K., Klausmeier, C.A., *et al.* (2017). Temperature – nutrient interactions exacerbate sensitivity to warming in phytoplankton. *Glob. Chang. Biol.*, 1–12

206.Thomas, M.K., Kremer, C.T., Klausmeier, C. a. & Litchman, E. (2012). A Global pattern of thermal adaptation in marine phytoplankton. *Science.*, 338, 1085–1089

207.Thomas, M.K., Kremer, C.T. & Litchman, E. (2015). Environment and evolutionary history determine the global biogeography of phytoplankton temperature traits. *Glob. Ecol. Biogeogr.*, 25, 75-86

208.Tylianakis, J.M., Didham, R.K., Bascompte, J. & Wardle, D.A. (2008). Global change and species interactions in terrestrial ecosystems. *Ecol. Lett.*, 11, 1351–1363

209.Vancoppenolle, M., Bopp, L., Madec, G., Dunne, J., Ilyina, T., Halloran, P.R., *et al.* (2013). Future arctic ocean primary productivity from CMIP5 simulations: Uncertain outcome, but consistent mechanisms. *Global Biogeochem. Cycles*, 27, 605–619

210.Vasseur, D.A., Delong, J.P., Gilbert, B., Greig, H.S., Harley, C.D.G., Mccann, K.S., *et al.* (2014). Increased temperature variation poses a greater risk to species than climate warming Increased temperature variation poses a greater risk to species than climate warming. *Philos. Trans. R. Soc. B Biol. Sci.*, 1779, 2013612

211.Vona, V., Di Martino Rigano, V., Lobosco, O., Carfagna, S., Esposito, S. & Rigano, C. (2004). Temperature responses of growth, photosynthesis, respiration and NADH: nitrate reductase in cryophilic and mesophilic algae. *New Phytol.*, 163, 325–331

212.Walther, G.R. (2010). Community and ecosystem responses to recent climate change. *Philos. Trans. R. Soc. Lond. B. Biol. Sci.*, 365, 2019–24

213.Walther, G., Post, E., Convey, P., Menzel, A., Parmesan, C., Beebee, T.J.C., *et al.* (2002). Ecological responses to recent climate change. *Nature*, 416, 389–395

214.Warton, D.I., Wright, I.J., Falster, D.S. & Westoby, M. (2006). Bivariate line-fitting methods for allometry. *Biol. Rev.*, 81, 259

215.Welter, J.R., Benstead, J.P., Cross, W.F., Hood, J.M., Huryn, A.D., Johnson, P.W., *et al.* (2015). Does N_2 fixation amplify temperature dependence of ecosystem metabolism? *Ecology*, 96, 603–610

216.West-Eberhard, M. (2003). *Developmental plasticity and evolution*. Oxford University Press, New York

217.West, G.B., Brown, J.H. & Enquist, B.J. (2001). A general model for ontogenetic growth. *Nature*, 413, 628–631

218.West, G.B., Woodruff, W.H. & Brown, J.H. (2002). Allometric scaling of metabolic rate from molecules and mitochondria to cells and mammals. *Proc. Natl. Acad. Sci. U. S. A.*, 1, 2473–2478

219.White, C.R., Cassey, P., Blackburn, T.M., White, R. & Tim, M. (2010). Allometric exponents do not support a universal metabolic allometry. *Ecology*, 88, 315–323

220.White, E.P., Ernest, S.K.M., Kerkhoff, A.J. & Enquist, B.J. (2007). Relationships between body size and abundance in ecology. *Trends Ecol. Evol.*, 22, 323–30

221.White, E.P., Ernest, S.K.M. & Thibault, K.M. (2004). Trade-offs in community properies through time in a desert rodent community. *Am. Nat.*, 164, 670–676

222.Williams, P.J.l.B., Quay, P., Westberry, T.K. & Behrenfeld, M.J. (2013). The oligotrophic ocean is autotrophic. *Ann. Rev. Mar. Sci.*, 5, 551–569

223.Williamson, T.J., Cross, W.F., Benstead, J.P., Gíslason, G.M., Hood, J.M., Huryn, A.D., *et al.* (2016). Warming alters coupled carbon and nutrient cycles in experimental streams. *Glob. Chang. Biol.*, 22, 2152–2164

224.Wu, B.J. (2004). Membrane lipids and sodium pumps of cattle and crocodiles: an experimental test of the membrane pacemaker theory of metabolism. *AJP Regul. Integr. Comp. Physiol.*, 287, R633–R641

225.Xia, J., Chen, J., Piao, S., Ciais, P., Luo, Y. & Wan, S. (2014). Terrestrial carbon cycle affected by non-uniform climate warming. *Nat. Geosci*, 7, 173–180

226.Yamori, W., Hikosaka, K. & Way, D. a. (2014). Temperature response of photosynthesis in C3, C4, and CAM plants: Temperature acclimation and temperature adaptation. *Photosynth. Res.*, 119, 101–117

227.Yvon-Durocher, G. & Allen, A.P. (2012). Linking community size structure and ecosystem functioning using metabolic theory. *Philos. Trans. R. Soc. Lond. B. Biol. Sci.*, 367, 2998–3007

228.Yvon-Durocher, G., Allen, A.P., Bastviken, D., Conrad, R., Gudasz, C., St-Pierre, A., *et al.* (2014). Methane fluxes show consistent temperature dependence across microbial to ecosystem scales. *Nature*, 507, 488–491

229.Yvon-Durocher, G., Allen, A.P., Cellamare, M., Dossena, M., Gaston, K.J., Leitao, M., *et al.* (2015). Five years of experimental warming increases the biodiversity and productivity of phytoplankton. *PLoS Biol.*, 13

230.Yvon-Durocher, G., Caffrey, J.M., Cescatti, A., Dossena, M., del Giorgio, P., Gasol, J.M., *et al.* (2012). Reconciling the temperature dependence of respiration across timescales and ecosystem types. *Nature*, 487, 472–476

231.Yvon-Durocher, G., Hulatt, C.J., Woodward, G. & Trimmer, M. (2017). Long-term warming amplifies shifts in the carbon cycle of experimental ponds. *Nat. Clim. Chang.*, 1–6

232.Yvon-Durocher, G., Jones, J.I., Trimmer, M., Woodward, G. & Montoya, J.M. (2010). Warming alters the metabolic balance of ecosystems. *Philos. Trans. R. Soc. Lond. B. Biol. Sci.*, 365, 2117–2126

233.Yvon-Durocher, G., Montoya, J.M., Trimmer, M. & Woodward, G. (2011). Warming alters the size spectrum and shifts the distribution of biomass in freshwater ecosystems. *Glob. Chang. Biol.*, 17, 1681–1694

234.Zhang, Q.G. & Buckling, A. (2011). Antagonistic coevolution limits population persistence of a virus in a thermally deteriorating environment. *Ecol.*

Lett., 14, 282–288

235.Zhou, J., Deng, Y., Shen, L., Wen, C., Yan, Q., Ning, D., *et al.* (2016). of microbes in forest soils. *Nat. Commun.*, 7, 1–10

236.Ziehn, T., Kattge, J., Knorr, W. & Scholze, M. (2011). Improving the predictability of global CO_2 assimilation rates under climate change. *Geophys. Res. Lett.*, 38, 1–5

237.Zwart, J., Solomon, C.T. & Jones, S.E. (2015). Phytoplankton traits predict ecosystem function in a global set of lakes. *Ecology*, 96, 2257–2264